Exposure to sparsely and densely ionizing irradiation results in an immediate activation of K^+ channels in A549 cells and in human peripheral blood lymphocytes.

TECHNISCHE UNIVERSITÄT DARMSTADT

Vom Fachbereich Biologie der Technischen Universität Darmstadt

Zur Erlangung des akademischen Grades

eines Doctor rerum naturalium

genehmigte Dissertation von

Dipl. Biologe Bastian Roth

aus Darmstadt

1. Referent/ Referentin: Prof. Dr. Gerhard Thiel

2. Referent/Referentin: Prof. PhD. Marco Durante

Tag der Einreichung: 16. Dezember 2013

Tag der mündlichen Prüfung: 7. Februar 2014

Darmstadt, 2014

D17

1. Table of contents

2. Abstract

Increasing evidence suggests that the activity of ion channels is intimately related to the control of the cell cycle and involved in a modulation of fundamental processes like apoptosis or proliferation and migration of cells. Because of this prominent role in the physiology of humans it is important to understand the impact of sparsely and densely ionizing irradiation on channel function in the context of exposure to natural radiation, radiotherapy and even space missions. The present experiments address the question on whether ionizing irradiation could have any implications on channel activity in the plasma membrane of mammalian cells. In particular there was a special focus on any fast events early on after treatment. For this purpose we examined the conductance of K^+ channels in mammalian cells by patch clamp technique before and soon after exposure to sparsely or densely ionizing irradiation. The possibility of electrophysiological recordings with a high temporal resolution makes it possible to observe the initial steps in signal transduction cascades. Our data show that radiation exposure to sparsely and densely ionizing irradiation results in an immediate activation of K^+ channels in A549 cells and in human peripheral blood lymphocytes. The data stress that in particular the human intermediate Ca^{2+} activated channel hIK (KCNN4) is activated within minutes after irradiating cells with low doses in the cGy range. The response is cell type specific and only cells, which functionally express the hIK channel, respond to radiation stress by a change in membrane conductance. The consequence of hIK activation is a hyperpolarization of the cells towards the Nernst voltage for K^+. With the use of specific blockers (Clotrimazole, Tram-34) and activators (1-EBIO) of hIK channels, it was possible to uncover the causal relation between radiation and channel function in general, and in particular the cellular impact of an up-regulation of K^+ channels. Experiments in which cells were challenged with H_2O_2 or in which the cytosolic Ca^{2+} buffer concentration was altered show that an increase in K^+ channel activity is presumably the result of a serial scenario: radiation causes an increase in radicals in the cytosol, which in turn triggers an elevation of $[Ca^{2+}]_{cyt}$; the latter is the established trigger for hIK activation. Flow cytometry experiments in the presence and absence of hIK channel blockers show that these events are instrumental for the induction of proliferation and migration of hIK expressing cells. Altogether these data provide important insights into potential side effects of ionizing irradiation and they may be helpful to improve radiation therapy of cancer.

3. Zusammenfassung

Es gibt immer mehr Beweise dafür, dass die Aktivität von Ionenkanälen eng mit der Kontrolle des Zellzyklus verbunden und damit an fundamentalen Prozessen wie Apoptose, Zellteilung und Migration beteiligt ist. Auf Grund dieser bedeutenden Rolle für die Physiologie des Menschen, ist es wichtig, die Auswirkungen von dicht- und dünn-ionisierender Strahlung auf Ionenkanäle zu verstehen. Dies ist gerade für die Auswirkungen von Strahlentherapie, Langzeit-Aufenthalten im Weltall, aber auch für die natürliche Hintergrundstrahlung von Interesse. Die vorliegende Arbeit soll Aufschluss darüber geben, ob ionisierende Strahlung eine Auswirkung auf die Ionenkanalaktivität in der Plasmamembran von Säugetier-Zellen hat. Zu diesem Zweck wurde in der Arbeit die Leitfähigkeit von tierischen Zellen mithilfe der "Patch-Clamp Technik" vor und sofort nach Bestrahlung mit dünn- oder dicht-ionisierender Strahlung überprüft. Da die elektrophysiologischen Messungen mit einer hohen zeitlichen Auflösung durchgeführt werden konnten, war es möglich, den Beginn der Signaltransduktionskaskade zu beobachten. Die vorliegenden Daten zeigen, dass eine Bestrahlung mit dünn- und dicht-ionisierenden Strahlen zu einer unmittelbaren Aktivierung von Kaliumkanälen in A549 Zellen und in humanen peripheren Blut-Lymphozyten führt. Insbesondere der humane intermediäre Ca^{2+} aktivierbare Kaliumkanal hiK (KCNN4) wird innerhalb von Minuten nach Bestrahlung, mit niedriger Dosis im cGy-Bereich, aktiviert. Diese Zelltyp spezifische Reaktion ist von der funktionellen Expression des hIK Kanals abhängig und äußert sich durch eine Veränderung der Membranleitfähigkeit. Dabei wird die Membranspannung in Richtung der Nernst-Spannung für K^+ verschoben. Mithilfe von spezifischen Blockern (Clotrimazol, Tram-34) und Aktivatoren (1-EBIO) für den hIK Kanal, konnte der kausale Zusammenhang von Bestrahlung und Kanalaktivierung aufgedeckt werden. In weiteren Experimenten wurden A549 Zellen mit H_2O_2 und unterschiedlichen zytosolischen Ca^{2+} Pufferkonzentrationen behandelt. Die Ergebnisse zeigen, dass der Anstieg an K^+ Kanalaktivität vermutlich das Ergebnis einer seriellen Abfolge ist: Bestrahlung führt zu einem Anstieg an Radikalen im Zytoplasma, dadurch kommt es zu einer Erhöhung der zytosolischen Ca^{2+}-Konzentration. Letzteres ist ein bekannter Auslöser der Aktivierung des hIK. Mithilfe von Durchflusszytometriexperimenten in Gegenwart und Abwesenheit von hIK Blockern, konnte gezeigt werden, dass eine Aktivierung des hIK zu Proliferation und Migration in A549 Zellen beiträgt. Zusammenfassend können die Ergebnisse der vorliegenden Arbeit wichtige Einblicke in mögliche Nebeneffekte von ionisierender Strahlung geben, die für die Verbesserung von Bestrahlungstherapien von Bedeutung sein können.

Chapter 1 - Changes in the activity of ion-channels in epithelial lung cancer cells upon exposure to ionizing irradiation

3.1. General Introduction

Ion channels are membrane tunnels, which allow the selective and regulated passive flow of ions across membranes. This class of membrane proteins is formed by a diverse group of proteins, which are located not only in the plasma membrane but also in the membrane of intracellular compartments including mitochondria, endoplasmic reticulum and nucleus (Hille, 1992). The activity of ion channels is in human cells involved in a large variety of physiological reactions, which range from the excitability of cells to the regulation of hormone secretion. They also modulate heart-beat and control the cell cycle (Hille, 2001; S. Wang et al., 1998; Wonderlin et al., 1995). The quasi-universal role of ion channels in human physiology has many medical implications. One aspect is related to the fact that mutations in genes, which code for channel proteins, are a frequent cause of genetic diseases. Prominent examples for a phenomenon, which is called “channelopathy”, are mutations in the CFTR anion channel (Heitzmann & Warth, 2008); these mutations are the cause of cystic fibrosis. A further well studied channel related disease is the so-called long-QT syndrome. In this case an aberrant function of K^+ or Na^+ channels results in an elongation of the heart-beat rate; this is a frequent reason for heart failure and sudden death (Shieh et al., 2000).

About a decade ago it was realized that ion channels are also involved in cancer (Kunzelmann, 2005). In some types of cancer cells, the presence of specific ion-channels is tightly associated with the aggressiveness of tumors (Bielanska et al., 2012; Catacuzzeno et al., 2012). The reason is presumably related to the fact that channels affect cell survival, proliferation, and migration of cancer cells (Catacuzzeno et al., 2012). Additional targets of ion channels, which could affect aggressiveness of cancer cells, are correlated with their ability to modulate the activity of enzymes in signaling cascades and to control expression of specific genes (Lewis & Cahalan, 1995). Furthermore ion channels are able to transmit their signals through conformational coupling to integrin; in this case their activity is even independent on their ability to conduct ions (Arcangeli & Becchetti, 2006).

The activity of ion channels is tightly regulated by many physical (voltage, mechanical stress) and chemical factors (chemical ligands, Ca^{2+}, pH) in cells. In this way the activity of the channels can be integrated into physiological processes of cells (Clapham, 2003; Horváth et al., 2002; Zhang et al., 2012). Under pathological conditions the regulation of channels can also go wrong with the consequence that cells suffer. Prominent examples are toxins, which block ion channels (Nicholson, 2007; Quintero-Hernández et al., 2013). This can under

extreme conditions prevent the excitability of nerve cells and/or muscle cells. With the beginning of the industrial revolution, which gave rise to environmental pollution, humans are increasingly exposed to various xenobiotics. Many of them augment the formation of metal radicals and reactive oxygen species (Gazzarrini, 2003; Gupta et al., 2012; Pietenpol & Stewart, 2002). Many of these exogenous oxidative-stress factors interfere with signal cascades which in turn regulate ion-channels (Restrepo-Angulo et al., 2010).

Because of their crucial relevance in human physiology and with their sensitivity to many stress related signals it is also important to understand the response of ion channels to ionizing irradiation. It is obvious that any direct or indirect effect of ionizing irradiation on ion channels can have immediate or long-term consequences on human health. In the context of radiation protection and radiotherapy but also for the risk assessment of long-term space flights (Durante & Cucinotta, 2008), it is important to understand how channel activity is affected by radiation. Based on this knowledge it will be possible to judge the consequences of radiation on cell-cycle control (Wang et al., 1998; Wonderlin et al., 1995) cell-migration (Catacuzzeno et al., 2012) and apoptosis (Elliott & Higgins, 2003; Remillard & Yuan, 2004).

Traditionally the DNA has been considered as the main target of ionizing radiation. It is well established that radiation induced damage of DNA can be repaired; alternatively cells with damaged genomic DNA may be eliminated. The latter strategy is much more a cell biological process and not directly coupled any more to the DNA damage. The elimination of cells with damaged DNA can occur, depending on the severances of the damage, either via the induction of apoptosis or necrosis. In the case of less severe DNA damage, cells can also alter their program of genetic differentiation. For example, fibroblasts can accelerate their differentiation with the result that they reach a final state of senescence much earlier than non-irradiated control cells (Schmidt-Ullrich et al., 1997, 1999). Hence although radiation-induced cell responses have been interpreted for a long time from a DNA-centric view, which is undisputed crucial, newer evidence shows that other targets like the plasma membrane are also important in the field of radiobiology (Corre et al., 2010). In this context it is worth recalling that irradiation is able to directly ionize the lipid/protein network of biological membranes (Bionda et al., 2007; Mothersill & Seymour, 2012; Stark, 1991). The plasma membrane is the host of several cytokine receptors like epidermal growth factor (EGF) and tumor necrosis factor (TNF). These receptors are crucial in the regulation of cell proliferation and cell death. The importance of membrane associated events in the radiation response is in agreement with the finding that irradiation, causes within 2 min of exposure an enhanced level of inositol-triphosphate (IP_3). The production of this second messenger was 2-4 fold increased in MDA-MB-231 cells as a consequence of an activation of phosphoinositid-phospholipase C. The latter

enzyme was stimulated by the membrane resident EGF receptor, which presumably was the primary target of radiation (Schmidt-Ullrich, 2000).

In addition to the membrane also water molecules, which are with 80% the most abundant molecule in the cell, can be ionized. Upon ionization water is decomposed into free radical species (Mikkelsen & Wardman, 2003). The concentration of the stress induced reactive oxygen species (ROS) is much lower than those which are constitutively generated in metabolic reactions. Nevertheless, a delayed increase in the rate of ROS can be detected up to 15 min after irradiation (Narayanan, 1997). Stress induced ROS have been shown to distinctly affect several K^+ channels in a manner, which is very much depending on the species of the radical. Hydrogen peroxide for example increase the activity of the Kv1.5 channel expressed in a mammalian cell line (Caouette et al., 2003). Similar effects on voltage-gated Na^+-channels are described in response to nitric oxide NO* (Mustafa et al., 2009; Restrepo-Angulo et al., 2010). Other studies have shown that radicals are not only affecting channels in a direct but also in an indirect manner. Several studies have reported that radicals are able to affect distinct signal cascades, which use the free concentration of cytosolic calcium $[Ca^{2+}]_{cyt}$ as a second messenger. An example for this activity of radicals is the activation of store-operated Ca^{2+} channels (ICRAC) by hydrogen peroxide (Grupe et al., 2010). Since the activity of many ion-channels is in turn regulated by $[Ca^{2+}]_{cyt}$ (Maher & Kuchel, 2003; Sze & Solomon, 1979) it is apparent that a modulation of channel activity by irradiation is in many cases the indirect consequences of radical formation in cells.

In the present study we show that exposure to low doses of x-ray, alpha-particles and high-energy iron/ nickel ions causes in A549 cells a rapid activation of two types of K^+ channels. One of the responsive channels has been identified as the human intermediate conductance Ca^{2+}-activated potassium channel hIK. The effect of irradiation on K^+ channels is cell type specific and has a half maximal effect at ca. 0.1 Gy. Similar effects on the currents were achieved by elevated $[Ca^{2+}]_{cyt}$ or by addition of external hydrogen-peroxide. The results of these experiments imply that activation of K^+ channels and the consequent hyperpolarization of cells can be part of a signal cascade following radiation stress.

3.2. Basics in radiation physics and chemistry

Ionizing radiation interacts with atoms by ionization. The biological effects of these ionizations are the final product of a series of physical, physicochemical and finally chemical events.

3.2.1. Physical basics

There are two main types of radiation. On the one hand energetic-particle radiation, which include electrons, protons, neutrons and alpha-particles which have a mass >0 at rest. On the other hand radiation by electromagnetic-waves that transport energy and have no mass, like photons. If the energy of the radiation is high enough it is possible to ionize atoms by absorbing a part of the energy. This physical process is fast and occurs in 10^{-15} sec. Radiation with this property is called ionizing radiation. With longer wavelength the electromagnetic radiation becomes weaker and is no longer ionizing.

The expression ionizing radiation surmises direct and indirect ionizing radiation. Indirect ionizing radiation is mainly caused by photons and neutrons. They produce charged secondary particles, which finally ionize matter. In contrast the direct ionizing radiation which is for example caused by charged particles is mainly caused by the radiation itself.

Experiments in this thesis deal with sparsely and densely ionizing radiation. The difference between sparsely and densely ionizing radiation is the zonal structure of energy deposition along the particle trajectory. A relative homogenous distribution with a wide range between the different ionization accumulations is called lose ionization radiation; it is generated by x-rays. In contrast, ionizing radiation is called dense if the ionizing events are closely around the ion-track and heterogeneous distributed. Typical examples of these radiations are caused by heavy-ion irradiation and alpha-particles. The local density of the heavy-ion track depends on the kind of ion and energy.

X-ray

Roentgen-rays are called after Wilhelm Roentgen who discovered in 1895 this at that time unknown kind of radiation; he called them therefore x-rays. They are produced when accelerated electrons collide with matter. A device to produce x-rays is an x-ray tube. The tube contains a cathode, which emit electrons into the vacuum. On the opposite site is the anode, which collects the electrons. By applying a high-voltage between cathode and anode the electrons are accelerated and establish an electron-beam. The electrons collide with the material of the anode, which is usually copper or tungsten. Electrons which are deflected by another charge emit electromagnetic radiation. About 1% of the deposed energy in x-ray tubes is emitted as radiation; the rest is released as heat. The generated radiation can be separated into *bremsstrahlung* and characteristic x-rays. There are three different types of interactions of photons with matter, which are important for x-rays. The photoelectric effect

(PE) occurs when an electron from an inner shell is ejected after absorbing a photon. It then causes *bremsstrahlung* or ionizes other atoms. The PE is the dominant process for x-ray absorption at energy lower than 500 keV. The Compton-effect (C) also known as incoherent scattering, occurs when an outer shell electron is ejected by the incident photon or the photon loses some energy and changes direction. The relative importance of this effect increases with energies higher 100 keV. The third effect is the pair production at energies higher 10 MeV. The incident photon can turn into a particle-antiparticle pair of electron and positron, which can both ionize other atoms or cause *bremsstrahlung*.

Highly charged ions

When electrons are removed from atoms the positive charge of the nucleus dominates and charged ions are produced. Because of this positive net charge the ions can be accelerated in a magnetic field to very high velocities. Ions are called heavy, if their atomic mass is higher than that of helium. When accelerated ions pass matter they lose energy by Coulombic repulsion with the electrons present in the atoms of the target, whereby ionizations and excitation take place (Kraft G, Krämer M, 1992; Krämer & Kraft, 1994). This is quantified as total mass stopping power; it is given as the energy transferred per ion track divided by the density of the medium. As the weight of the particles is very high compared to the weight of an electron, the former is not deflected and the track of the particle is almost linear. The heavy-ions in the following experiments were produced at the Universal Linear Accelerator (UNILAC, GSI Darmstadt) and at the Heavy Ion Synchrotron (SIS, GSI Darmstadt).

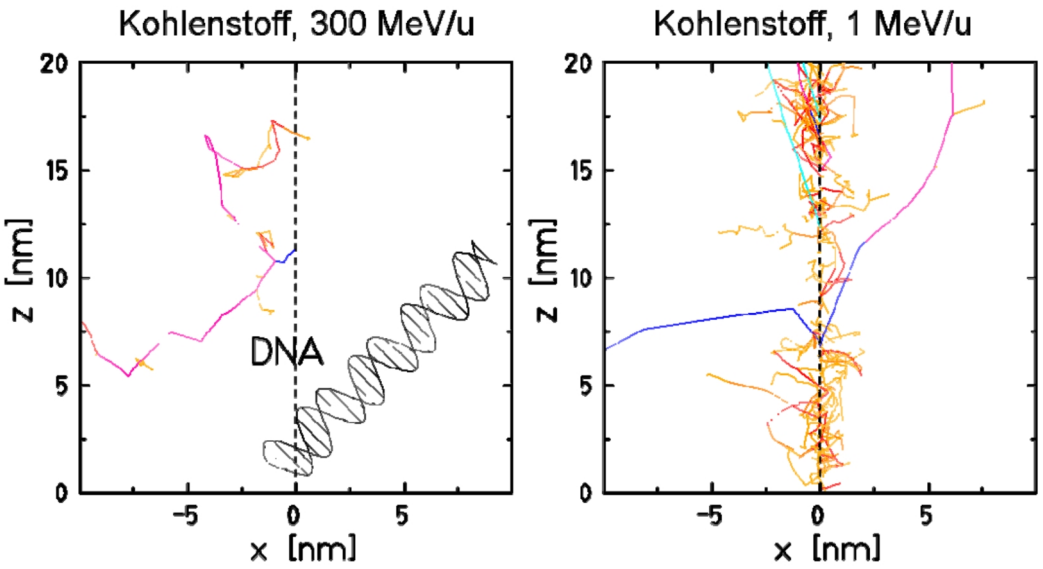

Fig. 1 Simulation of ionization-events along accelerated carbon-ion tracks.

A broken line describes the ion-track (high-energy (300 MeV/u, left and low-energy 1 MeV/u, right). A DNA molecule is shown in scale for comparison of size. Because the LET decreases with increasing energy the number of ionization events decrease with increasing energy. (Krämer & Kraft, 1994)

Alpha-particles

α-particles consist of two-fold positively charged helium atomic-nuclei. They spontaneously emerge from the decay of heavy atoms. Because α –particles are much heavier than electrons, they are not deflected by the atoms in matter, which they penetrate.

If the energy in the ionization-event is very high, the excessive energy is transferred into kinetic energy. These secondary electrons are for their part also able to ionize. α–particles have a much lower velocity than β-emitters because of their mass. Additionally the electromagnetic interaction of α–particles with other atoms is much higher because of their two positive charges. Therefore they have a high ionization density and high LET (linear energy transfer). The ionization distance of α–particles in air is depending on their energy and they reach about 1 cm per MeV. In water the distance is 0.12 mm at 10 MeV.

3.2.2. Chemical Basics

In the physical-chemical phase of ionization the products of the physical-phase react with the environment. Separation of functional groups, breaks in amino-acid chains and generation of water-radicals is the result. This physical-chemical phase persist between 10^{-13} and 10^{-10} sec.

Ionizing radiation effects on the cell

Various kinds of radiation with different energy deposition have at the same dose different relative biological effectiveness (RBE).

The RBE is a dimensionless value and it is defined by equation (1) as the ratio between the energy-dose of the reference and the energy-dose of the radiation of interest for obtaining the same biological effect (Failla, 1931).

$$RBE = \frac{D\ ref}{D\ ion} \qquad \textbf{(1)}$$

RBE: relative biological effectiveness

D ref: dose of the reference

D ion: dose of analyzed radiation

The RBE depends on the spatial distribution of energy deposition along the ion-track.

X-rays deposit their energy homogenous over the irradiated surface. Accelerated ions in contrast pass the irradiated surface in a straight-line and depose their energy depending on their primary energy. The RBE of a particle beam increases with higher atomic number. The typical radial distribution of an ion-track is around several micrometers; the rest of the energy is released for the production of secondary-ions, which form the *Penumbra*. For heavy carbon-ions (25.5 MeV/nucleon) for instance, the radius of the penumbra is about 3.7×10^4 nm (Muroya et al., 2006).

The LET is a good scale to characterize the density of ionization. The LET is defined by equation (2) as the energy-loss (ΔE) along the track (Δs) of a primary charged particle. In general high-LET radiation corresponds to a larger RBE than low-LET radiation (Hollaender, 1954).

$$LET = \frac{\Delta E}{\Delta s}$$

(2)

LET: linear energy transfer [keV/μm]

ΔE: energy deposition of a primary charged particle [keV]

Δs: distance of the charged particle [μm]

Because of the different distribution of energy deposition along the ion tracks, nonhomogeneous scattering of the main radio-lytic species are the result. The formation of free radicals immediately after exposure to ionizing radiation is known for many years. Even if these initial radicals only last for milliseconds it is well established that these radicals can interfere with intracellular metabolic red-ox-reactions; as a consequence the irradiation induced radicals can elicit secondary radical production which may persist for minutes or hours (Mikkelsen & Wardman, 2003).

In the case of particle irradiation the dose depends on the sum of all irradiating particles on the target. The dimension of the amount of applied particles is the fluency. The dependence is shown in the following equation (3).

$$D = 1.602\ x\ 10^{-9}\ x\ LET\ x\ F\ x\ \frac{1}{p}$$

(3)

D = dose [Gy]

LET = linear energy transfer [keV/μm]

F = fluency [1/cm^2]

p = density [g/cm^3]

To estimate the consequences of particle irradiation on cells it is important to know the number of particles, which pass through a cell. At low energy and low fluency it is possible

that not all the cells of an irradiated population are indeed hit. The distribution of particles is described by the equation (4) according to Hall (Hall, 2005):

$$P_{\lambda}(n) = \frac{\lambda^n}{n!} e^{-\lambda}, \qquad \lambda = AF \tag{4}$$

P = probability of n impacts

A = cell surface

F = fluency

λ = average number of particle impacts per cell

n = impacts

Radiation effects on nucleus

Since the pioneering experiments on Chinese hamster fibroblasts (Munro TR., 1970) it is well established that the nucleus with the genetic information is the most important target of ionizing radiation in cells.

Radiation damage of DNA

DNA-lesion evolve by direct hits, but also by indirect radiation effects. The latter occur as a result of hydroxyl-radicals, which are generated in the hydrated envelope of the DNA (Kauffmann G.W., 2006). The most abundant DNA modifications following irradiation with a dose of 1 Gy X-ray are in descending order: i) base-modifications, ii) single-strand breaks, iii) sugar molecule modifications, iv) DNA-Protein cross-linkage and v) double-strand breaks. When DNA-lesion occur the cell-cycle arrests at the next check-point and the DNA is repaired. The duration of the arrest depends on the number and types of DNA modification. As a brief summary it can be said that the irradiated cells are slower in passing the cell-cycle than non-irradiated cells (Scholz M, Kraft-Weyrather W, Ritter S, 1994). When the DNA damage is not repairable, the cell-cycle arrest can be permanent. In this case cells go into programmed cell-death (Apoptosis); alternatively mutations, which result from DNA damage can cause carcinogenesis (Dimitrijevic-Bussod, Balzaretti-Maggi, & Gadbois, 1999)

Radiation effects to plasma-membrane

With a thickness of around 5 nm and a large surface area the plasma-membrane is the largest target for ionizing radiation. In particular the fluidity and permeability of the membrane are directly affected by irradiation. Since the membrane is surrounded on both sides by water, free radicals, which occur as consequence of water radiolysis, find an immense surface to chemically modify the lipid components of the membrane (Stark, 1991). One example is the modification of sphingolipids one of the four most abundant lipids in the plasma membrane. Minutes after irradiation sphingomyelins are hydrolyzed by sphingomyelinase to ceramide. In recent studies the potential of ceramide as signal transduction molecules is discussed. In the context of the present work it is worth noting that also ion-channel activity is altered in association with ceramide (Corre et al., 2010).

Radiation effects to Cytoplasm

The effect of radiation, which is provoked solely by the penetration of the cytoplasm, is usually ignored. However, since it became possible to irradiate only distinct parts of a cell via a micro beam it became evident that also an extra-nuclear irradiation could induce cellular effects; these effects were similar to those observed after a direct damage to the nucleus (Zhou et al., 2009). In other experiments it was found that even an extra-cellular radiation of the surrounding medium is in some cases able to stimulate radiation-responses in cells (Singh et al., 2011; Zhou et al., 2009). The current view is that radiation generates cytotoxic intracellular substances, which then induce signal transduction cascades (AMENTA PS., 1962). Additionally also the idea that an amplification mechanism, which is elicited by a few primary ionization events (2000/Gy/cell), contributes to an activation of cytoplasmic signaling pathways has been advocated (Ward JF., 1994).

Oxidative Stress

Irradiation of water produces plenty of reactive products like hydroxyl radicals ($OH^{\cdot}$), hydrogen radicals (H*), hydrated electrons (e^{-}_{aq}) and hydrogen peroxide (H_2O_2). Additionally superoxide (O_2^{-}) emerges in the presence of oxygen. The latter can react with metal ions in the Fenton reaction to produce hydroxyl-radicals (Wardman, 1996). The relevant reactions are shown in the following scheme.

$$Fe-(Chelat)^{3+} + O_2^- \cdot \leftrightarrow Fe- (Chelat)^{2+} + O_2$$

$$(Chelat)^{2+} + H_2O_2 \rightarrow Fe- (Chelat)^{3+} + OH^- + OH \cdot \qquad Fenton\ Reaction$$

$$O_2^- \cdot + H_2O_2 \rightarrow O_2 + OH^- + OH \cdot \qquad Haber-Weiss-Reaction$$

The hydroxyl-radical is highly reactive, despite of its short lifetime of only 10^{-9} seconds. The radical is able to damage critical targets in its direct vicinity. In addition to irradiation oxidative stress by hydroxyl-radicals can also be caused by chemotherapy or by smoking. Chronic oxidative stress can support diseases like cardiac hypertrophy (Seddon et al., 2007) and it can play part in diabetes mellitus (Zatalia & Sanusi, 2013).

3.3. Ion-channels

The ionic conductance over the plasma membrane was first described by Alan L. Hodgkin and Andrew F. Huxley for which they received the Nobel Prize for medicine in 1963. Clay Armstrong and others showed that ion channels are integral membrane proteins, which form tunnels through which ions can diffuse. A particular feature of channels is that they move ions in a passive manner along their electrochemical gradient and that this movement is much faster than that provided by transporters. By changing the conformational state a channel opens and closes, a process, which is termed “gating”. Related to their particular function in a cell channels can be gated by the membrane voltage, specific ligands and even physical stimuli like temperature or pressure (Hille, 2001). The high selectivity of channels for certain ions is achieved by structural features of the channel proteins. K^+ channels, for which structure/function correlates are particular well known, contain a defined filter region with a characteristic signature sequence, which is responsible for the selectivity of these proteins (MacKinnon, 2004; Noskov & Roux, 2006). The specific residues of amino-acids in this filter compensate the energy relative to the hydration free energy; since this is more favorable for one type of ion than for another the transport of ions is selective (Noskov & Roux, 2006). It has been mentioned before that in particular potassium channels are well explored with respect to structure/function correlates but also with respect to their physiological roles. In this context also a function of potassium channels in cell differentiation is increasingly recognized. It is well established now that K^+ channels are involved in the process of cell proliferation and migration (Lang et al., 2000; Schwab et al., 2012) but also in the induction of apoptosis (Lehen’kyi et al., 2011).

Human intermediate conductance potassium channel (hIK)

One group of K^+-channels, which appears to be relevant in the context of irradiation elicited channel activity, is the Ca^{2+}-activated K^+-channels. Dependent on their pharmacological and physiological behavior the Ca^{2+} channels can be subdivided into three groups according to their unitary conductance; i) big (BK), ii) intermediate (IK) and iii) small (SK) conductance. Each of the three members can be modulated by Ca^{2+} (Cecilia Vergara, 1998). All members of the KCNN family are assembled by four identical α-subunits each spanning the membrane six times; the K^+-selective pore is built from the arrangement of the 5^{th} and 6^{th} trans-membrane domain of each monomer around a water filled pore. IK and SK channels are all encoded by the KCNN gene family, whereby the KCNN4 gene coding for the IK-channel shares only 40% amino-acid identity with the SK coding KCNN1-3 genes.

The intermediate conductance potassium channel (IK1) is also known as K_{Ca} 3.1, SK4 or Gárdos-channel named by a Hungarian scientist Gárdos who first described the channel in 1950. The activity of this channel is Ca^{2+} dependent and it gains its Ca^{2+}-dependency by calmodulin, which is constitutively bound to the C-terminus of the channel (Fanger et al., 1999). Channel activity is only measureable at calcium concentrations above 100 nM, meaning that the channel is essentially inactive at resting conditions. An electrophysiological characterization of the channel shows that it is apparently voltage independency; activation or inactivation shows no time-dependent features. hIK channels are expressed in a lot of tissues where they play diverse physiological roles. A physiological important activity of the IK-channel is known for intestinal epithelia (Devor et al., 1996) where these channels modulate the membrane voltage and with this Cl^- secretion. The same type of channels is also found with different physiological roles in placenta, lung, salivary glands, prostate, thymus, spleen, bone-marrow, lymph nodes and lymphocytes (Bo Skaaning Jensen et al., 1998; Vandorpe, 1998). Although the IK-channels are not found in the human nervous system the presence of the hIK in glioblastoma-cells has been confirmed (Catacuzzeno et al., 2012). In MCF-7 breast cancer cells the hIK-channel is responsible for the G1- to S-phase transition in the cell-cycle (Ouadid-Ahidouch et al., 2004) In primary cells like lymphocytes the hIK is required for continues proliferation (Ghanshani et al., 2000).

Voltage-gated potassium channel Kv1.3

The Kv1.3 channel also known as KCNA3 is a voltage-gated, delayed-outward rectifier potassium ion channel belonging to the Shaker-related subfamily. The channel consists of four identical subunits of about 500 amino acid residues (Roux, 2002). Each subunit constitutes

six membrane-spanning alpha-helices. The S5/S6 helices from each subunit, together with the extracellular loop between the fifth and sixth segment form the pore of the channel. The third and fourth segments together form the voltage-sensor where changes in membrane voltage are detected (Jiang et al., 2003). A movement of the voltage sensor domain following changes in membrane voltage directly affects the gating of this type of channels. Kv1.3 channels activate in a steep voltage dependent manner, at voltages more positive than ca. -60 mV; activity saturates at voltages positive of 0 mV (Cahalan, 1985). After activation the Kv1.3 channel undergoes at positive voltages a so called c-type inactivation during which the channel is non-conducting (Panyi et al., 1995). The Kv1.3 is most abundant in lymphocytes where it regulates the membrane voltage and calcium signaling. With these properties the channel plays an essential role in proliferation and activation of T-cells (Lin et al., 1993). The diverse functions also include cytokine production and cell death (Valencia-Cruz et al., 2009). Specific blockers of the Kv1.3 channel are developed as therapeutics for diverse autoimmune diseases like rheumatoid arthritis (Wulff et al., 2004).

3.4. Material and Methods

3.4.1. Cells used in this study

A549 cells

The A549-cell line is an epithelial lung cancer cell line, which was established from a 58-year old Caucasian man and initiated by Giard et al. (1972). The cell line is hypo triploid with a modal chromosome number of 66 occurring in 24% of cells and with 64 chromosomes in 22% of the cells. Percoll gradient centrifugation showed segregation in four heterogeneously distributed subpopulations. The most abundant subpopulation includes 45% and an intermediate population 18% of the cells; two low populations compromise each only 5%. Growth rate analysis underlined the predominant role of the largest population. In contrast to the dominant population the three smaller ones showed no tumor formation in nude mice (Croce et al., 1999). The A549 cells were purchased from the Leibniz-Institut DSMZ (Deutsche Sammlung von Mikroorganismen und Zellkulturen GmbH).

HEK 293 cells

HEK293 cells are human embryonic kidney cells derived from a healthy, aborted fetus. The 293 line was initiated by the transformation and culturing of normal HEK cells with sheared adenovirus 5 DNA (Graham et al., 1977). The HEK cells were also purchased from the DSMZ.

82-6 hTERT cells

82-6 hTERT cells are immortalized human primary fibroblasts cells. They become immortalized by transfection with a vector that carries the gene for the human telomerase reverse transcriptase (hTERT) catalytic subunit under the control of a constitutive promoter (Yang, 1999). They are considered non-tumorigenic but still have an indefinite lifespan.

The hTERT cells used in this study were a generous gift of Prof. M. Löbrich (TU Darmstadt).

Human peripheral blood lymphocytes

Lymphocytes belong to the cell-mediated immune-response in higher animals and they recognize and respond to antigens. Human peripheral blood lymphocytes (PBL) are subdivided into three groups, the T- and B-cells represent 95% and the large granular lymphocytes form the small group of 5% of the total PBLs. The lymphocytes were generated from the lymphoid progenitor cell in the bone marrow. There they maturate to B-lymphocytes or natural killer cells; in the thymus they maturate to T-lymphocytes. The PBL´s used in this study were isolated from so called buffy coats (anticoagulated leukocyte concentrate) purchased from the Blutspendebank Frankfurt/Main (DRK-Blutspendedienst Baden-Württemberg/Hessen).

3.4.2. Cell culture cultivation

All cultures were maintained free of Mycoplasma as determined by a test from Minerva Biolabs, (Berlin, Germany).

Cultivation-media

82-6hTERT cells were kept in Minimal essential medium (MEM) plus L-Glutamine (200 mM), 20% fetal calve serum (FCS) and 1% non-essential amino acids (NEAA). A549 cells were

cultivated in Dulbecco´s modified minimal essential medium (DMEM) with L-Glutamine (200 mM), 10% FCS and 1% NEAA. HEK293 cells were grown in DMEM with L-Glutamine (200 mM), 10% FCS. Human peripheral blood lymphocytes were cultivated in Roswell Park Memorial Institute medium (1640 RPMI-Medium) plus 20% fetal calve serum (FCS), L-Glutamine (200 mM) and 1% 4-(2-hydroxyethyl)-1-piperazineethanesulfonic acid (HEPES). All media contained 1% streptomycin and penicillin respectively.

Isolation of human peripheral blood lymphocytes from Buffy-coats

Human peripheral T lymphocytes were isolated from the blood of healthy volunteers. Mononuclear cells were isolated by Ficoll-Hypaque density gradient centrifugation according to (Bøyum A., 1976).

The whole human heparinized blood sample was diluted 1:1 (by volume) with phosphate-buffered saline and mixed well. The blood/PBS mixture was underlayed with an equal volume of Ficoll-Hypaque by slow addition. The sample was then centrifuged at 900 x g (2500 rpm) in a Minifuge RF (Heraeus, Hanau, Germany) for 30 min using a swinging-bucket rotor at room temperature without brake. The mononuclear leukocyte cell layer, which collected at the Ficoll-Hypaque plasma interface was carefully removed and transferred to another centrifuge tube. The cells were washed with PBS three-times the volume of the sample tube and were then centrifuged at 400 x g (1300 rpm) for 10 min. The supernatant containing the platelets was discarded and the wash was repeated until most of the platelets were removed. Suspended mononuclear cells were diluted in culture media. One-half of the mononuclear cells were activated with 2 g/ml phytohemagglutinin (PHA), 48 h before electrophysiological measurements were made.

Cultivation of A549, hTERT 82-6, hEK293 and lymphocyte cells

Adherent cell cultures were grown as monolayers in cell-culture flasks of 75 cm^2 to full confluence. Cell lines were generally sterile passaged twice a week using phosphate-buffered saline (PBS) for washing the cells and the trypsin/EDTA solution from Sigma (St. Louis, USA) for detachment. To stop the enzymatic activity of trypsin, cultivation-media was added and cells were re-seeded in new 75 cm^2 flasks. Suspension cell cultures were washed with PBS and sub-cultivated once per week. Cells were cultivated under standard conditions at 37 ^0C ambient temperature and 5% CO_2.

Cell culture sub-cultivation

For experiments the adherent cells were sub-cultivated two days before patch-clamp recordings in 25 cm^2 flasks. The density was selected to reach 80% confluence on the day of measurements.

Cryopreservation of cell cultures

For cryo-conservation a sub-confluent cell culture was trypsinized as described above and centrifuged at 2400 rpm for 3 min. The pellet was suspended in cold FCS to a density of $2*10^6$ cells. From the dilution 0.5 ml were added to 0.5 ml ice-cold FCS supplemented with 10% (v/v) Dimethyl sulfoxide (DMSO). Cells were then placed 12 h at -20°C followed by 12 h at -80°C and for long-term storage the cryogenic vials were placed in liquid nitrogen at -120°C. To defrost the cells they were placed in a water bath at 37°C until half of the volume was melted. The complete content of the vial was added to 5 ml of fresh and warm cultivation-media in a 25 cm^2 flasks and incubated afterwards under standard conditions with 37°C ambient temperature and 5% CO_2. The complete media was replaced with fresh cultivation-media after 24 h. First experiments were done after the 5^{th} passage of the cells.

3.4.3. Patch clamp recordings

Membrane currents of cells were recorded in the whole cell configuration (Hamill et al., 1981) with the portable patch clamp device (port-a-patch, Nanion, Munich, Germany). Confluent cells were harvested according to standard procedure (Fertig et al., 2002). Cells were sealed in solution containing (in mM) 80 NaCl, 3 KCl, 10 $MgCl_2$, 35 $CaCl_2$, 10 HEPES /NaOH, pH 7.4. For recordings we used a buffer with (in mM) 4 KCl, 140 NaCl, 1 $MgCl_2$, 2 CaCl2, 5 D-Glucose, 10 HEPES /NaOH, pH 7.4 as an external bath solution. The intracellular solution contained (in mM) 50 KCl, 10 NaCl, 60 K-Fluoride and 10 HEPES/KOH, pH 7.2. The concentration of the Ca^{2+} buffer EGTA was either 1 or 20 mM and the condition used in the experiments is given in the text. Currents were elicited with a standard pulse protocol consisting of a 200 ms long step from a holding voltage at -60 mV to 800 ms long test pulses between -100 mV and +80 mV and a 200 ms long post-pulse at -80 mV. In voltage ramp protocols cells were clamped from -100 mV to +100 mV over a period of 800 ms; subsequently the voltage was stepped for 50 ms to a post-pulse of -60 mV. The sealing process and the access into the whole-cell mode were achieved with the help of PatchControl Software (Nanion, Munich, Germany). Solution exchange was executed by a rapid perfusion-

system (Nanion, Munich, Germany) or manually. Currents were recorded with an EPC9 amplifier under the control of the Patchmaster Software (both from Heka Electronic, Lambrecht, Germany). Instantaneous currents were sampled 5 ms after onset of the test voltage; in this way the transient-capacitive current was eliminated from the current measurements. The steady-state currents were sampled at the end of the test pulses (usually at 800 ms), at which the slow outward rectifiers were close to their steady state. The time of data collection is indicated in the figures by symbols. Data were analyzed with Patchmaster and Fitmaster software (Heka Electronic, Lambrecht, Germany).

3.4.4. Cell irradiation

Asynchronous cells were exposed to x-ray irradiation in culture flasks for population measurements or alternatively directly on the port-a-patch device. As described in Fig. 2 the portable patch-clamp device was therefore directly placed over the x-ray tube. This adjustment offers the possibility to measure a single cell directly before and after irradiation as fast as possible. We used an x-ray tube (Isovolt160 Titan E from GE Sensing & Inspection Technologies, Ahrensburg, Germany) for all x-ray irradiations. Cells were irradiated with a voltage of 90 kV and 19 mA filtered by a 2 mm aluminum sheet. The dose rates were controlled by a dosimeter (DIADOS T11003 Diagnostikdosimeter). Different doses were achieved by varying the distance between the x-ray source and the cells and the duration, for which cells were irradiated.

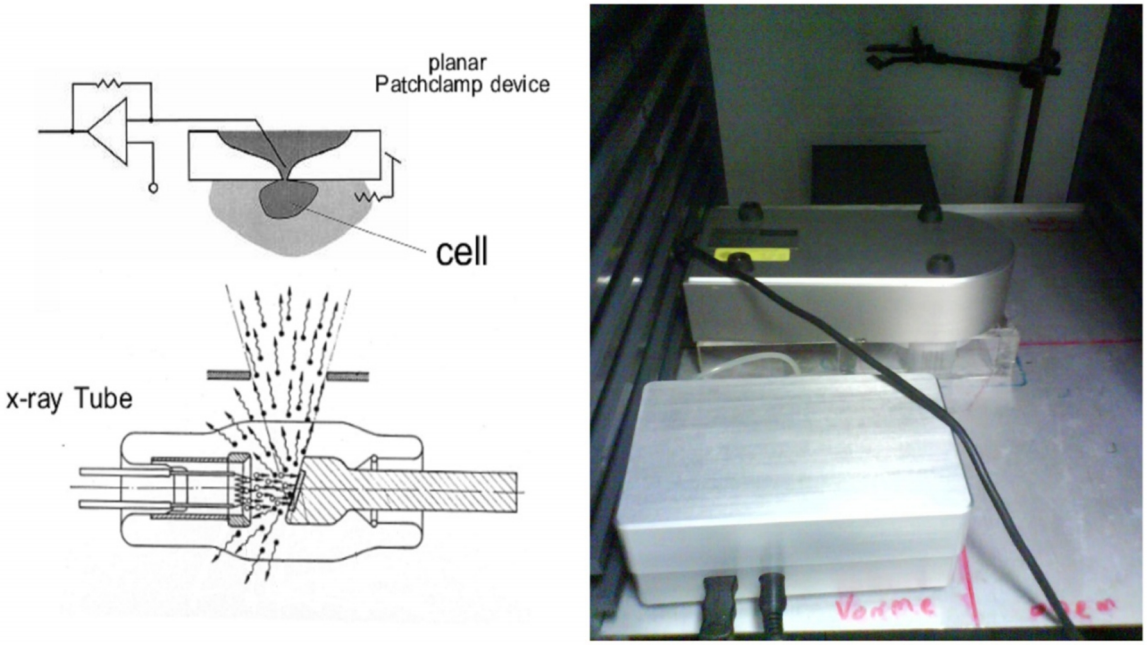

Fig. 2 Installation for measuring cell currents online with patch-clamp device on the irradiation chamber for x-rays.

The portable, planar patch-clamp system Port-A-Patch™ (Nanion, Munich) was placed upside-down over the x-ray tube. The currents of cells in the whole-cell configuration were measured before and after irradiation. Left: schematic drawing of cell on electrophysiological measuring over an x-ray source, right: photograph of port-a-patch (back) and vacuum pump (front) on x-ray source at TU-Darmstadt. (modified from RWTH-Aachen, 2000 & Fertig N. 2002)

Cells were also exposed to accelerated heavy iron or nickel ions (1 GeV/u, LET=150 or 170keV/µm, respectively) at the heavy ion synchrotron (SIS) or low energy iron ions (9.8 MeV/u, 3050keV/µm) at the Universal-Linear-Accelerator (UNILAC) facility (both GSI, Darmstadt, Germany) as described elsewhere (Becher et al., 2002) (Fig. 3). The irradiation at the SIS was delivered in upright standing culture-flasks, which were completely filled with DMEM. After irradiation, the cells were harvested from the culture containers and prepared for electrical recordings as described above. The time between the end of the irradiation and the electrical recordings was between 30 min and 1.5 hours. For each experiment we also recorded the properties of cells, which were not exposed to irradiation, but which underwent otherwise at the same day the same procedure, as controls.

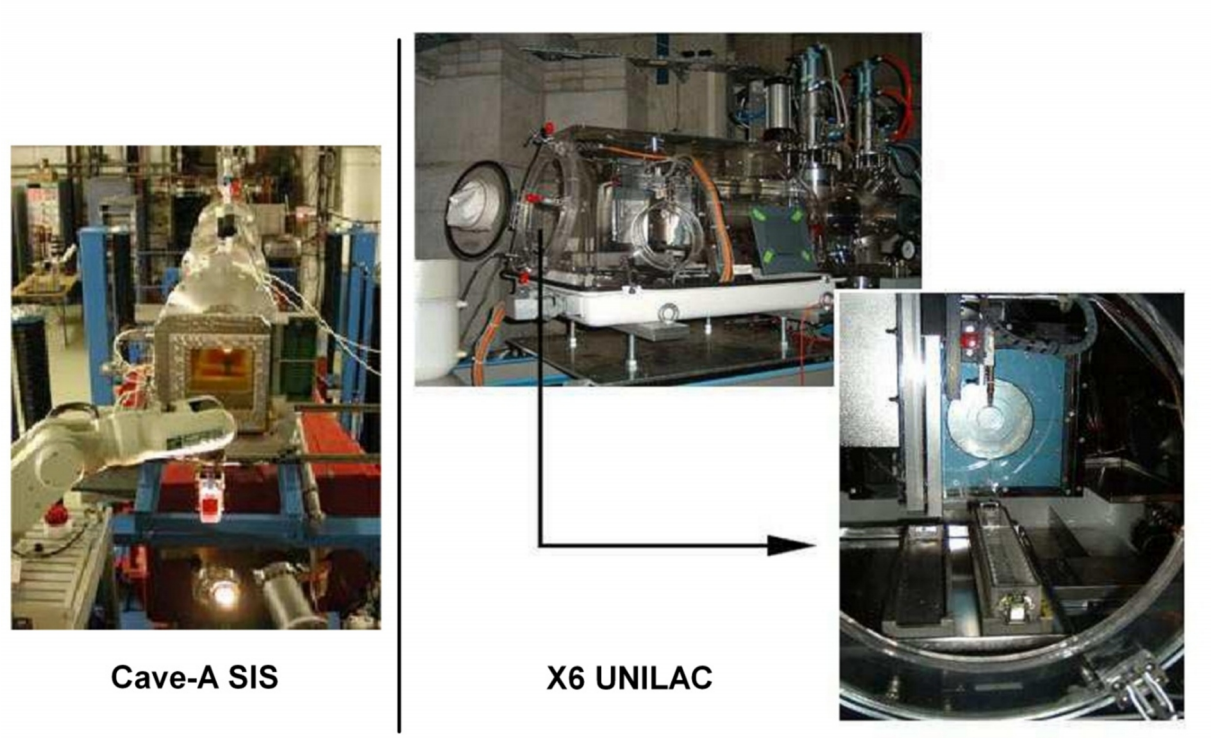

Fig. 3 Installations for the heavy-ion irradiation experiments at GSI (Darmstadt).

The left picture shows the irradiation facility at the SIS experimental hall. The robot-arm places the cell-culture flask directly in front of the beam-line. On the right the experimental hall X6 of the linear accelerator (UNILAC) with the BIBA (Biologische Bestrahlungs-Anlage) is shown. An automatic vacuum grabber system places the cell-culture dishes into the beam and after irradiation back in the cell-culture medium filled magazine. (modified from GSI Helmholtzzentrum für Schwerionenforschung, 1991)

Additional irradiation experiments were done with an alpha-emitter Americium-241. The alpha-particle source used in the respective experiments was ^{241}Am with a specific activity of 3.5 Ci/g and a radiation energy of 5.49 MeV. The dosimetry showed a rest radiation energy of 3.66 MeV (Löbrich-lab, TU-Darmstadt), which was delivered on target at the time of the experiments; the deviation of the actual energy from the specification of the particle source must be a matter of age and a respective decay time. Due to the short range of alpha-particles the NPC®-1 chips had to be unscrewed from the mounting station of the patch-clamp device for irradiation. The free chip was therefore placed upside down directly over the alpha-source for the relevant time to receive the desired dosage. After the estimated time of exposure the chip was mounted back on the holder and measurements were started. Control measurements (Fig. 4c) confirmed that this procedure had no effect on the electrophysiological behavior of A549 cells.

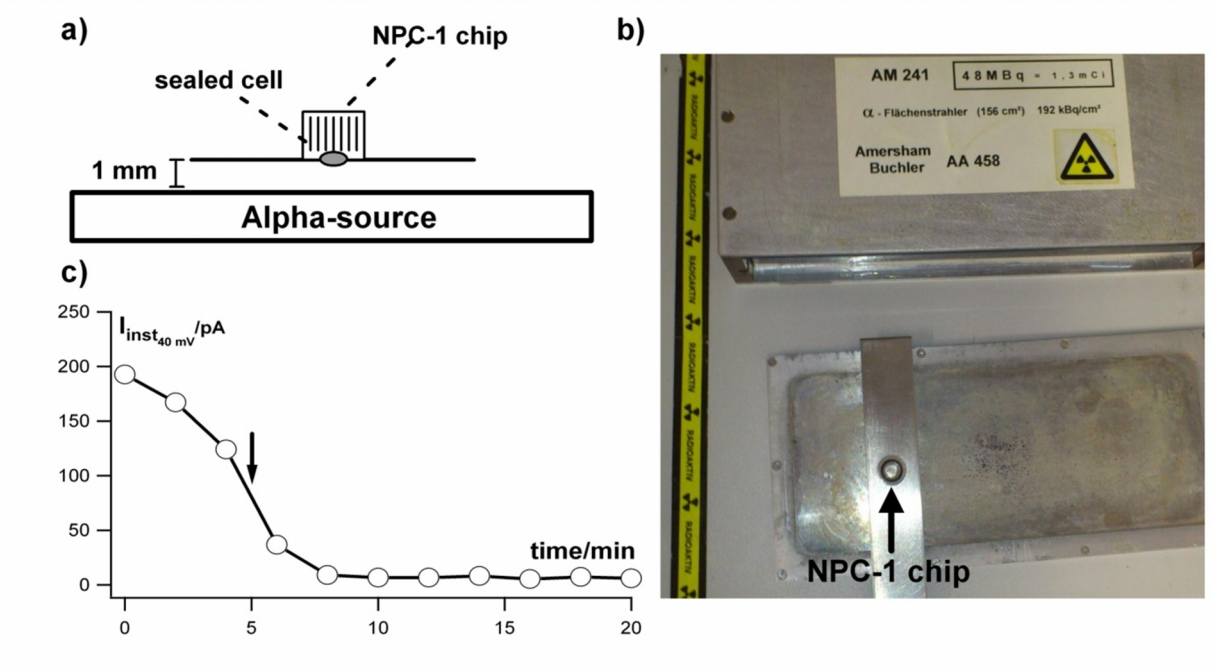

Fig. 4 Setup for patch-clamp measurements of cells in response to alpha-irradiation.

The sketch in a) shows the NPC®-1 chip (Nanion, Munich) with a successfully sealed cell. The chip is fixed upside down on a holder and placed directly at a distance of 1 mm over the plane alpha source ^{241}Am. The photograph in b) illustrates the real setup with the alpha-source, and the holder for the NPC-1 chip. Control-measurement in c) shows the current response of the I_{inst} at 40 mV every 2 min. The arrow indicates the short-term un-mounting of the chip. Only a slight decrease in current could be observed.

3.4.5. Reverse Transcription-PCR

RNA extraction

Total RNA was extracted from 80% confluent cultured cell lines by using RNAtidy (Applichem, Darmstadt, Germany). RNA was purified with a Direct-zol™ RNA MiniPrep Kit according to provider instructions (Zymo, Freiburg, Germany). RNA-content and -purity was determined by NanoDrop (Thermo-Scientific, Wilmington, USA).

Reverse transcription

cDNA was transcribed from 1µg total RNA using Supercript III reverse transcriptase (Invitrogen, Carlsbad, USA) as follows:

Mixture I	1 μg	total RNA
	1 μl	Oligo-T-Primer (100 pmol)
	1 μl	dNTPs (10 mM each)

H_2O_{bidest} was added to a total volume of 13 μl and incubated 5 min at 65 °C. Afterwards the mix was stored on ice. To the mixture 4 μl fivefold First-Strand Buffer, 1 μl 0.1 M DTT, 1 μl RNase Inhibitor (40 U) and 1 μl Superscript III RT (200 U / μl) was added. For randomized primers an incubation time of 5 min at 25°C was used. Oligo $(dT)_{12\text{-}18}$ primers were incubated for 60 min at 50°C and 55°C for gene-specific primer and GC-rich content, followed by a heat-inactivation of the Superscript III RT at 70°C for 15 min. RNA primer were removed by adding 1 μl RNase H and 2 μl RNase buffer and incubating for 20 min at 37°C and 20 min at 65°C.

PCR reaction

RT-PCR expression assays were performed in a Labcycler PCR system (Biolab, Hamburg, Germany) as follows:

PCR-reaction (50μl):

10x Taq-PCR Buffer [200 mM Tris-HCl (pH 8.4), 500 mM KCl]	5 µl
25 mM $MgCl_2$	3 µl
10 mM dNTP Mix (10 mM each)	1 µl
Forward primer (10 µM)	1 µl
Reverse primer (10 µM)	1 µl
Taq DNA polymerase (5 U/µL)	0.4 µl
cDNA	2 µl
H_2O_{bidest}	36.6 μl

Samples were cycled under the following conditions:

hot start	94 °C	2:00	
denaturation	95 °C	0:30	~24 cycles for ~200 bp
annealing	58 °C	0:30	
extension	72 °C	0:40	
final extension	72 °C	7:00	

The PCR product was size fractionated by a 1.8% agarose gel electrophoresis.

Table 1: Summary of the genes of interest and their NCBI reference sequence.

Abkürzung	Name	NCBI Reference Sequence
GAPDH	Glycerinaldehyd-3-phosphat-Dehydrogenase	NM_002046.3
β-Actin	Homo sapiens actin, beta	NM_001101.3
hEAG	Homo sapiens potassium voltage-gated channel, subfamily H (eag-related), member 1 (KCNH1)	NM_172362.2 / NM_002238.3
hERG	Homo sapiens potassium voltage-gated channel, subfamily H (eag-related), member 2 (KCNH2)	NM_000238.3 / NM_172362.2
hIK	Homo sapiens potassium intermediate/small conductance calcium-activated channel, subfamily N, member 4 (KCNN4)	NM_002250.2
Kv1.3 / 1.4	Homo sapiens potassium voltage-gated channel, shaker-related subfamily, member 3 (KCNA3) member 4 (KCNA4)	NM_002232 NM_002233.3

Table 2: Overview of primers used in experiments

Gene	Sequence: sense (se) / anti-sense (as)	Fragment-size (bp)
GAPDH	se 5´ CAACTACATGGTTTACATGTTC 3´ as 5´ GCCAGTGGACTCCACGAC 3´	181
β-Actin	se 5´ CAGAGCAAGAGAGGCATCCT 3´ as 5´ GTTGAAGGTCTCAAACATGATC 3´	210
hEAG	se 5´ TTCGGCGGTCCAATGATACTAAT 3´ as 5´ TTTGCCGCACTTTTTCAATCGT 3´	192
hIK	se 5´ AGAGATGAAGGAGTCCGCTGCC as 5´ GGATCATGTGCATCTTGGAGAT	206
Kv1.3 / Kv1.4	se 5´ GCATGCGGGAACTGGGCCTT 3´ as 5´ TGGCACACAGGGACCCGACA 3´	216
hERG	se 5´ TGTCAGGCGCCTTCTCAGGA 3´ as 5´ GGTCTCCAGCCTGTTGAGCTG 3´	203

3.4.6. Cell cycle analysis by flow cytometry

Flow cytometry was performed on propidium iodide (PI) stained nuclei using a Cytomics FC500 FACS (Beckmann Coulter) and the WinMDI 2.9 software for analysis (The Scripps Institute, Flow Cytometry Core Facility). A549 cells were grown for 24 hours at 37°C and 5% CO_2 at a confluency of 70% in 25 cm^2 cell culture flasks. Six hours prior fixation they were treated with staurosporine [5 μM] and/or TRAM-34 [1 μM]. In other experiments they were irradiated with 1 Gy x-ray. Control cells were only treated by DMSO, which was used as vehicle. For fixation cells were washed with PBS and harvested as described with Trypsin/EDTA. Cells were then fixed drop wise in 1 ml cold 70% ethanol under continuous vortexing; cells were then stored over night at -20°C. Before staining the cells were centrifuged and washed twice with SubG1 phosphate-citrate buffer (200 mM Na_2HPO_4; 8 mM citric acid adjusted at pH 7.8) at room temperature and treated with RNase A [100 μg/ml]. Cells were stained by adding propidium-iodid (PI) [50 μg/ml] or 4`, 6-diamidin-2-phenylidol (DAPI) [1μg/ml] and incubated for 20 min. Samples were then analyzed by flow cytometry.

The percentages of cells in G0/Gl, S, and G2/M phases of the cell cycle were determined by single-parameter histograms of DNA content. Apoptotic cells were distinguished from normal cells by their fractional DNA content, as revealed by a sub-G0/G1 peak in DNA content in the histogram (Nicoletti et al., 1991).

3.4.7. Wound healing and 2D invasion assay

For in vitro real-time mobility assays, the IBIDI Culture-Inserts System was used. The respective cell-culture inserts were placed on a cell-culture surface, and the A549 cells were then seeded in each well of Culture-Inserts at a density of 1×10^5 cells/ml. After incubation for 6 hours, the Culture-Insert was removed, and a standardized 500 μm cell-free gap was created. Alternatively also a second migration assay was used. A549 cells were therefore seeded onto six-well plates and after 24 hours the cell layer was scratched once across the entire well using a pipette tip. The cells were subsequently washed with medium to remove cell debris and were then treated by irradiation or ion channel-blockers. Finally they were incubated in complete growth medium. The cell culture dish or the the 6-well plates were placed in an incubator, which provides constant temperature at 37 °C and 5% CO_2. Inverted microscopes equipped with digital cameras (Juli, Smart Fluorescence Cell Imager for culture dishes Axiovert 10, Zeiss, digital camera DMK 41BF02 for 6-well plates) inside the incubation chamber allowed a monitoring of serial images of cell movement. To determine the migration path and cell front velocity of cells in the cell-free gap region, video movies were analyzed with appropriate image analysis software (TScratch, ETH Zürich, Swiss). The net migration distances were obtained by comparing the initial and final positions over 48 hours.

3.4.8. Statistical analysis

Data are expressed as means ± standard deviations of at least three different experiments. Significance was estimated by using the Student's t-test. A $P < 0.05$ was considered as significant.

3.5. Results

A previous study has reported that gamma irradiation results already at very low doses in an increase in the conductance of a K^+ outward rectifier in A549 cells (Kuo et al., 1993). To further examine the molecular mechanism of this rise in channel activity and the impact on

the cellular response to radiation we conducted the same kind of experiments but with different radiation qualities. In the initial experiments the currents of A549 cells were measured on a portable patch clamp device, which was placed directly under an x-ray source. This allows monitoring of currents in a single cell before and directly after irradiation.

3.5.1. Electrophysiological characterization of the epithelial lung cancer cell line A549

To interpret alterations in the electrophysiological behavior of A549 cells in response to stressors like irradiation it is crucial to first characterize the ensemble of endogenous ion-channels in these epithelial lung cancer cells. Endogenous potassium channels play an important role in epithelial cells such as A549 cells for stabilizing the membrane voltage and for maintaining the driving force for the electrogenic transport of Na^+ and Cl^-. Also the release of K^+ into secreted fluids is an important function of these channels. The typical ensembles of K^+ channels in the lung are voltage-gated ion-channels such as Kv1.1, Kv1.3, Kv4.2 and also ATP- or Ca^{2+}-dependent ion-channels. Even though also Cl^--channels are ubiquitously expressed in lung cells and functionally important in this epithelial tissue, there is currently not much known about the molecular nature of their Cl^--channels. It is only known that the cystic fibrosis transmembrane regulator (CFTR) is the most dominant Cl^--channel in the lung (Sheppard & Welsh, 1999; Warth et al., 1999).

In Fig. 5 the typical current responses of an A549 cell recorded under the prevailing experimental conditions are shown. Measurements were conducted with an extracellular concentration of 4 mM K^+ and an intracellular concentration of 50 mM KCl and 60 mM K-fluoride. The data show that the typical current response to voltage steps can be divided into two kinetically different components, an instantaneous activating (I_{inst}) and a time dependent (I_{td}) conductance.

The corresponding current/voltage (I/V) curve for both current components shows that the instantaneous current carries the main part of conductance.

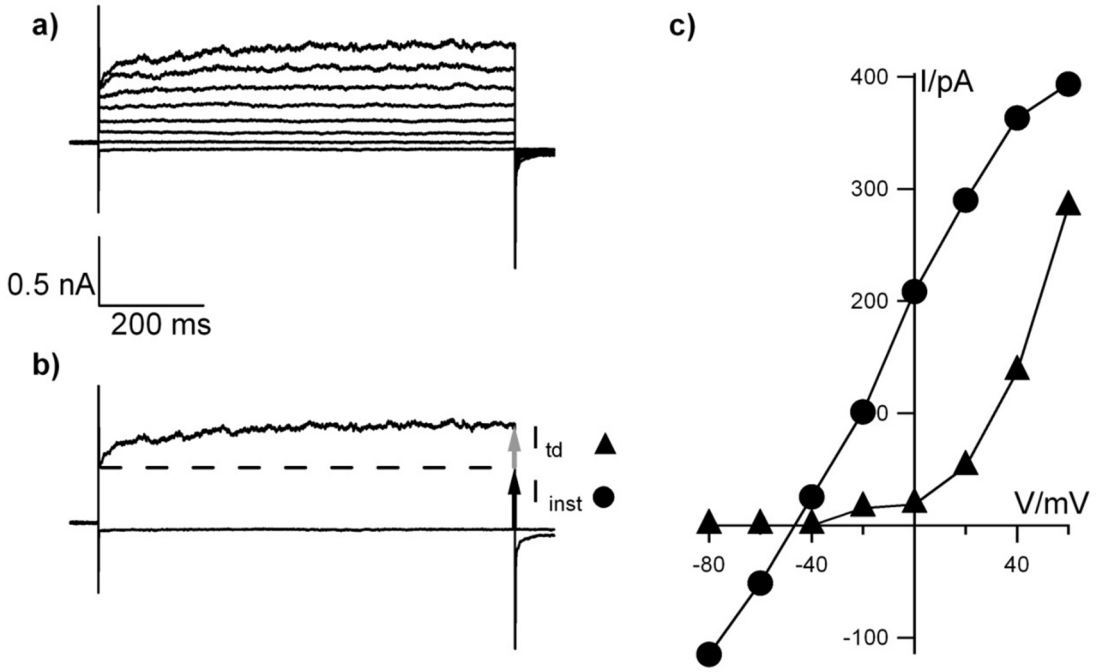

Fig. 5 Current/voltage relation of A549 cells.

Data show the current response of an exemplary A549 cell to a standard pulse protocol from a holding voltage (-60 mV) to test voltages between −80 mV and +60 mV in 20 mV steps (a). Currents, which are elicited by positive voltages here 60 mV, can be decomposed into two kinetically different components: an instantaneous activating conductance and a slow activating outward conductance (b). Instantaneous and steady-state currents were sampled after 5 ms and at the end of the voltage step (usually 800 ms) respectively. The corresponding current/voltage (I/V) relation of the two current components is shown in c. Currents were measured in an external buffer with 4 mM K^+.

To test whether the endogenous currents in A549 cells are carried by K^+, currents were measured with different external K^+ concentrations. Elevating the external K^+ concentration from 4 mM to 40 mM significantly decreased the amplitude of the outward currents by 67% at +40 mV. After a tenfold increase in KCl concentration the reversal voltage of the I/V relation was shifted by 50 mV towards positive voltages (Fig. 6c). The positive shift of the reversal voltage together with the lower outward current with a reduced chemical driving force for K^+ indicates that the outward currents of A549 cells are carried mainly by K^+; from the Nernst equation a positive shift by 57 mV would have been expected if the conductance were only determined by K^+.

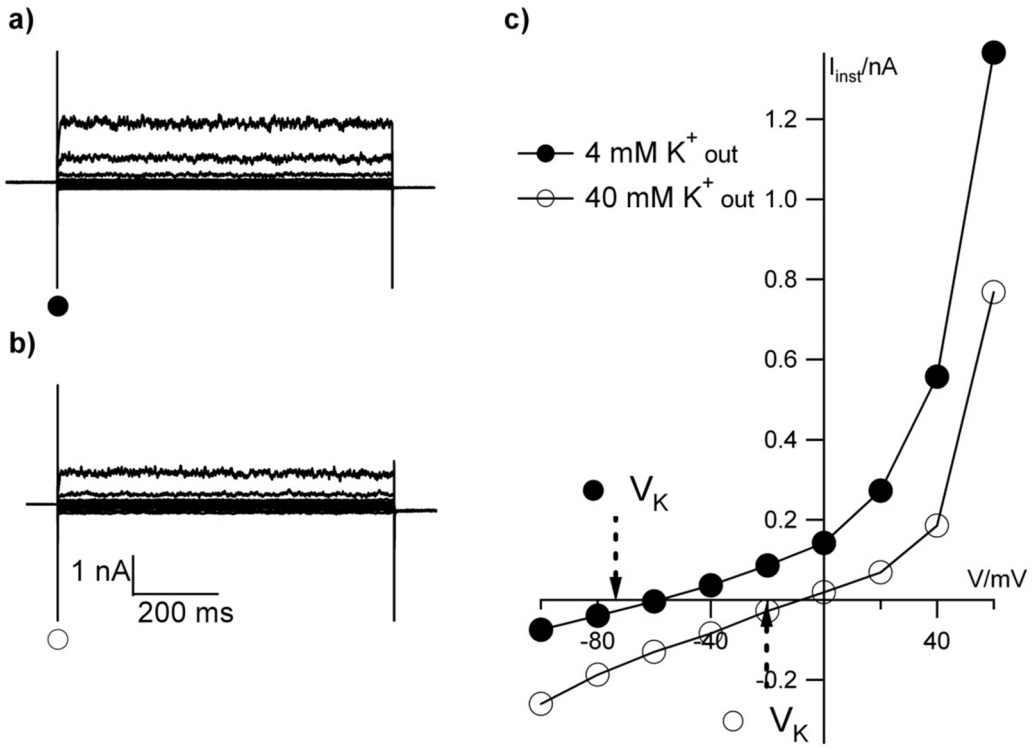

Fig. 6 Endogenous currents in A549 cells and their relationship to different transmembrane K^+ gradients.

(a,b) Representative current traces of one A549 cell recorded with different K^+ concentrations in the external buffer; currents were recorded as in Fig. 5 but with test pulses between −100 mV and +60 mV.(c) The I/V-relationships of the instantaneous activating currents in 4 mM (filled circles) and 40 mM $[K^+]_o$ (open circles). Instantaneous currents were sampled after decay of transient capacitive current 5 ms after onset of voltage step. The arrows indicate predicted K^+ Nernst-voltage (V_K) for the two measuring conditions. The K^+ Nernst-voltage for the different solutions was calculated by using K^+ activities (Robinson, R.A. and Stokes, 1965).

In order to further specify the contribution of K^+ currents to the two conductances, we replaced in the same cell the permeable K^+ in the internal solution by the impermeable Cs^+ (50 CsCl, 60 Cs-fluoride), a cation of the same valence. This should eliminate K^+ outward currents (Fig. 7). The results of representative experiments, in which currents were recorded with KCl and later with CsCl in the cytosolic solution show that the replacement of K^+ by Cs^+ causes a substantial reduction of the outward current and a positive shift of the reversal voltage. The data support the aforementioned conclusion that the outward rectifier is carried

by K^+ ions. The reduction of the instantaneous activating current implies that also this current must include K^+ channel activity.

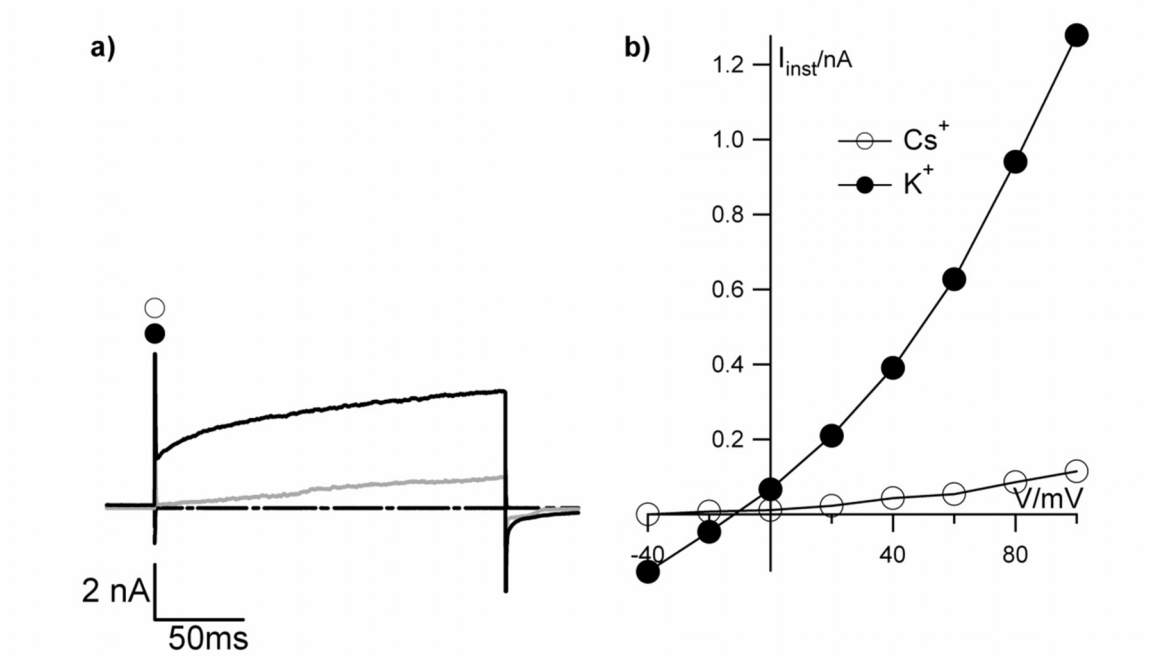

Fig. 7 Substitution of intracellular K^+ for Cs^+ abolishes currents in A549 cells.

(a) Current response of an A549 cell to steps from a holding voltage of -60 mV to a test voltage of 100 mV with K^+ (black line) and after replacing K^+ for Cs^+ (grey line) in the cytosolic buffer solution. The substitution of K^+ with the impermeable Cs^+ results in a strong reduction of membrane currents. The zero current value is illustrated by the broken line. (b) The I/V-relationships were obtained from the instantaneous activating currents at voltage steps from -40 mV to 100 mV indicated by arrow in (a) for measurements with $[K^+]_i$ (filled circles) and $[Cs^+]_i$ (open circles). Instantaneous currents were sampled after decay of transient capacitive current 5 ms after onset of voltage step.

Similarly, replacement of external Na^+ by N-methyl-d-glucamine (NMDG) should eliminate voltage–dependent sodium currents. Since replacement of Na^+ has in the exemplary experiments shown in Fig. 8 no appreciable consequences on the reversal membrane voltage and on the amplitude of I_{inst}, endogenous Na^+ channels in A549 cells can be neglected.

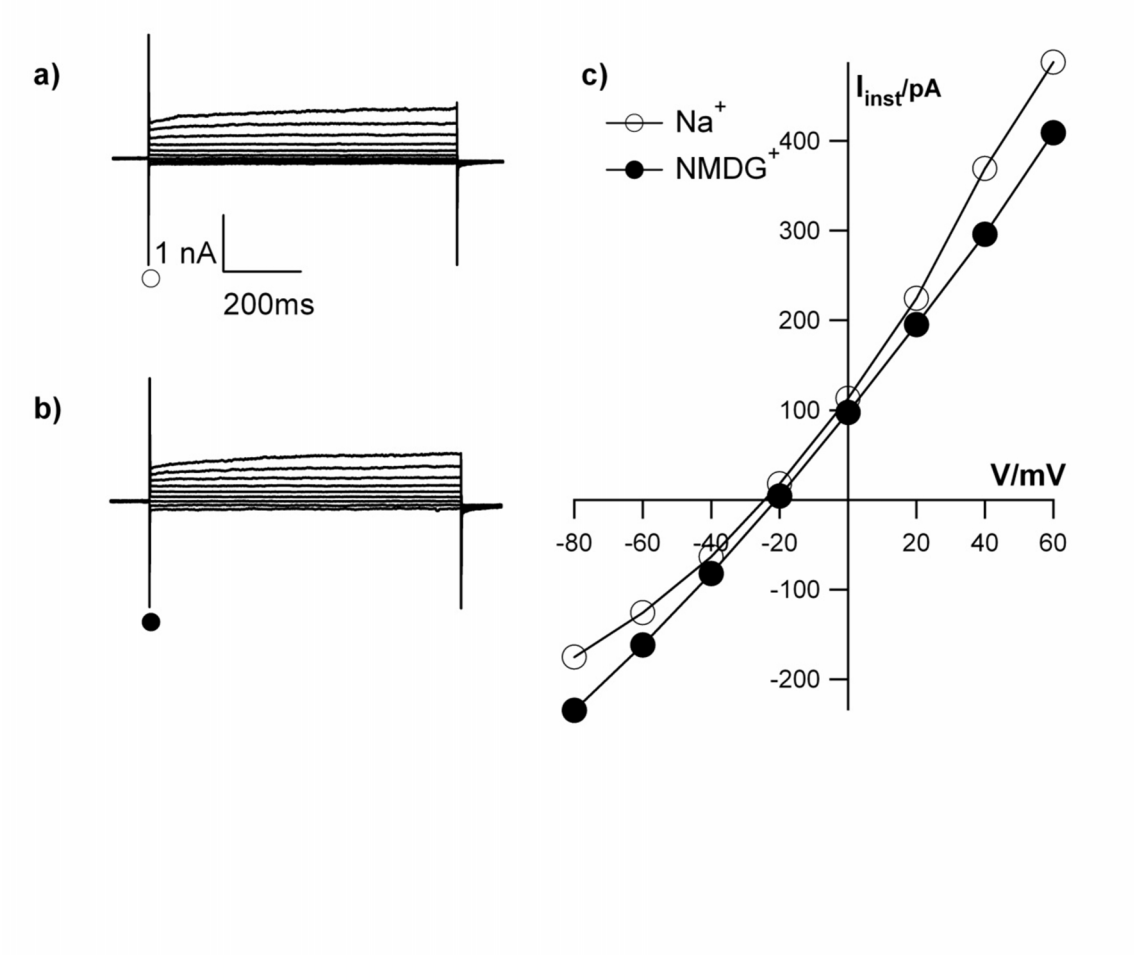

Fig. 8 Replacement of external Na^+ by NMDG has no perceivable effect on I/V relations in A549 cells.

Representative current traces obtained from standard voltage pulses from −80 to +60 mV in 20 mV increments with (a) $[Na^+]_e$ or (b) $[NMDG^+]_e$ in external buffer. (c) The I/V-relationships of the instantaneous current, with $[Na^+]_e$ (open circles) and $[NMDG^+]_e$ (closed circles). Instantaneous currents were sampled after decay of transient capacitive current 5 ms after onset of voltage step in an external buffer with 4 mM K^+.

In summary, it can be concluded that the conductance in A549 cells is under the experimental conditions mostly carried by K^+ ions. From the kinetics of the current responses to positive voltage steps it is apparent that at least two different K^+ channels contribute to the membrane conductance. One of these channels exhibits an instantaneous activation (I_{inst}) and the second a time dependent (I_{td}) activation. In order identify the molecular nature of the two K^+ channels we carried out further molecular biological experiments.

The presence of selected candidate ion-channel genes in A549 cells was confirmed by reverse transcription (rt) PCR (Fig. 9). The transcripts reveal the typical ion-channels, which are prominent in cancerous cells. This includes the human ether-a-go-go (hEAG) potassium channel, a protein with a role in cancer cell proliferation (Ouadid-Ahidouch & Ahidouch, 2008). Also the Human ether à-go-go related (hERG) ion-channel is present in A549 cells; this channel has been shown as a modulator of tumor progression (Jehle et al., 2011). Also transcripts of the voltage-gated, Shaker-related subfamily potassium channel Kv1.3/1.4 are detected; finally also the human intermediate conductance potassium channel (hIK) is present in A549 cells. The latter two channels were included into the screening by RT-PCR because their kinetics is reminiscent to those of the instantaneous activating endogenous K^+ channels detected in A549 cells.

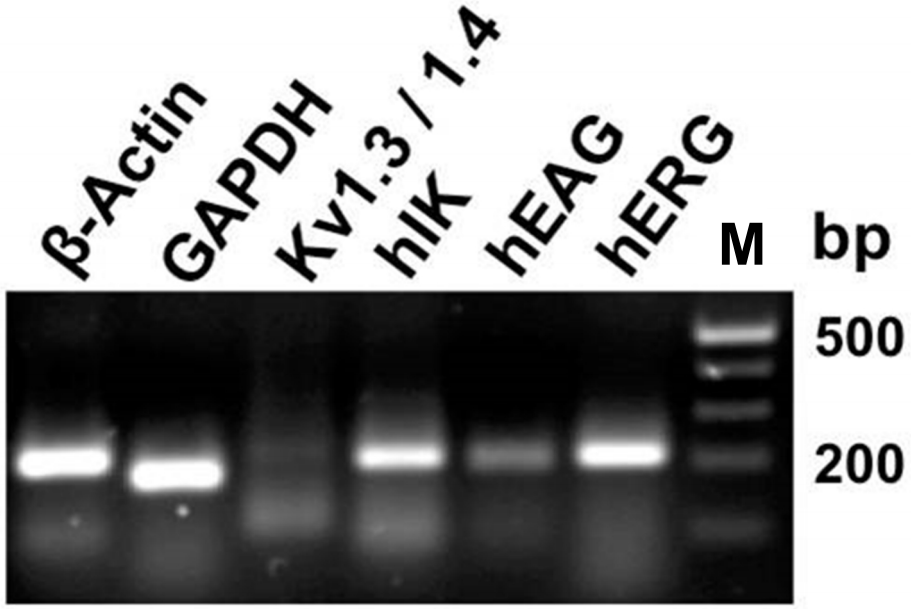

Fig. 9 RT-PCR of common ion-channels in A549 cells.

Total RNAs of A549 cells were reverse transcribed, followed by PCR using A549 cell cDNA and specific primers amplifying the Kv1.3/1.4 (216 bp), hIK (206 bp), hEAG (192 bp) and hERG (203 bp) potassium channel cDNA, as described. Amplified fragments were resolved by 2% agarose-gel electrophoresis and visualized by ethidium-bromide staining. M, molecular weight marker; Sample with GAPDH (181 bp) and ß-Actin (210 bp) were used as positive controls.

To further specify the K^+ channels, which are involved in the endogenous conductance of A549 cells, we used a selective blocker margatoxin (MGTX) at 1 nM. This blocker is very specific because it has at this concentration no effect on calcium-activated potassium channels

but inhibits Kv1.3 (Garcia-Calvo et al., 1993). The efficacy of this blocker on the endogenous current is shown in Fig. 10. The conductance shows after addition of the blocker a reduction of 61% at +60 mV and a shift of the free running membrane voltage 12 mV towards more positive voltages. Additionally the difference-currents at 40 mV (Fig. 10c), which was obtained by subtracting the currents in the presence of the blocker (Fig. 10b) from that in the absence (Fig. 10a), exhibits the characteristic kinetics of Kv1.3 with a slow activation and a c-type inactivation. The results of these data imply that Kv1.3 is active in A549 cells and that it contributes to the conductance at the free running membrane voltage.

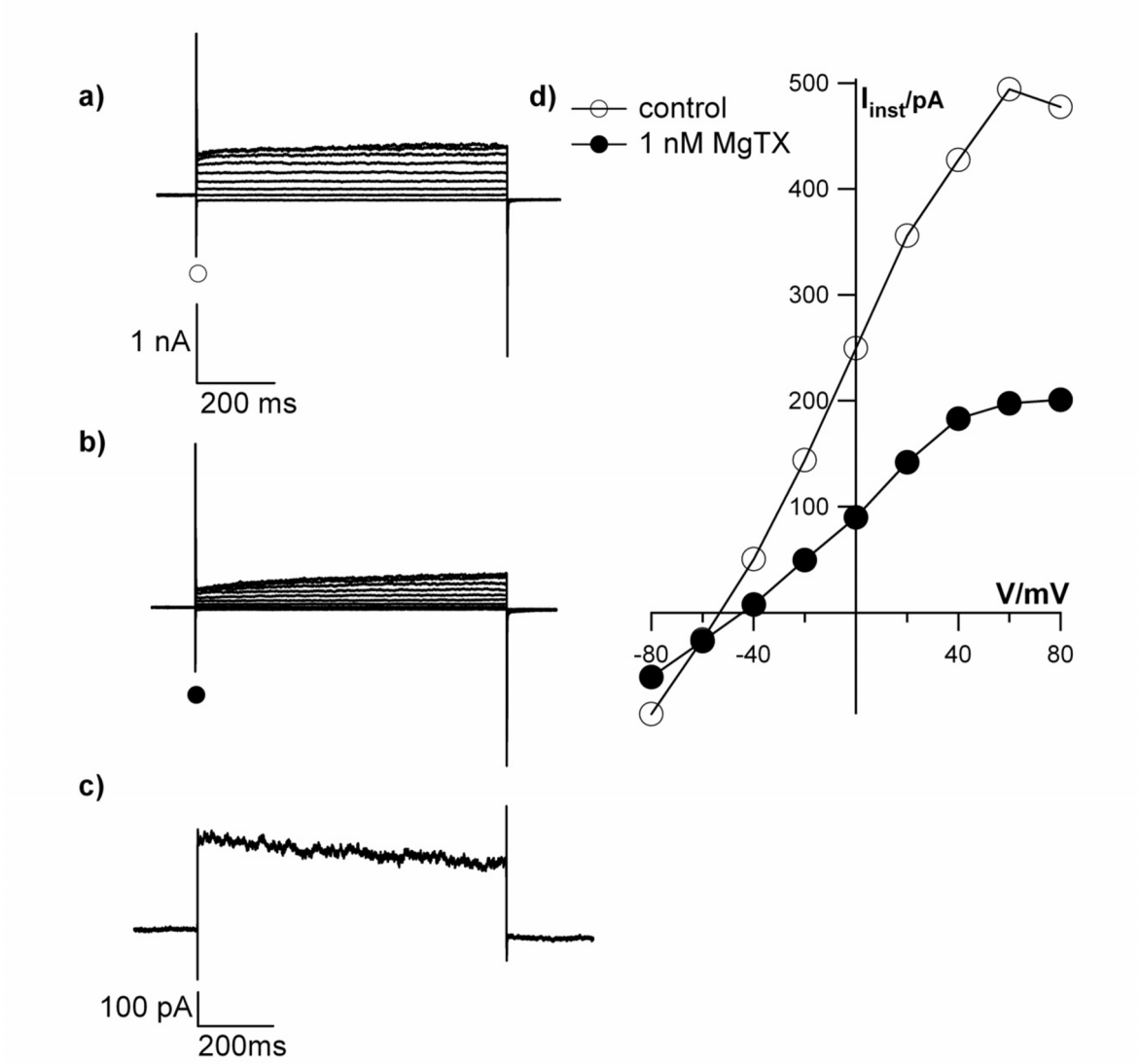

Fig. 10 The inhibitor margatoxin blocks a current with the kinetic feature of a channel with c-type inactivation.

(a,b) Representative current traces recorded to standard pulses from −80 to +80 mV in 20 mV increments before and after adding margatoxin [1nM]. The block of conductance leads to 61% reduction in current density and a shift of 12 mV in membrane voltage towards more positive values. (d) Shows the I/V-relationships of the instantaneous current with and without margatoxin [MgTX] was added at 1 nM (filled circles) to standard external solution (open circles). The currents shown in c) are the difference-currents obtained by subtraction of the MgTX blocked currents from the control currents obtained for a voltage step to 40 mV. Instantaneous currents were sampled after decay of transient capacitive current 5 ms after onset of voltage step in an external buffer with 4 mM K^+.

In order to test for the contribution of hIK channels to the endogenous A549 conductance, cells were treated with 10 μM of the drug clotrimazole (CLT); the inhibitor was added to the

bath medium (Fig. 11). CLT was tested because it is reported as a specific inhibitor of hIK type K^+ channels (Brugnara et al., 1996). Fig. 11 shows the currents of an A549 cell recorded before and after addition of CLT. I_{inst} was reduced by 89% at +40 mV (mean 72 ±19% n=18) by 10 μM CLT (Fig. 12). Together with the data on the expression of the hIK channel in A549 cells the results of these experiments underscore that I_{inst} is largely carried by this Ca^{2+}-activated K^+ channel. The data in Fig. 11 show that CLT also inhibits to some extend the time dependent current. An effect of CLT on Kv-type channels, which are responsible for the slow activating outward-rectifier, has only been reported for Kv1.5. Since Kv1.5 seems not to be expressed in A549 cells, the molecular nature of this slow-activating outward rectifier remains unknown.

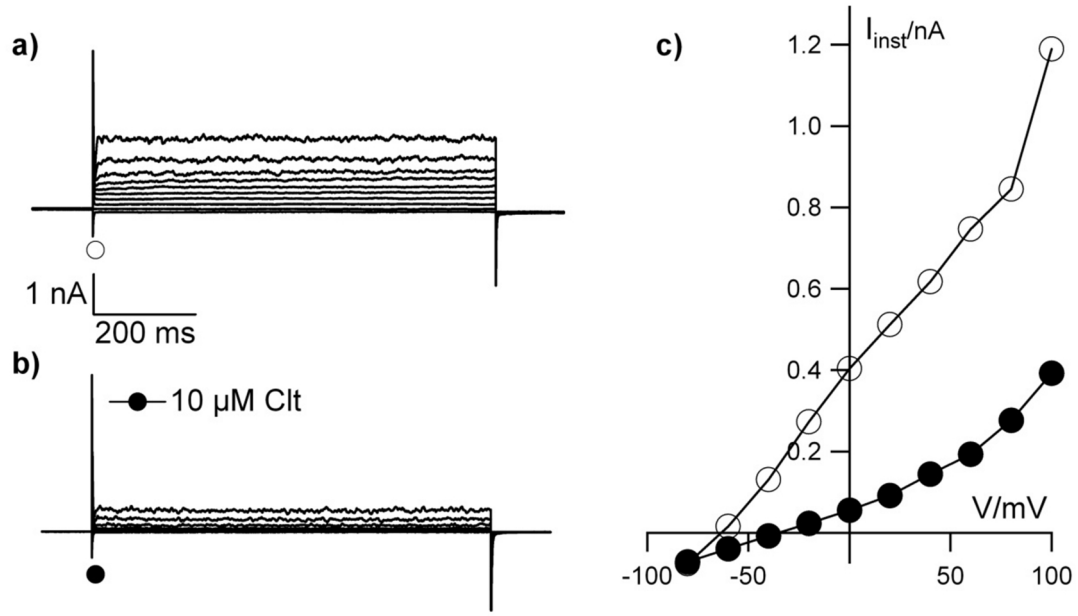

Fig. 11 The inhibitor clotrimazole generates a block of the instantaneous component in A549 cells.

(a,b) Representative current traces to standard pulses from −80 to +100 mV in 20 mV increments recorded before and after adding 10 μM clotrimazole. The block of conductance leads to 89% reduction in current density at 40 mV and a shift of 47 mV in membrane voltage towards more positive values. (c) Shows the I/V-relationships of the instantaneous current with and without clotrimazole. With $[CLT]_o$= 10 μM (filled circles), standard external solution (open circles).

While CLT generates in A549 cells an overall robust block, the data show a great variability between individual cells. The relative block can vary at a reference voltage of 40 mV from 28% to 95%. At this point it is important to mention that the activity of hIK channels is discussed in relation to the control of the cell cycle. It is known for example that an activation of hIK-channels is stimulating in MCF-7 cells the progression from G1- to S-phase (Ouadid-Ahidouch et al., 2004). It is further commonly accepted that cells control their progression through the cell-cycle with controlled excursions in the membrane voltage (Wonderlin et al., 1995). On the background of this putative function of hIK channels, we analyzed the membrane voltage distribution of a cell population of A549 cells. The data show that the free running voltage ranges in a population of randomly chosen A549 cells from -76 mV to -6 mV with a median at -23.7 mV ±21.9 mV (n=21 cells). From this we can assume that the A549 cells exhibit a rather heterogeneous distribution of membrane voltages. It is reasonable to assume that the variable membrane voltages reflect cells in different states of the cell-cycle. Together with the anticipated role of hIK channels in cell cycle control (Ouadid-Ahidouch & Ahidouch, 2008) it is possible that the heterogeneous response of cells to CLT reflects a difference in the background activity in the cells tested. To analyze this dependency we plotted the degree of CLT induced membrane depolarization as a function of the free running membrane voltage measured prior to addition of the inhibitor. The data in Fig. 12b clearly show a correlation between the resting membrane voltage and the ability of CLT to shift the membrane voltage as a consequence of blocking the hIK-channel. The data are consistent with the view that cells with a negative voltage have a high activity of hIK channels. As a consequence CLT has a strong effect on the membrane conductance and on the membrane voltage. In cells with a low membrane voltage the hIK channels are less active; the effect of the blocker is hence small.

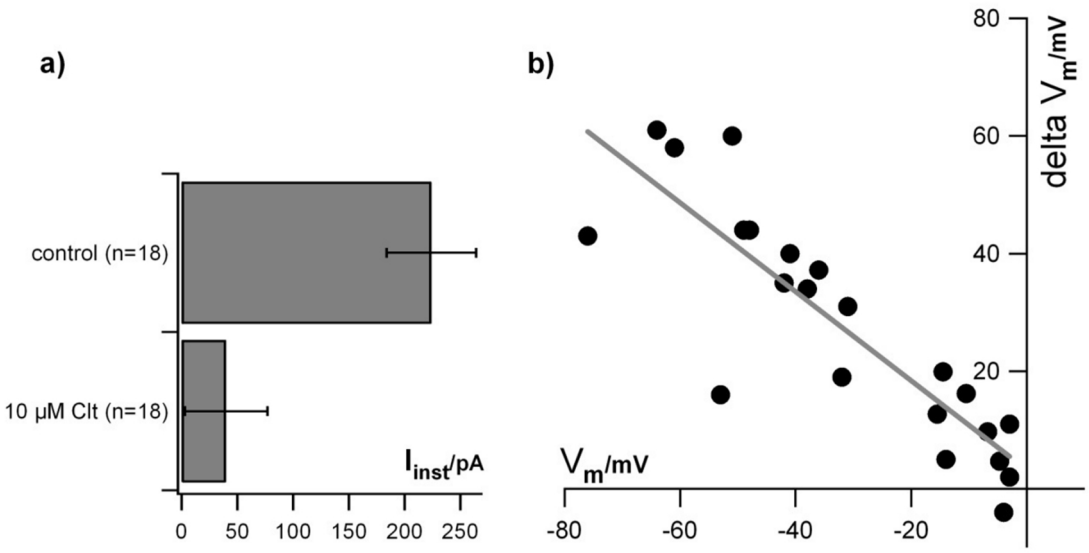

Fig. 12 Clotrimazole blocks the instantaneous outward current in A549 cells.

(a) 18 cells were measured at a holding voltage of +40 mV before (control) and directly after addition of $[10\ \mu M]_{ext}$ CLT. The conductance is blocked by 72 ±19.9% in the presence of the inhibitor. The graph in (b) demonstrates the dependency of CLT induced shift of the membrane voltage on the resting membrane voltage in A549 cells prior to treatment.

It has been reported that CLT is not entirely specific for hIK channels; it also blocks some voltage dependent channels such as Kv1.5 at higher concentrations (Iftinca et al., 2001) and leads to side-effects by its high affinity for cytochrome P450-dependent enzymes (Wulff et al., 2001). Therefore we conducted the same experiments as in Fig. 11 with 1 μM TRAM-34. TRAM-34 is an analog of CLT and blocks the hIK channel with a Kd of 20 nM; it is extremely selective for the hIK channel (Wulff et al., 2001). In A549 cells the inhibitor had a strong effect on the instantaneous conductance at 20 mV (mean 65 ±35% n=7) by 1 μM TRAM-34 leaving the slow outward conductance mostly unaffected (Fig. 13). Hence the presence of TRAM-34 sensitive hIK channels is very dominant in A549 cell.

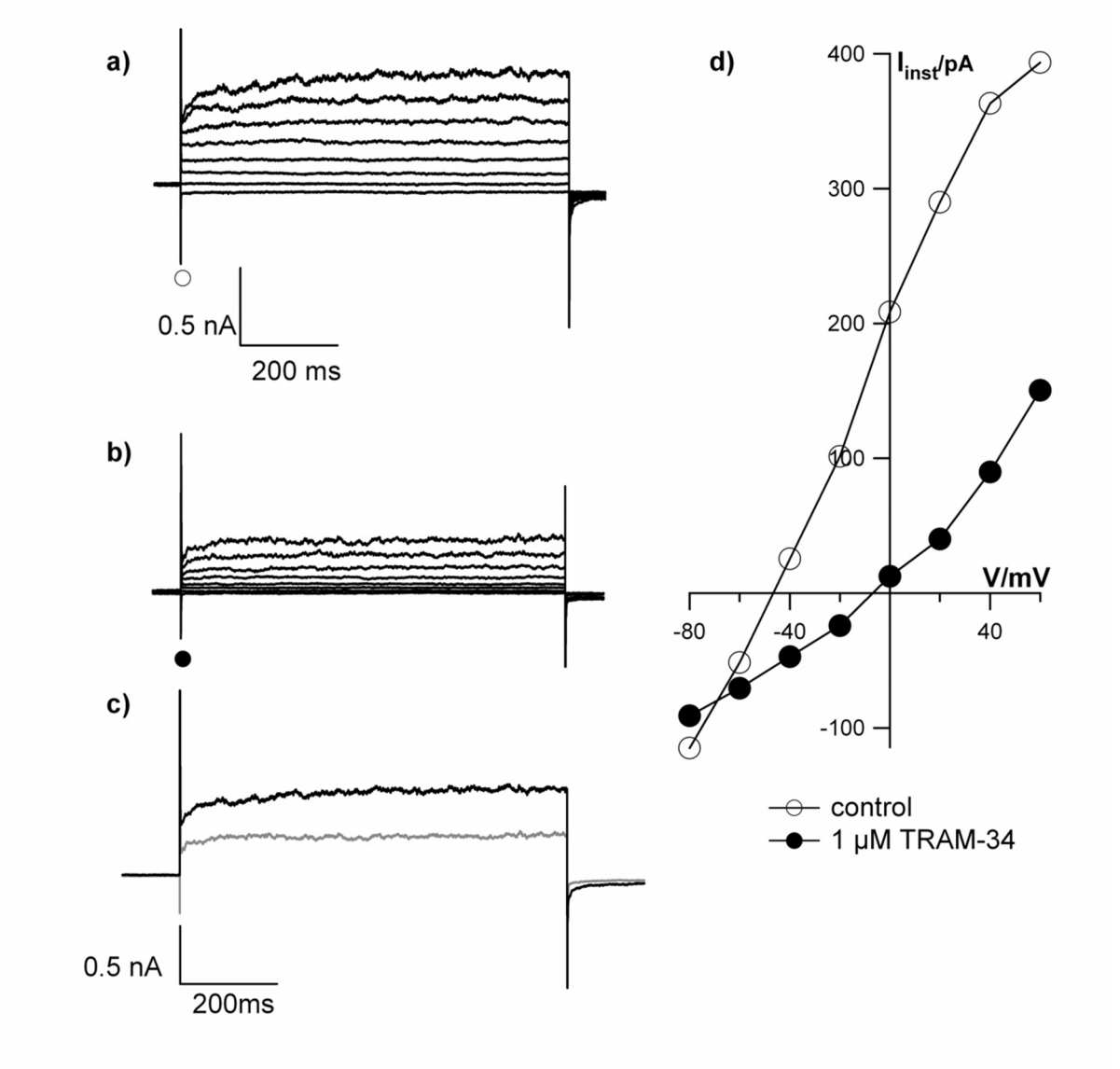

Fig. 13 The inhibitor TRAM-34 generates an even more specific block of the instantaneous component.

(a,b) Representative currents of an A549 cell recorded in absence and presence of 1 μM TRAM-34. Standard pulses from −80 to +60 mV in +20 mV increments were applied. The blocked conductance leads to a reduction of 67% at +60 mV in current response (c) and a shift of 38 mV in membrane voltage towards more positive values. (c) The I/V-relationships of the instantaneous current without (open circles) and with 1 μM TRAM-34 (filled circles).Instantaneous currents were sampled after decay of transient capacitive current 5 ms after onset of voltage step in an external buffer with 4 mM K^+.

The data so far show that A549 cells contain hIK channels, which can be blocked by CLT and TRAM-34. The variable response to the blocker and the variable membrane voltages in A549 cells suggest that these channels are not by default always active. To test this assumption, cells were treated with 1-ethyl-2-benzimidazolinone (1-EBIO), an opener of epithelial Ca^{2+}-

dependent K^+-channels (Pedersen et al., 1999). A typical result of an experiment is shown in Fig. 14. In this case 1-EBIO [100 μM] was added to a cell with a low conductance and a low resting voltage. After adding the channel opener, the conductance of the instantaneously activating current increases; as a consequence the membrane hyperpolarizes towards the K^+ Nernst-voltage (Fig. 14). The activated current could then be again blocked by adding 1 μM TRAM-34 (mean 82 $\pm$20% n=3) at +20 mV.

The result of this experiment further underlines the presence of hIK channels in A549 cells. Additionally there are evidences that the hIK channel activity is dependent on the cell-cycle phase. They furthermore show that they can be activated and that this activation results in a hyperpolarization of the cells.

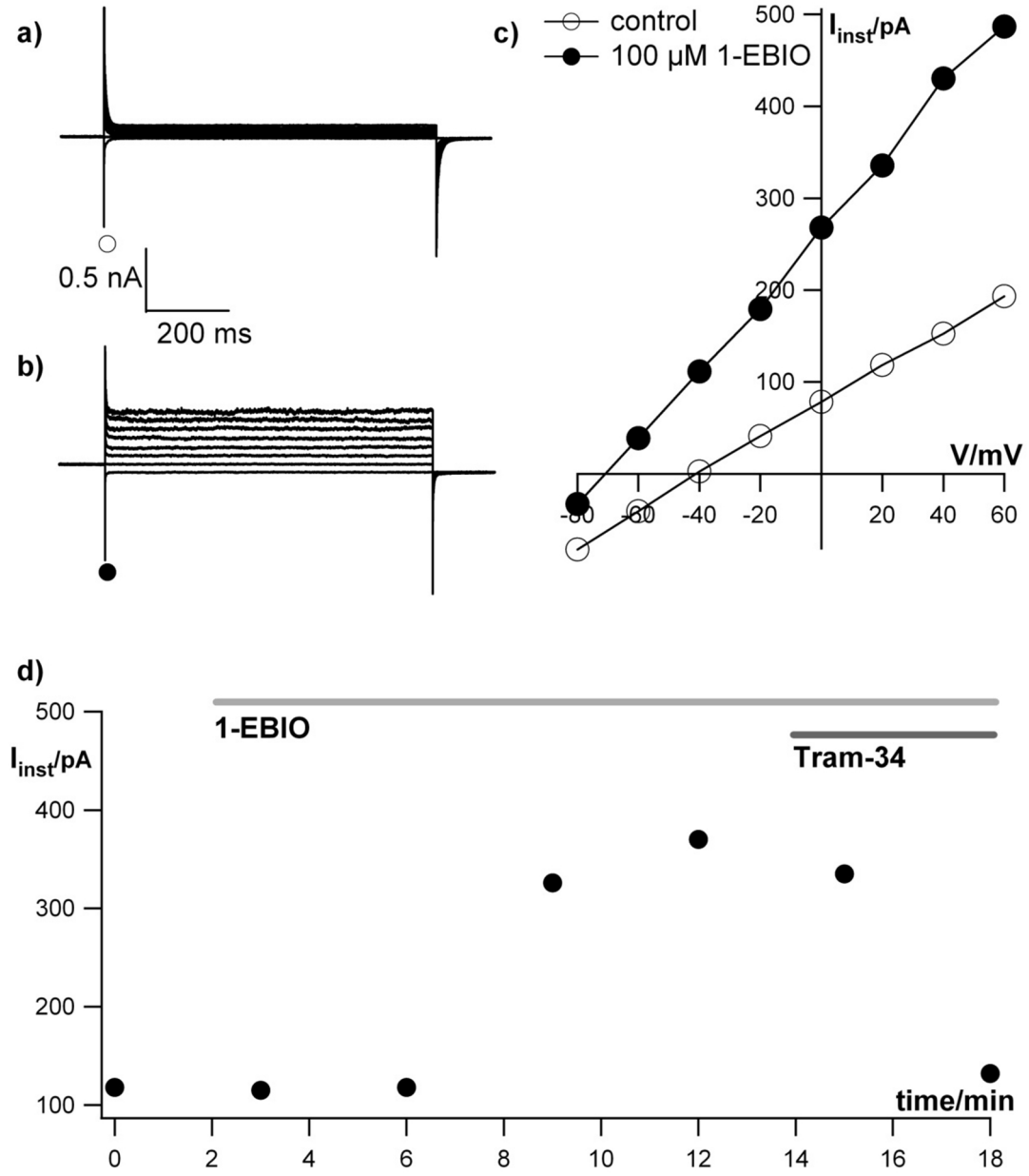

Fig. 14 Activation of the instantaneous current by 1-EBIO in A549 cells.

Current responses of A549 cell to a standard pulse protocol from −80 to +60 mV in 20 mV increments before (a) and (b) after the addition of 100 μM 1-EBIO to the external solution. The corresponding current/voltage (I/V) relations (c) of instantaneous currents in absence and presence of 1-EBIO show an increase in conductance and a shift of the membrane voltage in negative direction. (d) Time course of I_{inst} at 40 mV in 3 min interval after addition of modulators to the external medium. The perfusion time with 1-EBIO [100 μM] and TRAM-34 [150 nM] is illustrated with bars on top. Instantaneous currents were sampled after decay of transient capacitive current 5 ms after onset of voltage step.

The hIK channels are activated by $[Ca^{2+}]_{cyt}$ (Ouadid-Ahidouch & Ahidouch, 2008). To examine the dependency of the hIK channels in A549 cells, the Ca^{2+} ionophore ionomycin [1 μM] was added to the external medium. In the presence of extracellular Ca^{2+}, ionomycin induced a current activation by 115 ±31.3% (n=4). The exemplary data in Fig. 15 show that I_{inst} is significantly increased in A549 cells. These findings are a further evidence for the view that I_{inst} in A549 cells is a Ca^{2+}-dependent ion-channel, which can be activated at voltages between -40 mV and +60 mV.

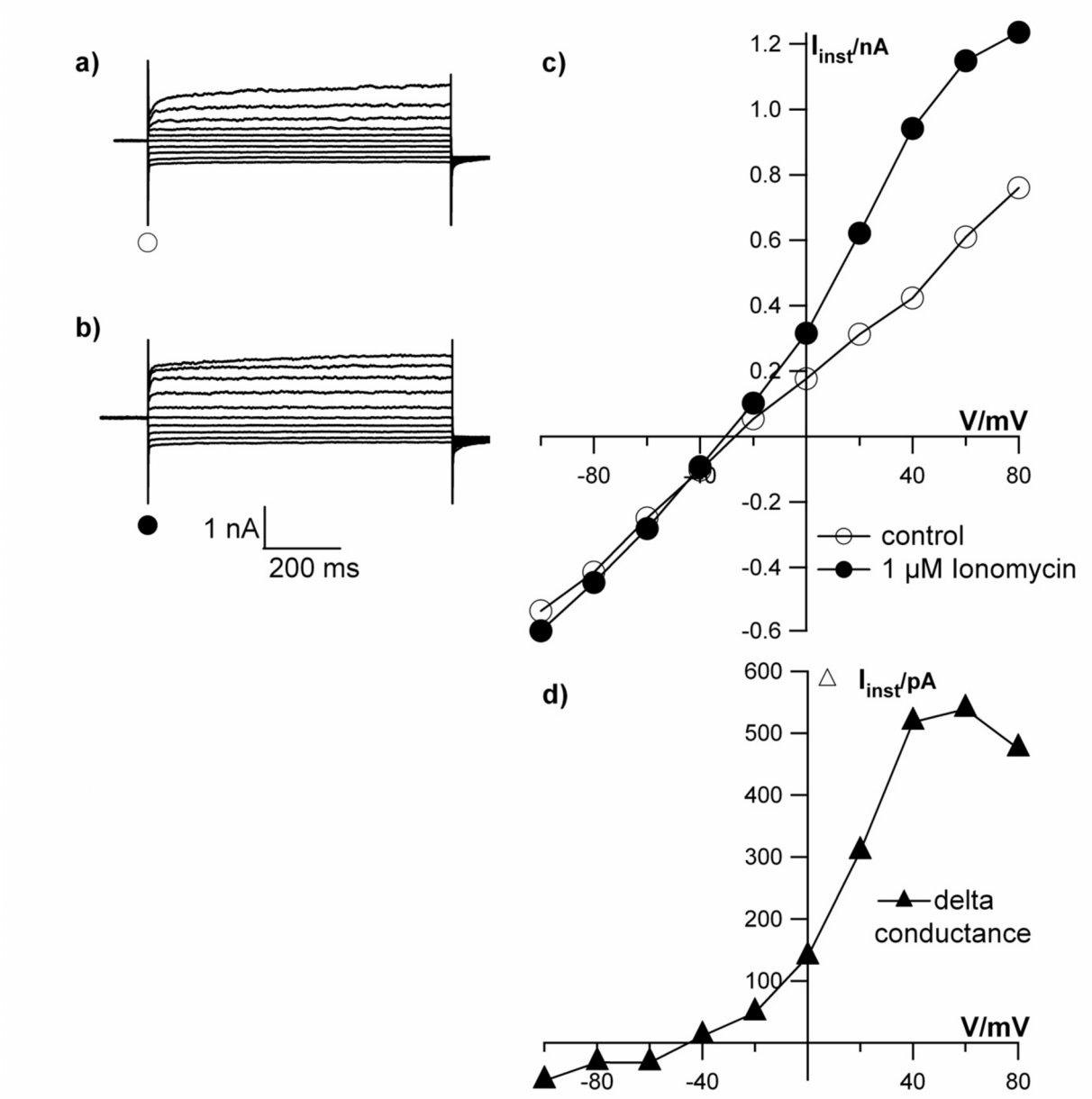

Fig. 15 Ca^{2+} ionophore ionomycin causes in A549 cells an increase in I_{inst}.

(a) Current traces of the same A549 cell in the absence (a) and presence (b) of ionomycin [1 μM]. Currents were elicited by voltage pulses from -100 mV to +80 mV in 20 mV increments. The resulting I/V-relations for I_{inst} were measured at the beginning of voltage pulses after relaxation of capacitive transient in the absence (open circles) and presence of 1 μM ionomycin (closed circles). The difference current shown in (d) represent the ionomycin induced current; data were obtained by subtracting the control current from that recorded in the presence of ionomycin. Currents were measured in an external buffer with 2 mM $CaCl_2$ and 4 mM K^+.

The experiment reported in Fig. 16, in which the hIK channel was activated in a voltage ramp protocol, shows that the same conductance, which is induced by 1 μM of ionomycin, is again blocked after adding CLT [10 μM] to the external solution (Fig. 16a). The results of these experiments imply that an increase in the concentration of cytosolic Ca^{2+} activates CLT sensitive hIK channels.

The time course of the currents at +40 mV (Fig. 16e) shows that the calcium dependent hIK conductance can be detected within a few seconds after addition of the ionophore (Fig. 16e). The rise in Ca^{2+}-activated current (Fig. 16b) is accompanied by a negative shift of the membrane voltage from - 18 mV to - 51 mV; this shift towards the K^+ Nernst-voltage (-85.1 mV) is expected as a consequence of an activation of a K^+ conductance. After blocking the hIK current with clotrimazole (Fig. 16a) the membrane depolarizes 28 mV towards positive voltages. The results of these experiments indicate that an elevation of $[Ca^{2+}]_{cyt}$ has activated CLT sensitive channels. The persistence of a hyperpolarized membrane voltage furthermore indicates that also other non CLT sensitive channels were activated by this treatment. To analyze the contribution of the hIK channels to the overall ensemble of Ca^{2+}-activated current in A549 cells we analyzed the current/voltage difference relation. For this purpose the current measured in the presence of clotrimazole was subtracted from that recorded in the presence of ionomycin. The resulting difference current should reflect the current voltage relation of the CLT-sensitive channels in these cells. A scrutiny of the respective difference current shows that it exhibits the typical features of hIK currents reported in the literature (Pedersen et al., 1999). The reversal voltage of the difference I/V relation is at -66 mV, a value close to the expected K^+ Nernst voltage for hIK (Fig. 16c). The data show that the hIK conductance is indeed contributing to the total Ca^{2+} activated conductance; in the present experiments it conducts at +40 mV ca. 59% to the Ca^{2+}-activated currents.

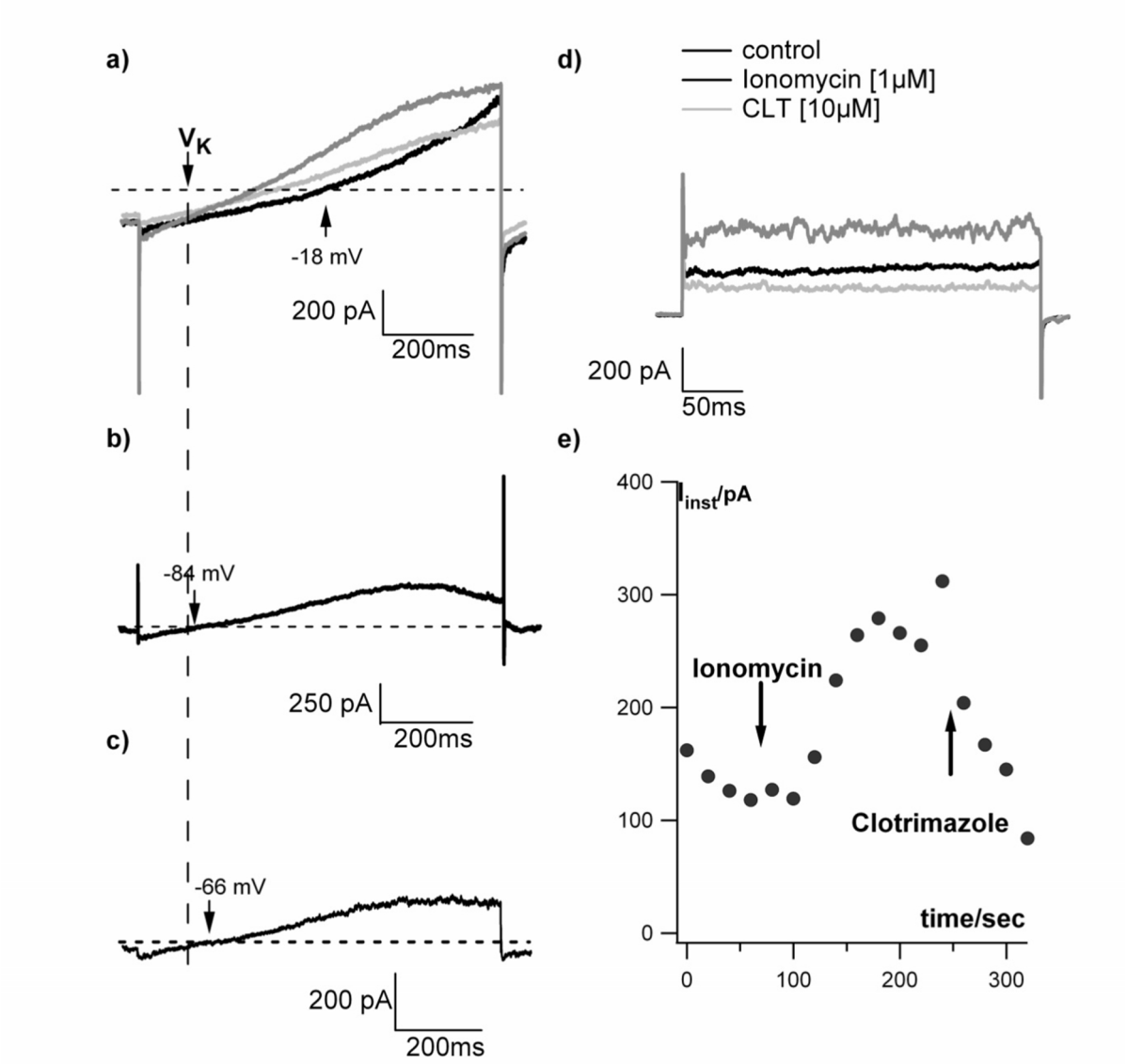

Fig. 16 hIK channels contribute to the calcium-activated currents in A549 cells.

Currents of an A549 cell were measured in the whole-cell configuration with a ramp protocol; the voltage was continuously increased by 0.25 mV/ms from a holding voltage of -100 mV to 100 mV. The data in (a) show the current before and 2 min after adding ionomycin $[1\mu M]_{ext}$ to the external bath. A third curve was obtained 3 min after adding CLT $[10\mu M]_{ext}$ on top of the ionophore, to the external buffer solution. The difference current shown in (b) represent the ionomycin induced current; data were obtained by subtracting the control current from that recorded in the presence of ionomycin. To isolate the hIK conductance the current measured in the presence of CLT was subtracted from that in ionomycin (c). The hIK current obtained from this procedure reverses at -66 mV; the estimated Nernst voltage for K^+ is -85.1 mV. The K^+ Nernst voltage for the different solutions was calculated by using K^+ activities (Robinson and Stokes 1965). The data in (d) show the current response of an A549 cell to voltage steps from -80 mV to 40 mV before and 2 min after adding ionomycin $[1\mu M]_{ext}$ and finally 3 min after adding CLT $[10\mu M]_{ext}$ on top of the ionophore. The time-course in (e) shows the current-response of one A549 cell at +40 mV in 20sec interval before and after

addition of the modulators. The addition of ionomycin [1 μM]$_{ext}$ and CLT [10 μM]$_{ext}$ is indicated by arrows.

3.5.2. Influence of ionizing irradiation on the electrophysiological behavior of the epithelial lung cancer cell line A549

X-ray irradiation

To examine the effect of x-ray radiation on the two K^+ conductance the I/V relations of individual A549 cells were measured before and after irradiation with 1Gy X-ray.

In control experiments we first conducted measurements of individual A549 cells on an x-ray tube. A 5 cm plump-shield was used to fully protect the cells from radiation. In this situation we could not detect any appreciable effect on operating the x-ray on the conductance of the A549 cells tested (Fig. 17). This indicates that the measuring condition and the electronics of the X-ray tube have no impact on the A549 conductance.

In long-term recordings with non-irradiated cells it occurred that the conductance slowly decreased with time. Fig. 17 shows a typical example of a plumb shielded control cell over a period of ca. 13 min; over time the currents relax gradually. This phenomenon is most likely caused by a rundown of KCa3.1 channel activity in ATP-free internal solution (Gerlach, 2000).

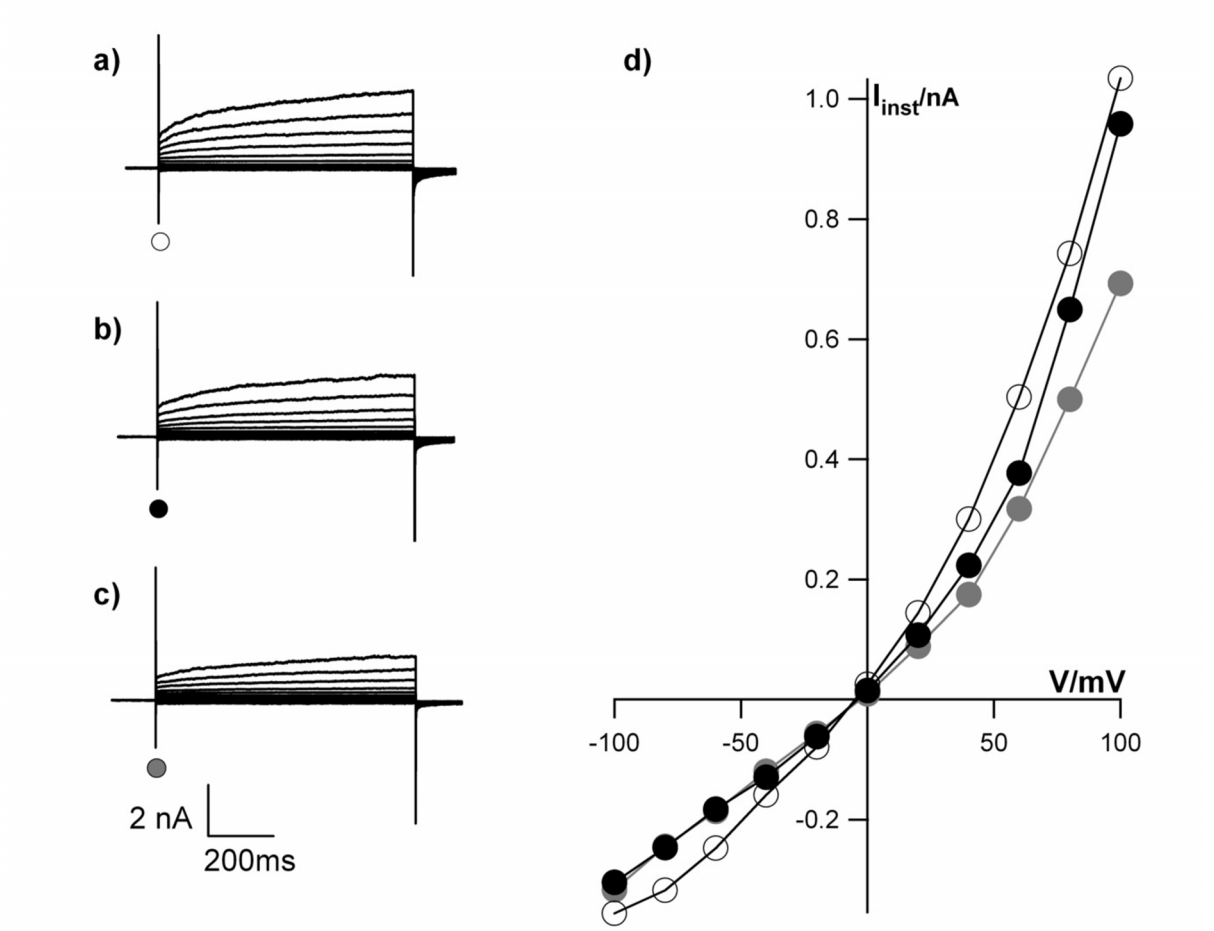

Fig. 17 Sham-irradiated cells show a slight decrease in current.

Current response of an A549 cell to voltage steps from -100 mV to 100 mV (a) 5 min before and (b) 4 min or (c) 8 min after 1 Gy x-ray sham-irradiated cells. The cell was protected from x-rays by a 5 cm thick plump shield. The resulting I/V-relations of the instantaneous currents (d) were measured at the beginning of voltage pulses after relaxation of the capacitive current (labeled by the markers). Currents show a slight reduction over time. Currents were measured in an external buffer with 4 mM K^+.

Fig. 18 reports a representative example of an A549 cell, which responds to x-ray exposure. The exemplary current responses taken before and 8 min after irradiation with 1 Gy x-ray are shown in Fig. 18a, b. The currents and the corresponding I/V relations of the different current components reveal that mostly the instantaneous conductance increases in response to 1 Gy x-ray. In some cells we could also observe an increase in the slow conductance component (Fig. 18b, d). In the context of the aforementioned characterization we can assume that irradiation augments two types of K^+ channels including hIK-type K^+ channels, which makes up a major part of I_{inst}. A close scrutiny of the I/V relation in Fig. 18c of a responsive A549 cell shows that

this treatment also has a profound impact on the free running membrane voltage; irradiation causes a hyperpolarization in the responsive cells.

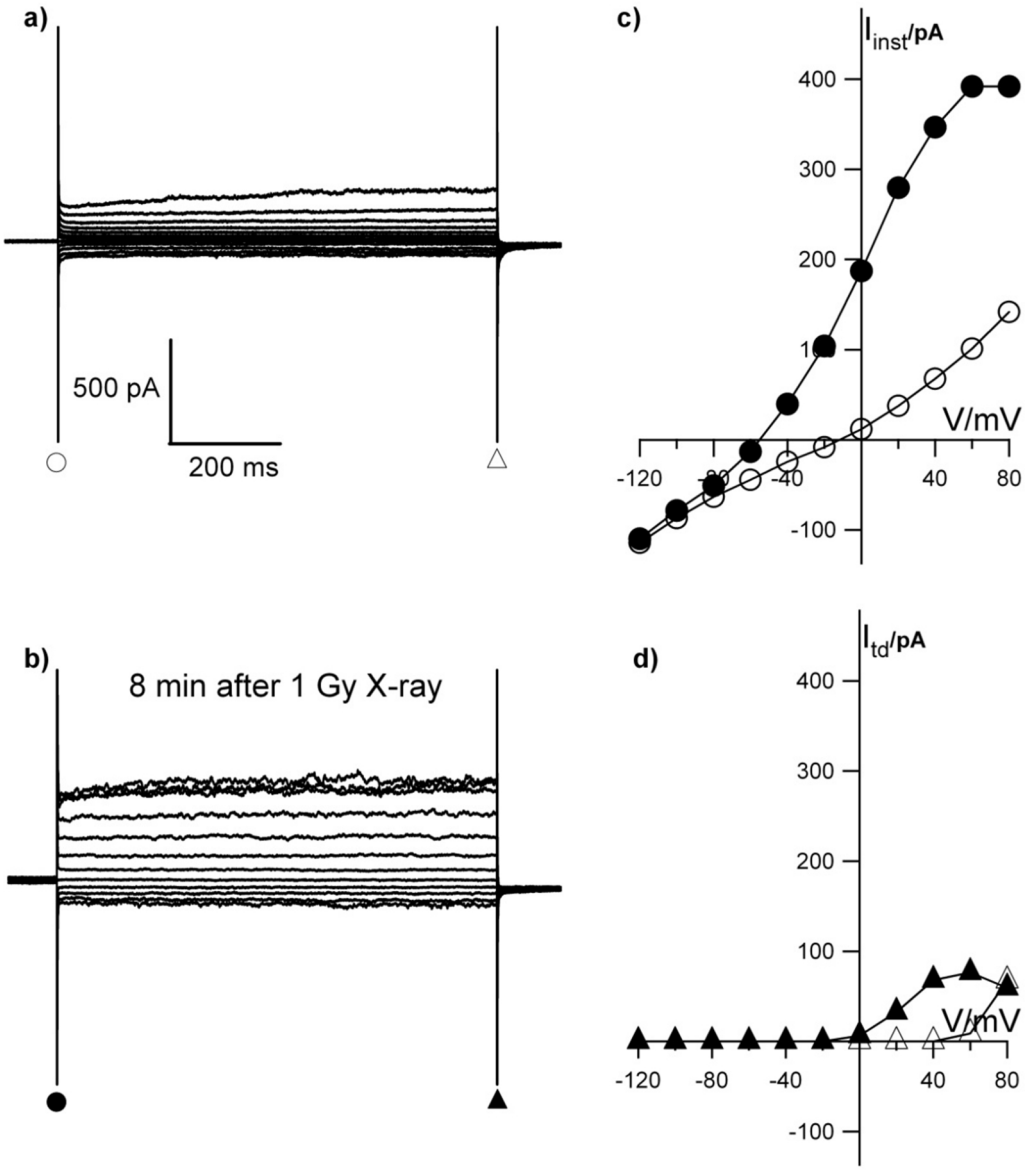

Fig. 18 Effects of ionizing irradiation on membrane currents in A549 cells.

Current traces were obtained as in Fig. 17 1 min before (a) and 8 min after (b) exposing the same cell to 1 Gy x-ray. Standard pulses from −120 to +80 mV in 20 mV increments were applied. The resulting I/V-relations of the instantaneous (c) currents were measured at the beginning of voltage pulses after relaxation of the capacitive current (labeled by the markers). The time-dependent (d) currents were obtained from steady-state current after subtracting the instantaneous currents. The time of data collection for the steady-state current is labeled by triangles. Currents were measured in an external buffer with 4 mM K^+.

A time course of the normalized instantaneous conductance recorded before and after treatment reveals that the effect of radiation is very fast (Fig. 19). Already 4 min after irradiation with 1 Gy x-ray the instantaneous activating K^+ conductance is increased over the pretreatment level. The same kind of increase in K^+ conductance has been observed in 42% of a total of n=48 cells tested under these conditions. The remaining cells were completely insensitive to the treatment.

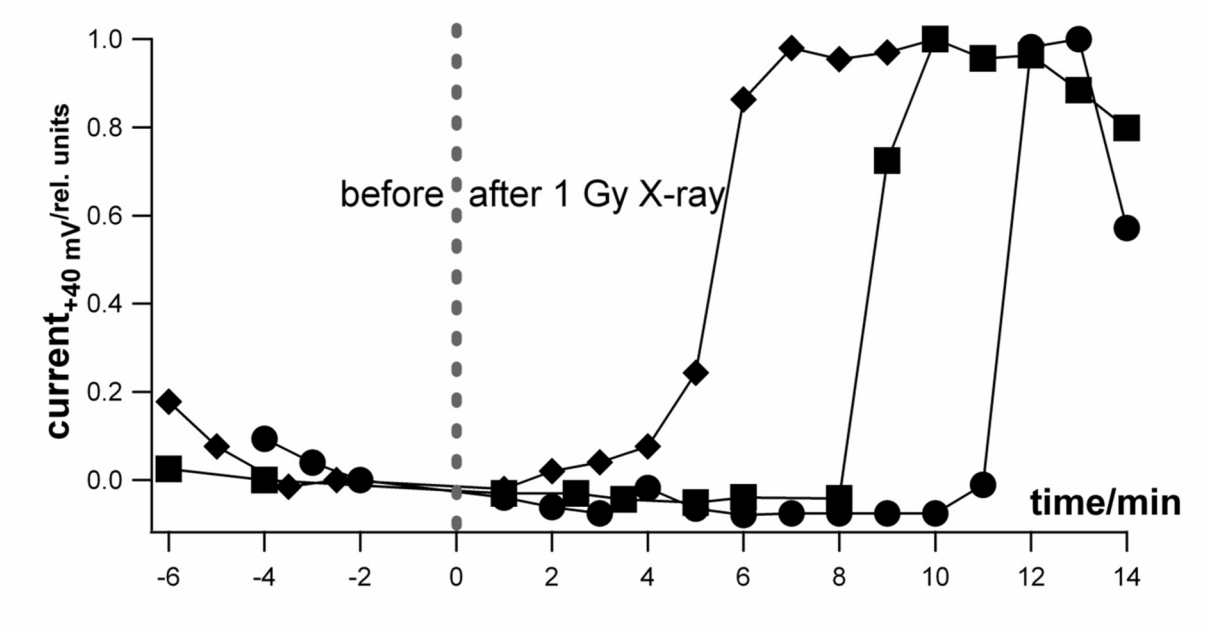

Fig. 19 Time-course of radiation induced changes in membrane currents in A549 cells.

The current-responses were recorded as in Fig. 18 in three different A549 cells before and after irradiation with 1 Gy x-rays. I_{inst} at +40 mV recorded before and after irradiating with 1 Gy x-ray (at 0 min) were normalized to the current measured before and the maximum after irradiation.

In the population of responding cells, it occurred that 1 Gy caused a maximal 19-fold and 3-fold increase of the instantaneous current (I_{inst}) and time dependent current (I_{td}) over the pre-treatment currents respectively (Fig. 20b). Hence the rapid activating K^+ conductance is affected more by radiation than the slow activating K^+ channels. Again the sham-irradiated control cells show a continuous relaxation in current; this is presumably caused by a rundown effect.

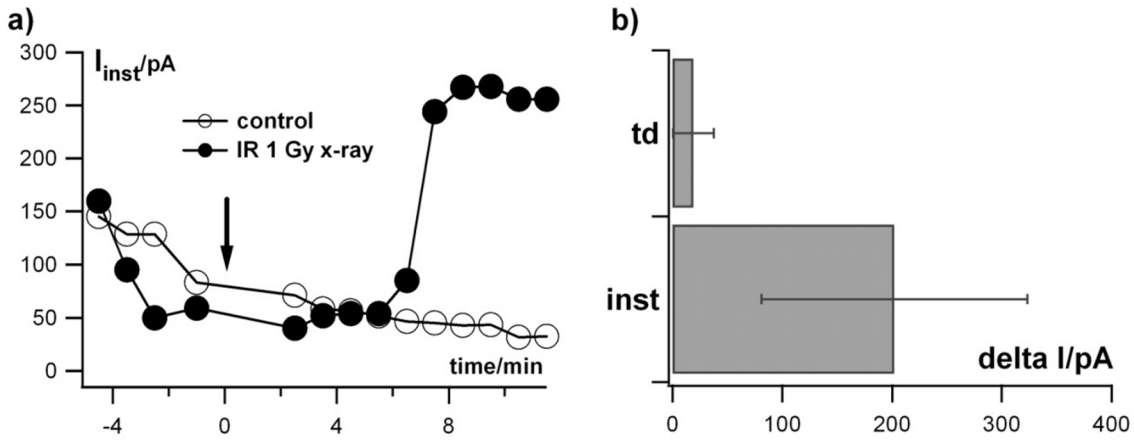

Fig. 20 Both conductances show an increase after ionizing irradiation.

(a) Shows the current responses of two A549 cells at +40 mV over time. One of the cells was irradiated at t=0 with 1 Gy x-ray (closed circles) the other remained un-irradiated (open circles). The plot in (b) shows the average ±SD increase of the time-dependent current (td) and instantaneous current (inst) at +20 mV ≥5 min after irradiation with 1 Gy x-ray of n=8 cells.

Mainly because of the increase in instantaneous K^+ conductance the cells hyperpolarize after irradiation; the elevated K^+ conductance shifts the free running voltage closer to the K^+-Nernst voltage. In the responsive cells the free running membrane voltage hyperpolarized in n= 12 cells under the influence of x-ray [1 Gy] by an average of -25.85 mV ± 22.14 mV. A plot of the radiation evoked hyperpolarization as a function of the free running voltage measured prior to the treatment shows that the shift in voltage is largest when the cells are depolarized before treatment (Fig. 21); cells which exhibit already a negative voltage before irradiation show only little increase in membrane voltage. The results are consistent with the view that x-ray irradiation causes the highest effects in cells, which exhibit at rest a low K^+ conductance.

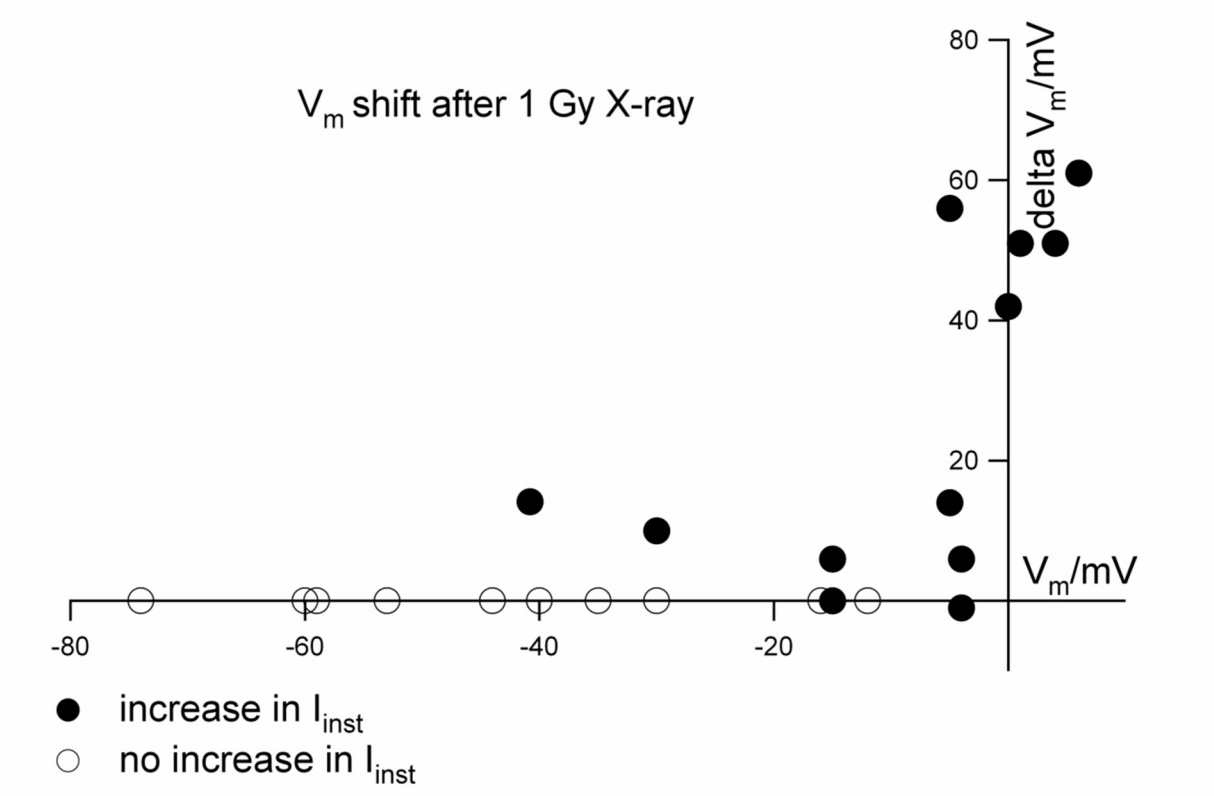

Fig. 21 Radiation induced hyperpolarization is largest when the cells were depolarized before treatment.

The scatter plot shows the difference in membrane voltage (delta Vm) of an A549 cell induced by irradiation of 1 Gy x-ray as a function of the resting membrane voltage prior to irradiation. Filled dots represent A549 cells, which showed an increase in instantaneous current. Empty dots display A549 cells, which exhibited no increase in current.

In order to test whether a block of the hIK channel could prevent channel activation by x-rays we treated populations of A549 cells before irradiation with 1 Gy x-ray with 10 μM clotrimazole $(CLT)_{ex}$, a blocker of hIK channels. Fig. 22 shows a plot of the mean current of A549 cells at +40 mV for three different treatments. The currents of 3 cells per treatment were measured at the same day in order to allow a direct comparison. The data show that I_{inst} was increased 3-fold at +40 mV over that of the control in response to irradiation. A pretreatment of A549 cells with CLT [10 μM] resulted in an I_{inst}, which was also after irradiation not larger than that of the control cells. These experiments indicate that irradiation leads to an increase in the instantaneous activating current, which is largely carried by the hIK-channel. The aforementioned variable response of individual A549 cells to irradiation does not yet allow interpreting these data as a proof for an involvement of hIK channel in the radiation response. However the experiment, which will be reported further down in Fig. 30

in which an irradiation induced increase in I_{isnt} can in the same cell be blocked by CLT, strongly supports this interpretation.

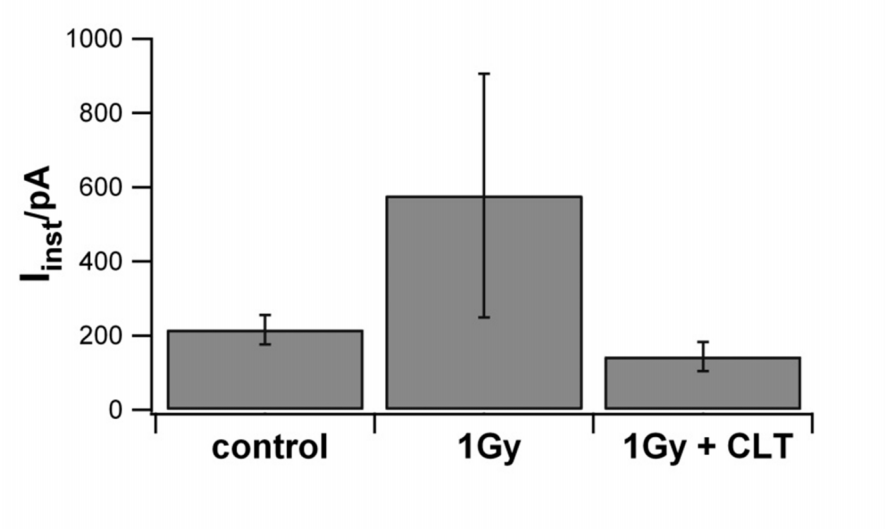

Fig. 22 A549 cells pretreated with clotrimazole show no IR evoked increase in conductance.

Average instantaneous current of A549 cells at +40 mV of untreated cells (control), cells treated by 1 Gy x-ray (1 Gy) and cells irradiated with 1 Gy x-ray after pretreatment with CLT [10 μM] (1 Gy + CLT) Data are mean ±SD of 3 cells.

It has been announced before that x-ray irradiation causes a hyperpolarization of the membrane voltage. This negative shift of the membrane voltage is similar to that observed with other modulators of the hIK channels. Some of these will be mentioned later in the text. To compare the effect of x-rays with other modulators the main effects of relevant treatments on the membrane voltage are summarized in Table 3. The table presents for comparison the final membrane voltage and the shift of the membrane voltage in a given treatment.

Table 3: Overview of modulator effects on membrane voltage in A549 cells

Modulator	'Shift in Vm'	'final Vm'	quantity
1-EBIO [100 μM]	-12.3 ±9.2 mV	-56 ±7.7 mV	n=3
H2O2 [100 μM]	-9.25 ±8.5 mV	-33 ±10 mV	n=11
X-ray [1 Gy]	-25.9 ±22 mV	-35 ±19 mV	n=12
TRAM-34 [1 μM]	26 ±18.7 mV	-17.9 ±16 mV	n=7
CLT [10 μM]	27 ±19 mV	-4.5 ±11 mV	n=18
MGTX [1 nM]	12 mV	-42 mV	n=1

It has been mentioned before that only 20 out of 48 cells tested in this way responded to an exposure to x-rays with an increase in membrane conductance. To investigate whether this heterogeneous response is related to a variability of the cell population we examined the distribution of cells in the cell-cycle. It is well-known that the cell-cycle phases can have an impact on the function of certain ion-channels (Sundelacruz et al., 2009). To obtain an overview on the relative distribution of A549 cells in different states of the cell cycle we expressed the cell-cycle sensor FUCCI (Premo™) in these cells. The color of this fluorescent probe is cell cycle specific and allows a discrimination of cells in G0/G1-phase, G1/S transition and S, G2, and M phases. The representative image of A549 cells expressing this probe (Fig. 23) shows that this population of cells exhibits basically all states of the cell cycle. Roughly about half of the cells are in the G1/G0 phase the rest is in the remaining phases. To obtain more quantitative insights into the cell-cycle states of A549 cells we stained A549 cells with 4',6'-diamidino-2-phenylindole (DAPI) and estimated the distributions of different cell-cycle states by flow cytometry in n=4 experiments. This approach reveals information on the distribution of cells in the three major phases of the cycle namely G0/G1, S and G2/M. The A549 cells showed a stable cell-cycle distribution under control conditions (Fig. 23a). The major part of the cells was with 50 ±3% detected in the G0/G1-phase; 35 ±2% were in the S-phase and 15 ±1% in the G2/M-phase. The data show that the cells, which were irradiated, were not uniform. Interesting to note is that the distribution of cells in G0/G1 versus the other states is roughly the same as that of irradiation sensitive versus insensitive cells (Fig. 23b). 42% of cells responded to x-ray exposure with an increase in membrane conductance; 58% showed no significant response.

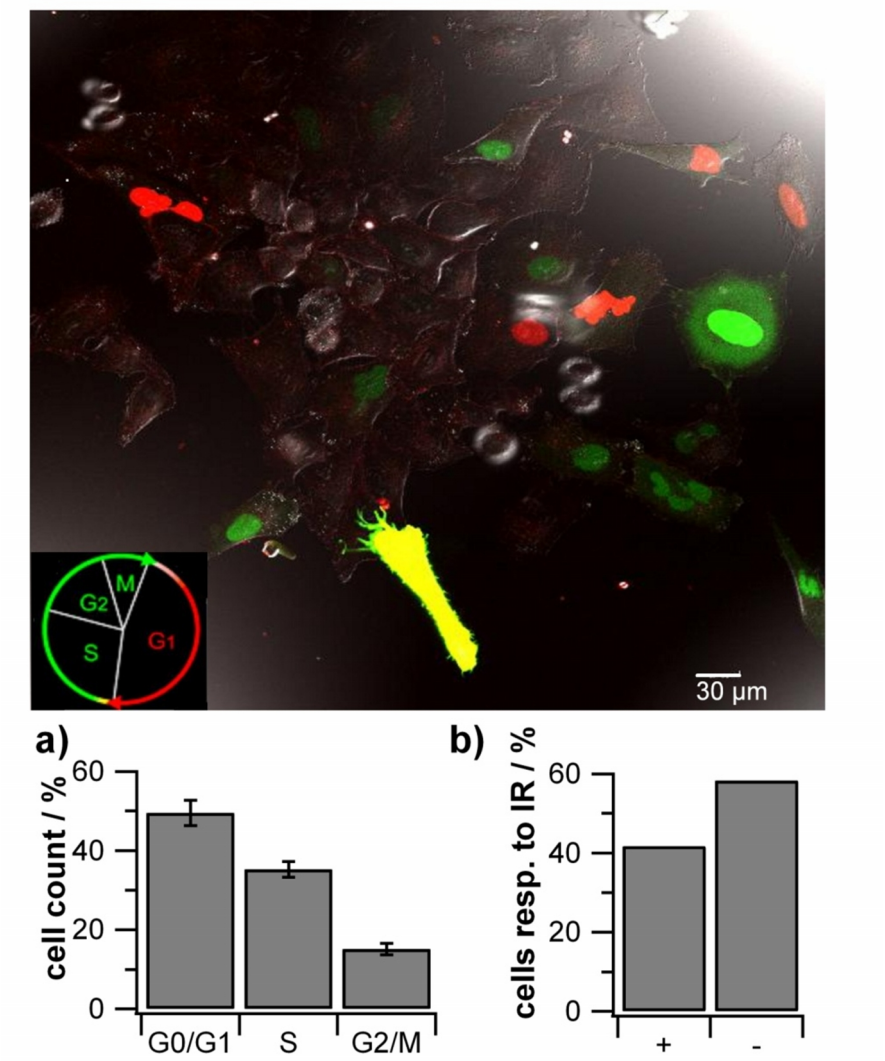

Fig. 23 Cell-cycle distribution shows a correlation with response to ionizing irradiation.

Overview-image of cell-cycle distribution in living A549 cells with Premo™ FUCCI Cell Cycle Sensor. Cells were transfected with Premo™ FUCCI Cell Cycle Sensor (top). The dynamic color change, from red via yellow to green, represents the progression through cell cycle. Mean percentage of A549 cells in G0/G1-, S- and G2/M-phase detected by flow cytometry of n=4 independent measurements (a). Overall statistic of live-measurements (b) of n=48 A549 cells tested. 42% showed an increase in conductance after irradiation of 1 Gy x-ray.

The same experiments as in Fig. 18 were repeated with different doses of x-ray radiation. Again at all doses tested about 58% of the cells were unaffected by the treatment. The remaining cells revealed a dose dependent increase in the two K^+ conductances. The plot in Fig. 24 illustrates the maximal increase in I_{inst} over the control in responsive A549 cells after treatment with different doses of x-ray. The relative rise in I_{inst} is measured as the difference

between the current at a reference voltage of +60 mV before and ≥ 4 min after stimulation; the plot shows that a half maximal activation of I_{inst} is achieved with as little as 0.11 Gy.

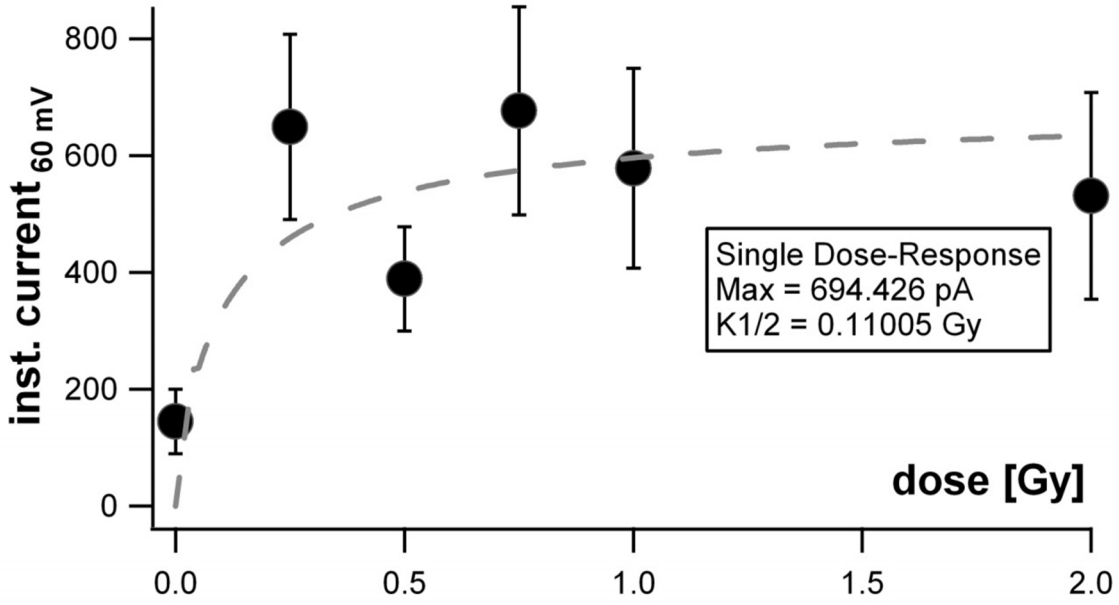

Fig. 24 The instantaneous conductance in A549 cells increases in a dose-dependent manner to ionizing irradiation.

A549 cells were measured before and after irradiation of different doses as described before. The different doses were achieved by varying the time of irradiation or the distance to the exit window of the x-ray tube. Each point shown is the instantaneous current at +60 mV of 4-12 cells at a given x-ray dose ±SD.

Heavy-ion irradiation

Next we wanted to examine whether the elevation of K^+ conductance in A549 cells is depending on the type of radiation. We therefore compared the effect of sparsely and densely ionizing irradiation on channel activity. Since for technical reasons we could not perform online measurements of cells in the course of heavy ion radiation we had to compare the effect on a population basis. For this purpose we measured I/V relations of A549 cells before and >30 min <60 min after radiation with x-ray or heavy ions. In all measurements on population basis the higher internal EGTA buffer concentration of 20 mM was used, because at that date it was not known that the irradiation effect on channel activity is $[Ca^{2+}]_{cyt}$ dependent. Fig. 25 shows the mean I/V relations recorded in A549 cells before and after exposure to 1 Gy x-ray. The results confirm the data obtained from the online measurements:

cells recorded soon after irradiation with 1 Gy x-ray reveal on average an elevated conductance over non-irradiated control cells from the same batch. The resulting conductance is the sum of an increased outward rectifier and an instantaneous activating K^+ current. A comparison of the two current components before and after x-ray treatment supports the aforementioned tendency in that the instantaneous component increases by about 10 pA/pF ± 3 and the slow component 13.8 pA/pF ± 6.5 after ionizing irradiation. Because of the elevated fast activating K^+ conductance we found also on a population basis an x-ray induced hyperpolarization of ca. 15 mV (Fig. 25).

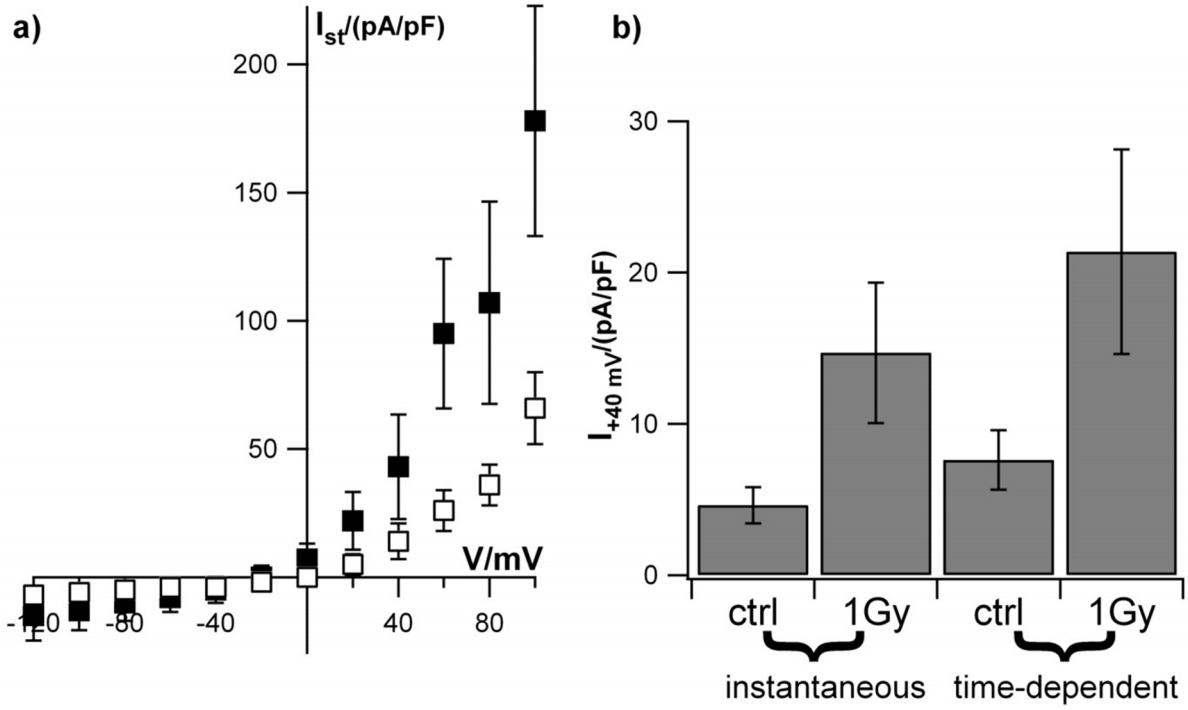

Fig. 25 Effects of x-ray irradiation on populations of A549 cells.

Mean steady state I/V relations in (a) of a population of A549 cells, which were (filled symbols) or were not (open symbols) exposed to irradiation with 1 Gy x-ray. Data were recorded as in Fig. 5. Currents of irradiated cells were measured ≥30 min after the treatment. Data are mean ± standard deviation of n=30 measurements of 6 individual experiments. To account for different cell sizes the currents were normalized to the membrane capacitance of the individual cell; the latter is an indirect measure of the cell surface. The plot in (b) compares the mean instantaneous and time-dependent current at +40 mV of non-irradiated control cells and of cells exposed to 1 Gy x-ray irradiation.

Using the same set up, we recorded I/V relations of A549 cells before and >30 min after exposure to heavy Fe and Ni ions of high and low energy. The response of cell populations

exposed to high energy Fe and Ni ions was similar to that obtained with x-ray irradiation; also heavy ion exposure causes a rise in the slow activating and in the instantaneous activating K^+ conductance. The effect of 7.5 Gy Ni ions on the membrane voltage causes a hyperpolarization towards a mean voltage of -31 mV ± 12 (n=4); control cells in contrast have a low mean voltage of -1.3 mV ± 6 (n=4). Even with the lower dose of 2 Gy Ni ions a negative shift of the membrane voltage towards -17 mV ± 9 (n=6) could be detected.

The plot in Fig. 27 illustrates the mean steady state current density at +40 mV of treated and untreated cells; the recorded currents of different cells were normalized to the membrane capacitance in order to account for differences in cell size. The effect of Fe ions on the membrane conductance was nearly identical to that measured with Ni ions. Cells irradiated with either Ni or Fe show an elevated conductance over that of non-irradiated control cells. The controls reveal an average current density at +40 mV of 12 ±2 pA/pF (n=18). After irradiation the value increases to 21 ±7 pA/pF (n=5).

The same types of experiments were also performed with low energy heavy ions. Because sparsely and densely ionizing irradiation has a different energy transfer they cause at the same dose a qualitative and quantitative different stress response in cells (Laverne & Laveme, 1996). For low energy particle beam irradiation it is important to know the target size. With this information it can be estimated whether all cells are transversed at least once by a particle. The mean cell diameter of an A549 cell is according to predictions from transmission electron microscopy (TEM) 14.93 μm (Jiang et al., 2010). Because the cells are approximately spherical we calculated a mean cell surface of 700 μm^2; the predicted irradiated area is about 350 μm^2. Because the particle impacts are Poisson distributed it is possible to quantify the hitting probability of a cell for different fluencies (4). The estimated probability for particle impacts in A549 cells for a heavy ion irradiation with Fe 9.8 MeV/u is shown in Fig. 26. It is obvious that the chance that a cell is not hit by a particle is very high when cells are exposed to a low dose such 2 Gy. To increase the probability of hitting a cell with at least one particle we used a fluency of $1.54 \cdot 10^6$ p/cm²; this corresponds to a higher dose of 7.5 Gy.

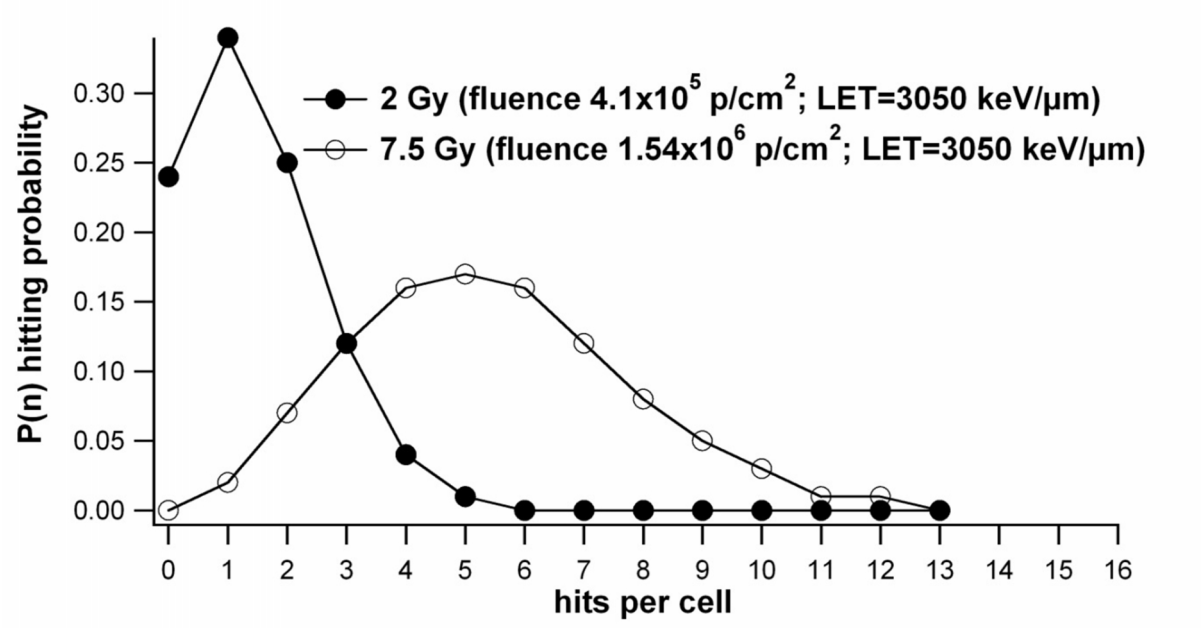

Fig. 26 Distribution of particle impacts in A549 cells as a function of different fluencies.

The graphs show the Poisson distribution for the hitting probability for low energy heavy ion irradiation with Fe 9.8 MeV/u. With 2 Gy (closed circles) nearly 25% of the cells are expected to evade a hit by a particle. With a dose of 7.5 Gy (open circles) the chance is very high that all cells are hit at least once.

The results of experiments, in which A549 cells were irradiated with low- and high-energy heavy ions are summarized in Fig. 27. The data show no apparent difference in the electrical properties of treated and untreated cells with low energy heavy ions. This implies that the response of A549 cells to heavy ion irradiation is depending on the energy in the sense that only exposure to radiation of ions with high energy generates the increase in K^+ channel conductance.

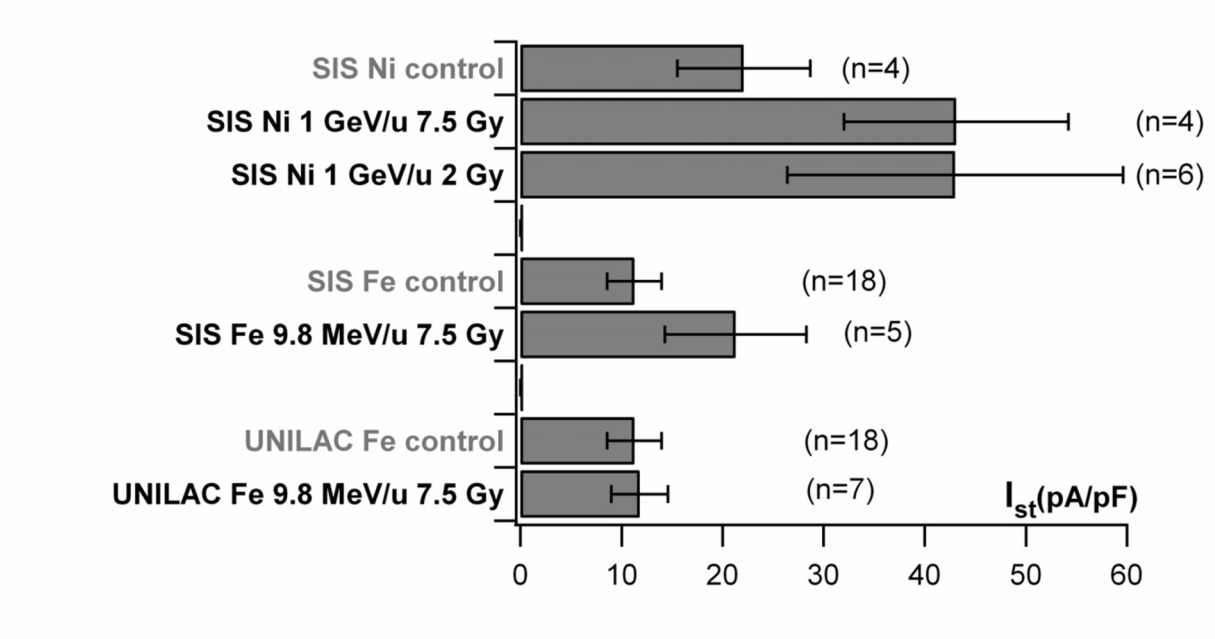

Fig. 27 The effect of irradiation on the membrane conductance of A549 cells depends on the type of radiation.

Mean steady state currents collected in A549 cells at +40 mV from populations of cells, which were or were not exposed to different types of heavy ion irradiation. The cells for the control and for the irradiation treatments were always from the same cell batch and measured on the same day. Irradiation was either administered from the "Universal linear accelerator" (UNILAC) or the "Schwerionen-Synchrotron" (SIS) at GSI at doses stated in the graph. Steady state currents were measured as in Fig. 5. To account for different cell sizes the currents were normalized to the membrane capacitance of the individual cell; the latter is an indirect measure of the cell surface. Data are means ± standard deviation of n cells.

Alpha-particles irradiation

In addition to low-dose radiotherapy, radon-therapy is a widely-used alternative cure of inflammatory diseases like Morbus-Bechterew, spondylarthrosis, osteochondrosis or eczemas (Zdrojewicz & Strzelczyk, 2006). But radon exposure is not only beneficial for human health; it also bears negative consequences when humans are exposed over long periods to alpha-particles emitted from radon (^{222}Rn). Also the daughter products of ^{222}Rn may cause health problems. This has been observed with uranium mine workers, which often developed lung cancers (Samet, 1989; Yao SX, 1994). The molecular mechanism of both the curative and the disease evoking effects of Rn remain so far unclear. A direct interaction of alpha particle with the DNA as for other sources of radiation can be excluded as the only explanation for ^{222}Rn effects. Alpha particles penetrate only over a very small distance into tissue and cells. Recent data suggests that alpha-particles cause DNA-damage by mechanisms, which are independent on a traversal of α-particle through the nucleus (Deshpande A, 1996; Nagasawa H, 1991). In

one study it has been shown that ROS levels were increased by 15% after 1 to 10 charged helium particles had traversed the cytoplasm of glioblastoma cells (Shao et al., 2004). These data are in good agreement with experiments of Narayanan and coworkers (Narayanan, 1997). They demonstrated that cells, which were irradiated by alpha-particles (0.4-19 cGy) exhibited an increase in ROS production; these occurred even without any direct nuclear hits by the particles (Narayanan, 1997). It has been reported that even sham-irradiated cells showed such an elevated concentration of ROS, when the cells were incubated with supernatants from irradiated cells. The results of these experiments advocate the idea that direct DNA damage is not required for eliciting cell-signaling cascades after low-dose irradiation; not only the nucleus but the entire cell should be considered as a target for radiation exposure.

In order to test whether the endogenous currents in A549 cells are affected by alpha-particles, we conducted whole-cell measurements before and after exposure of individual cells to an alpha source. Fig. 28 reports a representative example of an A549 cell, which responds to an exposure of alpha-particles with a rise in I_{inst} by 54%. The exemplary currents were measured immediately, and 3 min after irradiation with 12.5 cGy alpha-particle (3.66 MeV/u) (Fig. 28a, b). The currents and the corresponding I/V relations of the different current components reveal that again mainly the instantaneous conductance increases in response to the exposure of alpha-particles. In the context of the aforementioned characterization of the channels in A549 cells we can conclude that irradiation with alpha-particles augments the same types of K^+ channels as other sources of radiation. The rise of I_{inst} suggests that this also includes hIK-type K^+ channels. Out of 11 cells, which were tested in this way, n=5 responded to alpha-particle exposure with an increase in I_{inst}; on average I_{inst} increased at 40 mV in the responsive cells by 63.5 ±34%. There was no indication for a rise in the slow activating outward rectifier after alpha-particle treatment. Hence the rapid activating K^+ conductance is affected more by alpha-particle irradiation than the slow activating K^+ channels.

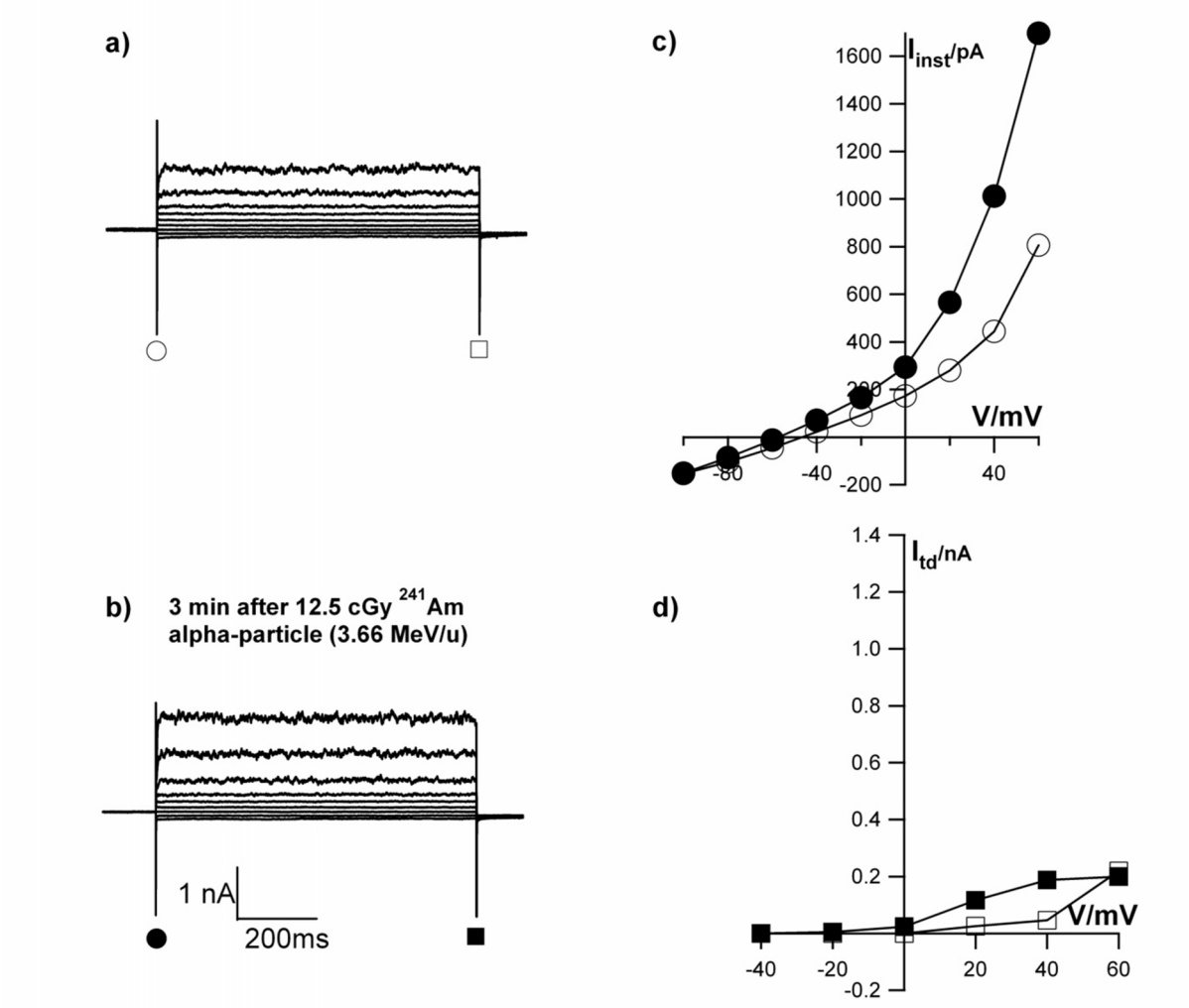

Fig. 28 Alpha-particles increase membrane conductance in A549 cells.

Current responses of one typical A549 cell recorded immediately (a) and 3 min after irradiation with 12.5 cGy alpha-particles (b) as described in Materials and Methods. Currents were measured with standard voltage protocol with test voltages from −100 mV to +60 mV. The resulting I/V-relations of the instantaneous currents (c) were measured at the beginning of voltage pulses, labeled by the markers in a) and b). The time-dependent currents (d) were obtained by subtracting I_{inst} from the steady-state current collected at the end of the pulses. Currents were measured in an external buffer with 4 mM K^+.

To estimate the possibility whether every cell was hit at least once by an alpha-particle at the dose used for irradiation we calculated the Poisson distribution of particle impacts. The probability of particle impacts in A549 cells for an irradiation with alpha particles from a source with ^{241}Am 3.66 MeV/u and a dose of 12.5 cGy are shown in Fig. 29. The estimated

distribution shows that we cannot fully exclude that a single cell may have not been hit by an alpha-particle. Still the probability for a single hit of a cell is with 91% very high.

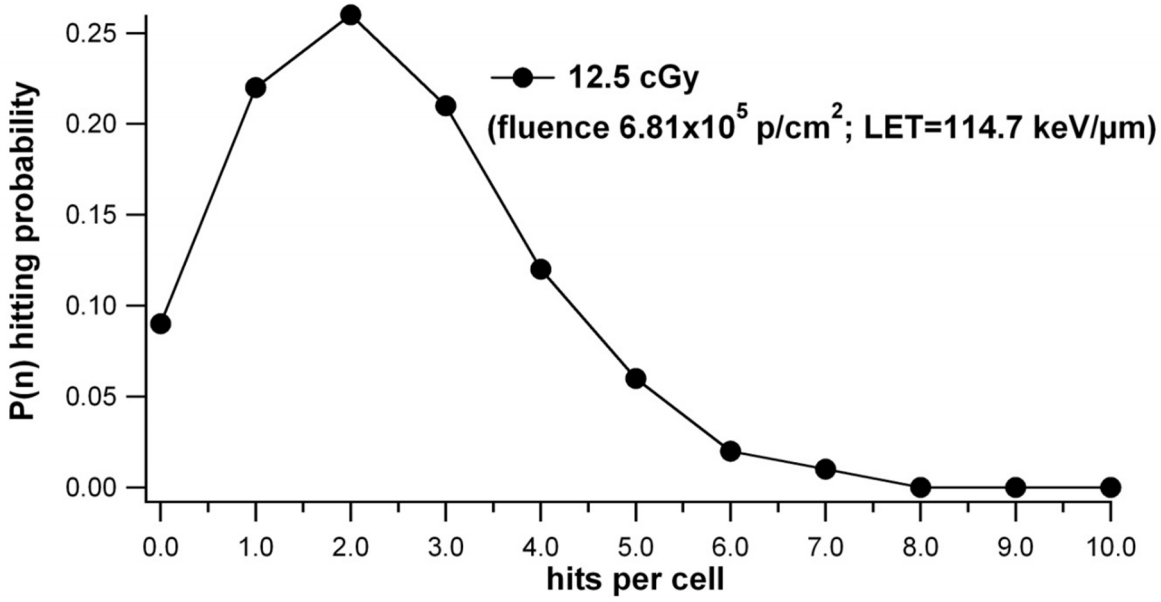

Fig. 29 Distribution of alpha-particle impacts in A549 cells.

The graph shows the Poisson distribution for the hitting probability of a cell by α-particles from a ^{241}Am source with 3.66 MeV/u. At a dose of 120 cGy (closed circles) 9% of the cells will exhibit no impact. The probability that a cell is hit at least once by a particle is 91%.

In order to test whether alpha-particles and x-rays activate in A549 cells the same ion channels we added after an α-particle treatment of A549 cells the blocker CLT at 10 μM to the external medium. Fig. 30 shows the currents of an A549 cell recorded 3 min after irradiation with 12.5 cGy alpha-particles; subsequently the cell was exposed to the hIK channel-blocker CLT. The exemplary data show that the conductance, which was augmented by irradiation, could be blocked by CLT. On average 10 μM CLT reduced the steady-state current of A549 cells irradiated with α-particles at +40 mV by 44 ±11% (n=3). These experiments underscore that also alpha-particle irradiation leads to an increase in I_{inst}, which is largely carried by the hIK-channel.

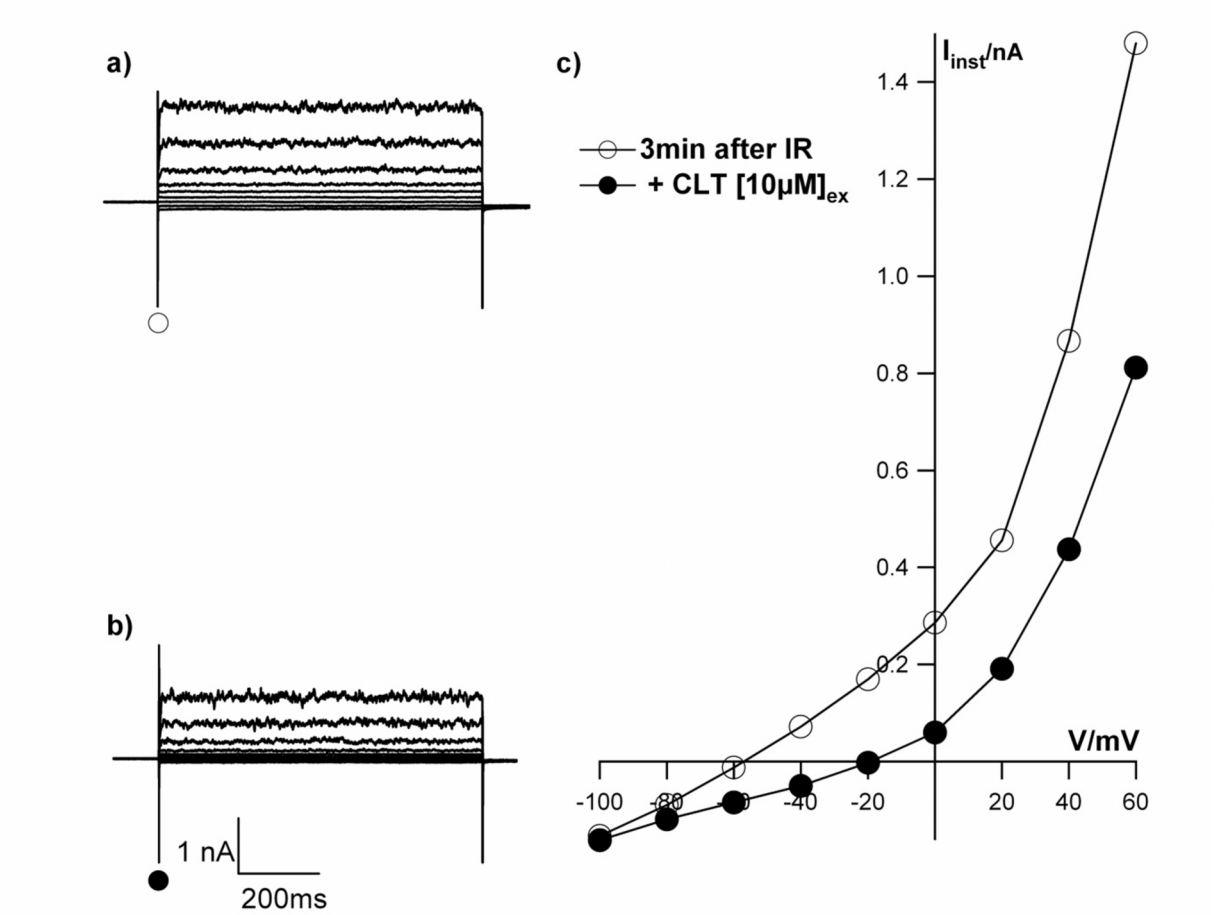

Fig. 30 The membrane conductance in A549 cells can be increased by exposure to alpha-particles and again inhibited by hIK blocker clotrimazole.

Currents of one typical A549 cell were recorded 3 min after irradiation with 12.5 cGy alpha-particles (a) as described before. Currents, which are elicited by alpha-particle irradiation, can be blocked by adding 10 μM of the hIK-specific blocker clotrimazole to the external medium (b). Currents were measured with voltage pulses from −100 to +60 mV in 20 mV increments. The resulting I/V-relations (c) of the instantaneous currents were measured at the beginning of voltage pulses at time indicated by symbols in a, b and c. Currents were measured in an external buffer with 4 mM K^+.

After finding that diverse forms of ionizing irradiation cause in A549 cells an increase in membrane conductance we addressed the question whether this effect is cell type specific. For this purpose we conducted the same kind of experiments as in Fig. 18 but with 82-6hTERT and HEK293 cells. These cells show current voltage relations, which are at first glance similar

to those of A549 cells (Fig. 31, Fig. 32). The current response of both cells to the standard pulse protocol is also dominated by two different kinetic components.

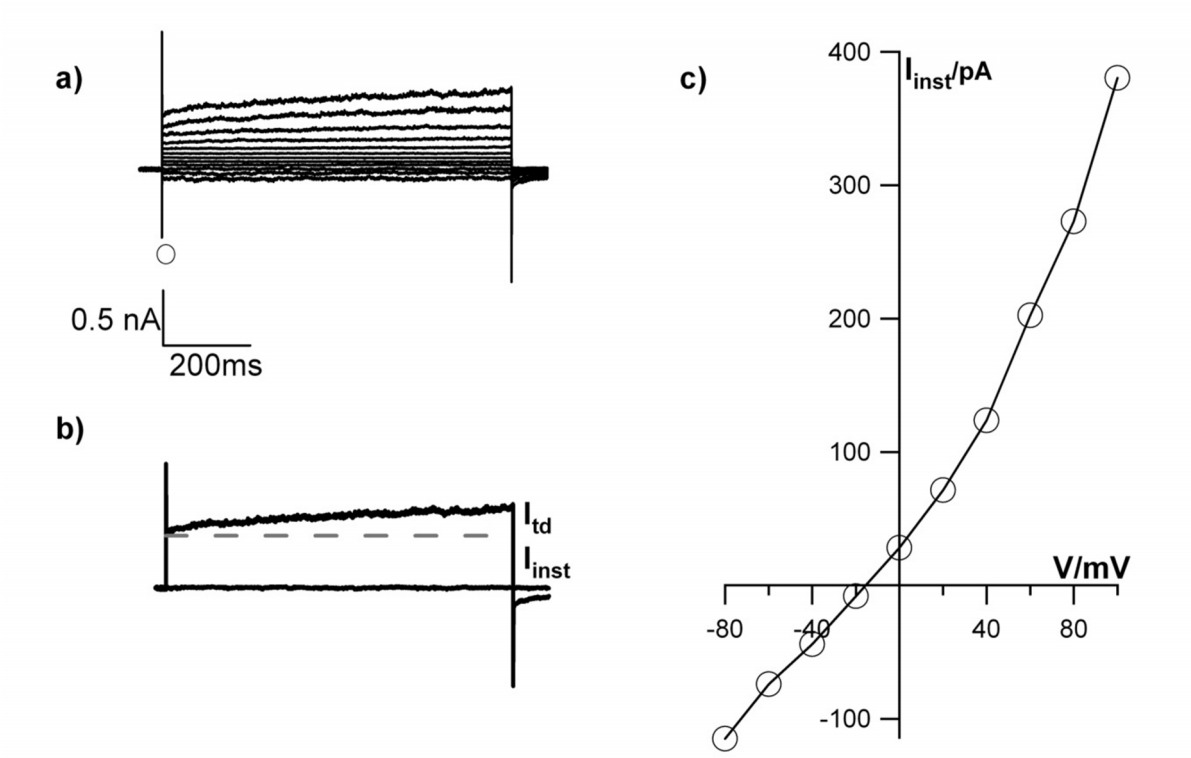

Fig. 31 Current/voltage relation of a 82-6hTERT cell.

Data show the current response of an exemplary 82-6hTERT cell to a standard pulse protocol from a holding voltage (-60 mV) to test voltages between -80 mV and +100 mV in 20 mV steps (a). Currents, which are elicited by positive voltages, can be decomposed into two kinetically different components: an instantaneous activating conductance and a slow activating outward conductance (b). The corresponding current/voltage (I/V) relation of the instantaneous conductance is shown in c. Currents were measured in an external buffer with 4 mM K^+.

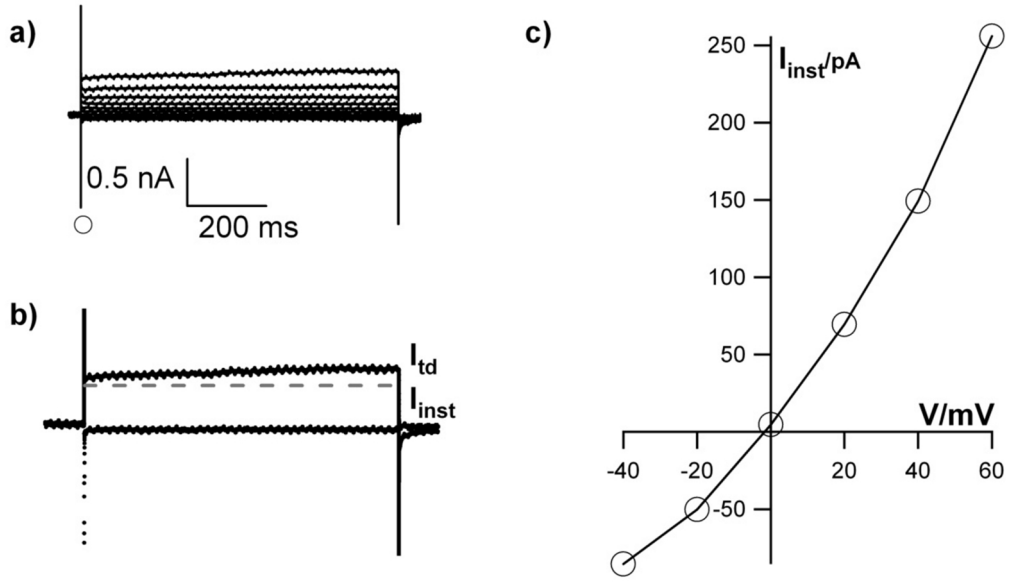

Fig. 32 Current/voltage relation of a HEK293 cell.

Current response of an exemplary HEK293 cell to a standard pulse protocol from a holding voltage (-60 mV) to test voltages between -40 mV and +60 mV in 20 mV steps (a). Currents, which are elicited by positive voltages, can be decomposed into two kinetically different components: an instantaneous activating conductance and a slow activating outward conductance (b). The corresponding current/voltage (I/V) relation of the instantaneous conductance is shown in c. Currents were measured in an external buffer with 4 mM K^+.

Exposing 82-6hTERT cells or HEK293 cells as in Fig. 18 to 1 Gy x-ray resulted in none of the experiments in any appreciable increase in conductance (Fig. 33) or hyperpolarization. The results of these experiments mean that the increase of K^+ channel activity is not a generic response of cells to radiation.

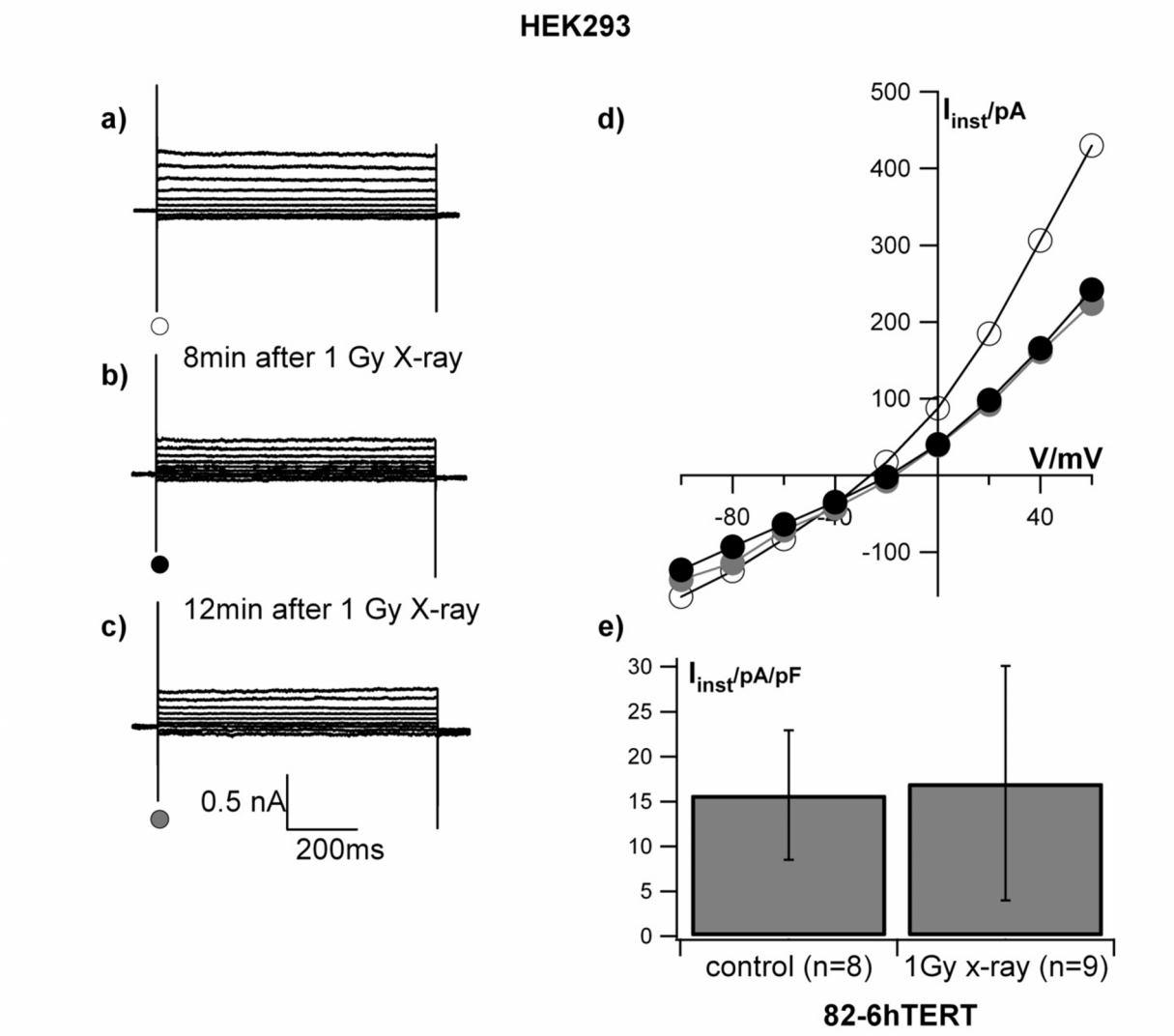

Fig. 33 The increase of membrane conductance after irradiation is cell specific.

(a) Current traces recorded 2 min before and (b) 8 min; (c) 12 min after 1 Gy x-ray. Standard pulses from −100 to +60 mV in 20 mV increments were applied. The resulting I/V-relations (d) of the instantaneous currents were measured after decay of transient capacitive current 5 ms after onset of voltage step (labeled by the symbols). Mean steady state currents in (e) collected at 40 mV from populations of 82-6hTERT cells, which were exposed or not exposed to 1 Gy x-ray. Currents were measured in an external buffer with 4 mM K^+. Instantaneous currents were measured as in Fig. 5. Data are means ± standard deviation of n cells as stated in the graph.

Additionally we wanted to examine whether the insensitivity of these cells is correlated with the presence/absence of hIK channels in these cells. Therefore we repeated the transcript analysis for the hIK genes in both cell lines by reverse transcription (rt) PCR (Fig. 34, Fig. 36). The transcripts from 82-6 hTERT cells reveal that the human ether-a-go-go (hEAG) potassium

channel and also the human intermediate conductance potassium channel (hIK) are transcribed albeit at a low level in these cells.

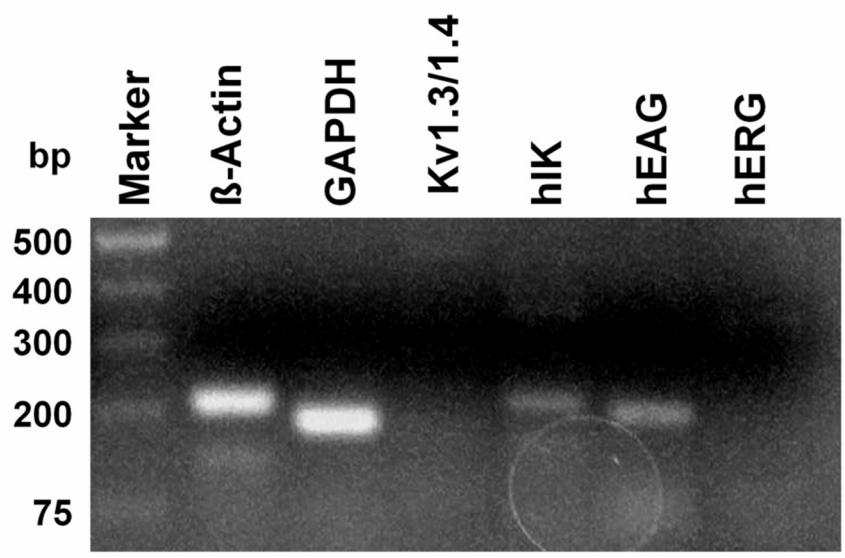

Fig. 34 RT-PCR of common ion-channels in 82-6hTERT cells.

Total RNAs of 82-6hTERT cells were reverse transcribed, followed by PCR using 82-6hTERT cell cDNA and specific primers amplifying the Kv1.3/1.4 (216 bp), hIK (206 bp), hEAG (192 bp) and hERG (203 bp) potassium channel cDNA, as described in Materials and Methods. Amplified fragments were resolved by 2% agarose-gel electrophoresis and visualized by ethidium-bromide staining. M, molecular weight marker; Sample with GAPDH (181 bp) and ß-Actin (210 bp) were used as positive controls.

Because the transcript analysis does not exclude the presence of the hIK in 82-6 hTERT cells we repeated the same experiments as in Fig. 11 and treated 82-6hTERT cells with the hIK blocker CLT. These experiments (Fig. 35) show no effect of CLT [10 μM] on the conductance in these cells. On average 10 μM CLT reduced the I_{inst} of A549 cells at +40 mV by -6 ±9% (n=3). This means that hIK channels provide no mayor contribution to the membrane conductance of 82-6hTERT cells.

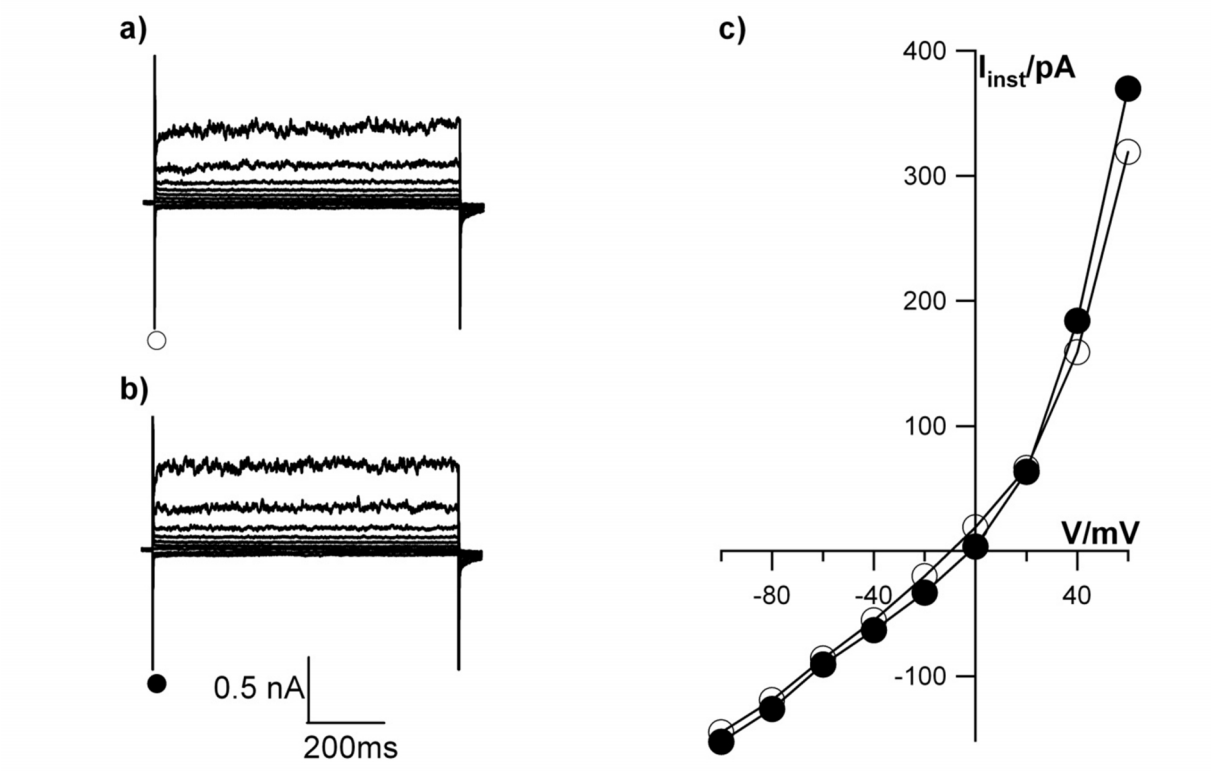

Fig. 35 Addition of 10 μM clotrimazole shows no effect on the conductance of 82-6hTERT cells.

Current of an exemplary 82-6hTERT cell elicited by standard pulse protocol with voltage steps from a holding voltage (-60 mV) to test voltages between −100 mV and +60 mV in 20 mV steps. Currents were measured before (a) and 3 min after (b) adding 10 μM CLT to the external buffer. The corresponding current/voltage (I/V) relation of the instantaneous conductance is shown in c. The symbols in a and b correspond to the symbols in c. Currents were measured in an external buffer with 4 mM K^+.

The presence of candidate ion-channel transcripts in non-responsive HEK293 cells was also revised (Fig. 36). In addition to the housekeeping genes also transcripts for hIK and hEAG were detected at very low level in these cells.

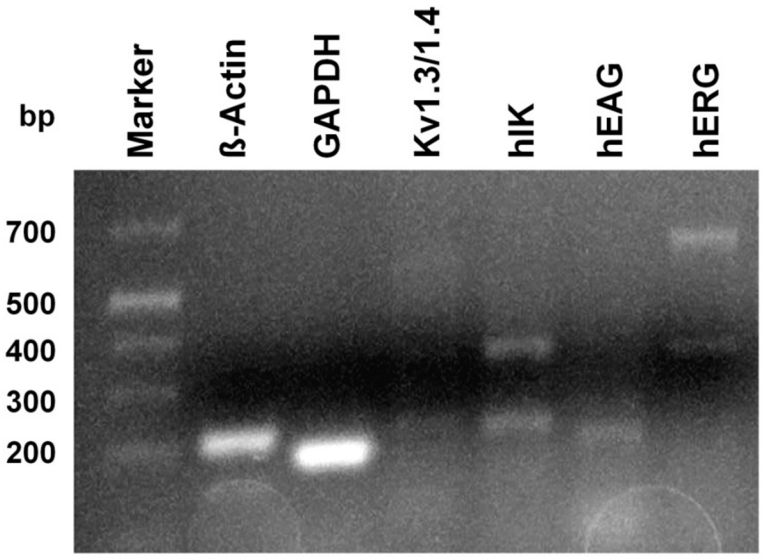

Fig. 36 Transcripts of common ion-channels in HEK293 cells.

Total RNAs of HEK293 cells were reverse transcribed followed by PCR using HEK293 cell cDNA and specific primers amplifying the Kv1.3/1.4 (216 bp), hIK (206 bp), hEAG (192 bp) and hERG (203 bp) potassium channel cDNA, as described in Materials and Methods. Amplified fragments were resolved by electrophoresis in a 2% agarose-gel and visualized by ethidium-bromide staining. M, molecular weight marker; Sample with GAPDH (181 bp) and ß-Actin (210 bp) were used as positive controls.

Because of the low expression of the hIK-channel in HEK293 cells we repeated the same experiments as in Fig. 13; cells were exposed to the hIK blocker Tram-34. Even though transcripts for the hIK-channel were detectable at a low level in HEK293 cells, the blocker Tram-34 [150 nM] had no appreciable effect on the current voltage relation of HEK293 cells (Fig. 37). The results of these experiments suggest that hIK channels contribute little if any of the conductance of HEK293 cells.

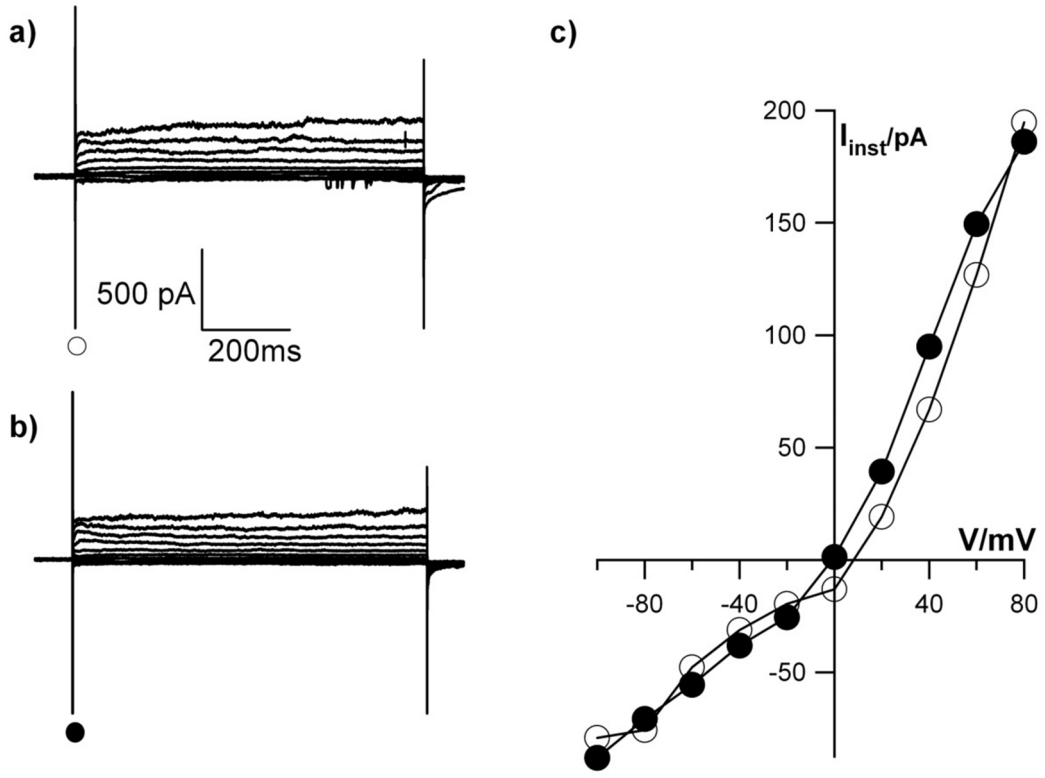

Fig. 37 hIK specific blocker Tram-34 has no effect on currents in HEK293 cells.

Currents of an exemplary HEK293 cell elicited by standard pulse protocol with voltage steps from a holding voltage (-60 mV) to test voltages between −100 mV and +80 mV in 20 mV steps. Currents were measured at the onset of the test pulse before (a) and 5 min after (b) adding 150 nM TRAM-34 to the external buffer. The corresponding current/voltage (I/V) relation of the instantaneous conductance is shown in c. The symbols in a and b correspond to the symbols in c. Currents were measured in an external buffer with 4 mM K^+.

In summary the results of a variety of experiments show that, the main conductance of A549 cells is carried by two types of K^+ channels. The instantaneous activating conductance is dominated by the hIK-channel; this channel can be blocked by Tram-34 and CLT. Both conductances can be activated in a dose dependent manner by different types of ionizing irradiation, the instantaneous conductance e.g. an increase in hIK activity. The effect of ionizing irradiation is cell type specific and can be attributed to the presence or absence of the hIK-channel.

3.6. Discussion

The present data confirm and extend a previous report in that ionizing irradiation augments already at very low doses the activity of K^+ channels in A549 cells (Kuo et al., 1993). We find that this treatment does not only stimulate the conductance of the slow activating K^+ outward rectifier but increases even more the conductance of an instantaneous voltage-independent K^+ conductance. The data are consistent with a model according to which only cells, which strongly express the Ca^{2+} sensitive and voltage independent hIK channel, exhibit a sensitivity to low dose ionizing irradiation. The rapid response to radiation stress is strongest in cells, in which the hIK channels are not yet active. In these cells irradiation causes a hyperpolarization of the cells towards the Nernst voltage for K^+. The large range of membrane voltages and the variability of currents in control cells, which can be blocked by TRAM-34 or CLT, suggest that a regulation of hIK activity is an endogenous process in these cells. In the context of published data on the function of hIK channels it is reasonable to speculate that hIK activity varies throughout the cell cycle. It has been reported for MCF-7 cells that a transition between G1- and S-phase is favored by a hyperpolarization and that the latter is caused by an activation of hIK channels (Ouadid-Ahidouch & Ahidouch, 2008). On the background of these data the present results imply that irradiation is modulating an endogenous physiological regulation, which could well be associated with the regulation of the cell cycle.

From the measurements it occur that hIK channels are rapidly activated upon irradiation but only after some short delay. This suggests that the hIK channels are not direct targets of irradiation but that the stress induces some signal transduction cascade.

The radiation-induced activation of hIK channels is an important issue for the evaluation of radiation responses in cells. This Ca^{2+} activated type of K^+ channel is present in many cell types including erythrocytes, endothelial cells, lymphocytes, and smooth muscle cells (Fanger et al., 1999; Tharp & Bowles, 2009). In these cells they have key regulatory functions related to their ability of modulating the free running membrane voltage. In motile cells for example hIK channels are essential players in the contractile motion through mitigating localized volume loss (Schwab et al., 2012). With this key role in controlling motility the hIK channels are important for cell development and pathologies. hIK channels are also required for endothelial cell hyperpolarization and subsequent smooth muscle relaxation, leading to vasodilation, which is crucial for the maintenance of cardiovascular homeostasis (Grgic et al., 2005; Tharp & Bowles, 2009). In erythrocytes and epithelial cells, hIK channels participate in osmoregulation (B S Jensen et al., 2001). Finally, the hIK channel plays a role in cell proliferation by hyperpolarizing the cell through the cell cycle stages mainly between G1- and

S-phase (Ouadid-Ahidouch et al., 2004). The prominent role of the hIK channel in key cellular reactions and the finding that these channels are activated by low dose ionizing irradiation suggests that an exposure of cells to this type of radiation stress can cause severe deregulation in cells, which express this type of channel.

4. Chapter 2 - Possible Signal Transduction Mechanisms for the activation of the hIK channel after ionizing irradiation.

Ionizing radiation is known to activate cytoplasmic signal transduction pathways, which are involved in important cellular processes like apoptosis and cell proliferation. More information on the interplay of ionizing irradiation and signal cascades is provided in the introduction. An interesting question in the context of the present study is to examine the signaling processes, by which ionizing irradiation activates potassium channels in A549 cells.

4.1. Results

4.1.1. Reactive oxygen species

A possible second messenger, which is produced by cytoplasmic ionization and which has the potency to activate channels, are reactive oxygen species (Sahoo et al., 2013). The relationship between irradiation and reactive oxygen species in cells has been reviewed by Mikkelsen & Wardman, (2003). To test for the contribution of reactive oxygen species as a link between radiation and channel activation we first recorded the typical current voltage relation of an A549 cell in Fig. 6. In the next step, hydrogen peroxide was added at a final concentration of 100 μM to the buffer medium. Hydrogen peroxide (H_2O_2) belongs to the reactive oxygen species (ROS); it is uncharged and relatively stable under physiological conditions. It is also membrane permeable and similar to water molecules it is conducted by the membrane and to a higher extend also by aquaporins (Bienert et al., 2007). A bulk of published data suggests that H_2O_2 is a potential second messenger, which can transmit the direct effect of irradiation to a regulation of enzyme activity. Altogether this can affect cell growth and development. Studies performed by Rhyu and coworkers (Rhyu et al., 2012) showed that a treatment of an epithelial cell line with as little as 500 µM H_2O_2 effectively transformed these cells into fibroblasts. In addition to profound effects on development it was reported that an elevation of H_2O_2 in the extracellular medium can also be anti-proliferative (Wang et al., 2002) and affect proliferation/migration (Gupta et al., 2012; Tochhawng et al., 2013).

The data in Fig. 38 show the current response of a characteristic A549 cell to a standard voltage protocol before and after addition of 100 μM H_2O_2 to the external buffer medium. A comparison of the currents and of the corresponding I/V relation recorded before and after addition of H_2O_2 [100 μM] shows that this treatment evokes a strong activation of I_{inst} in these cells. The same increase in I_{inst} was recorded in 11 of 15 cells challenged with H_2O_2. In the responsive cells the current increased on average by 37 $\pm$2.9% in response of this treatment.

Notably the response of A549 cells to H_2O_2 is similar to that generated by radiation shown in the previous experiments.

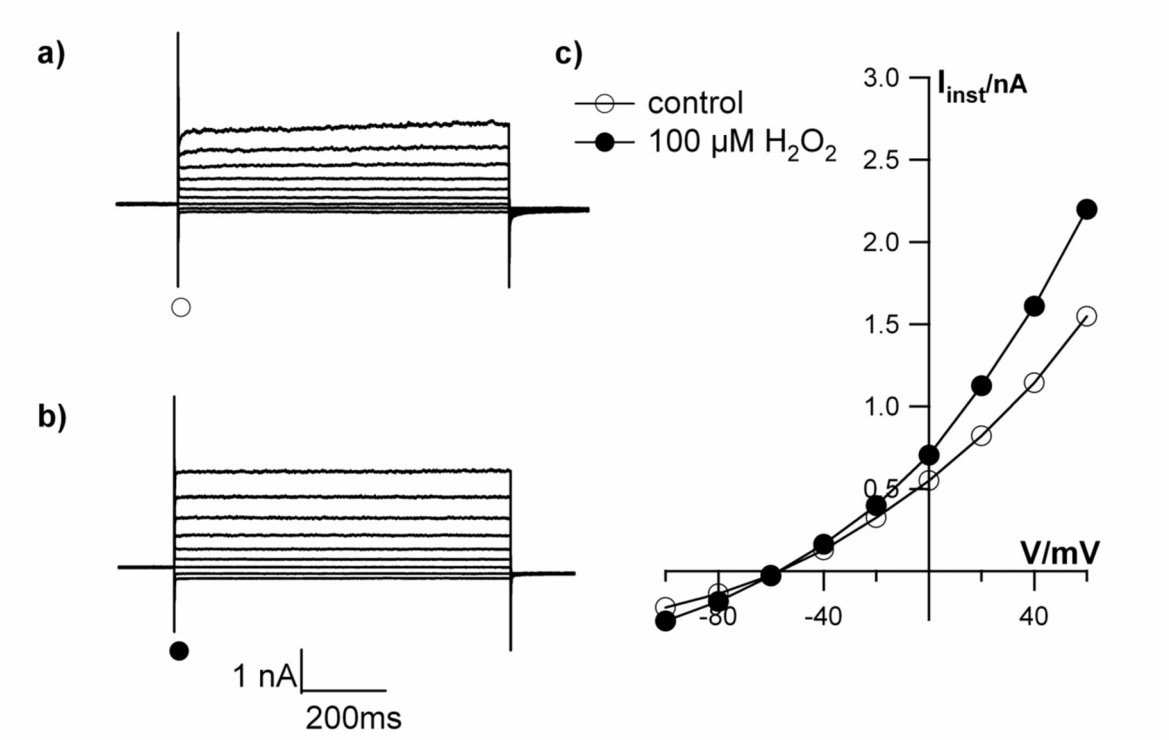

Fig. 38 Hydrogen peroxide activates membrane conductance in A549 cells.

Typical current responses of one A549 cell to voltage protocol in absence (a) and presence (b) of H_2O_2 [100 μM]$_e$. Voltage pulses from -100 to +60 mV in 20 mV increments were applied. The resulting currents were measured at the beginning of each voltage pulse in the absence (open circles) and presence of 100 μM H_2O_2 (closed circles) and plotted as an I/V relation (c). The symbols in c correspond to those in a and b.

To further examine the sensitivity of K^+ channels to H_2O_2 the same experiments as in Fig. 38 were repeated with different concentrations of hydrogen peroxide. The plot in Fig. 39 illustrates the relative increase in I_{inst} at +40 mV in responsive A549 cells; the currents were measured 2 to 5 min after adding H_2O_2 at different concentrations to the external buffer. The relative rise in I_{inst} is measured as the percentage of increase between the current at a reference voltage of +40 mV before and after stimulation; the plot shows that I_{inst} is increasing as a function of the H_2O_2 concentration. A Hill equation was fitted to the dose–response values with the following equation:

$$I = \frac{I_{max}}{\left[1 + \left(\frac{EC_{50}}{c}\right)^{n}\right]}$$

(5)

Where I is the amplitude of the H_2O_2-activated K^+ current, I_{max} the maximal amplitude of the H_2O_2-activated K^+ current, and c the H_2O_2 concentration. The fitting yields a Hill coefficient of n=0.8 and an EC_{50}-value of 0.45 mM. It is worth noting here that the latter is only an indirect value for the sensitivity of the K^+ channels to H_2O_2 since the cytosolic concentration is presumably lower than that in the external bath.

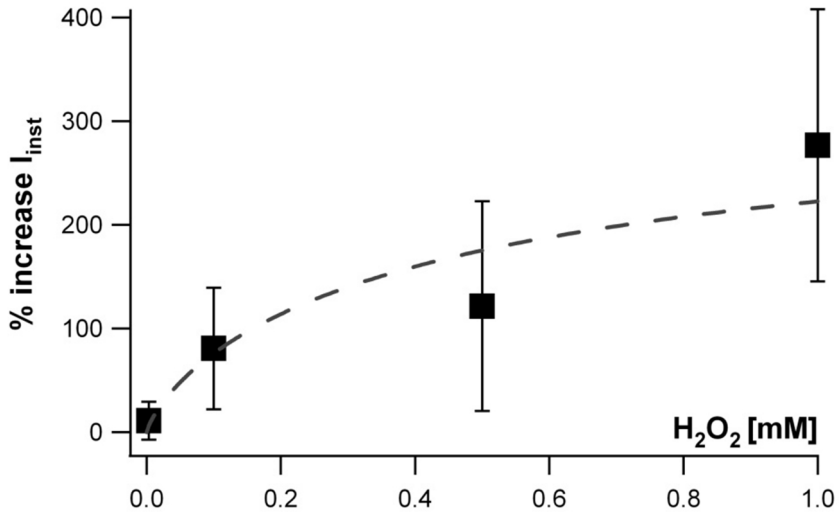

Fig. 39 H_2O_2 activates the instantaneous conductance in A549 cells in a dose-dependent manner.

Instantaneous activating currents in A549 cells were measured before and after addition of different concentration of hydrogen peroxide to the bath medium. Each data point gives the percentage increase of instantaneous current at +40 mV over the current recorded before treatment. Data are mean values ±SD from measurements in 4 cells. The line was obtained by fitting the data with equation 5 yielding a Hill coefficient of n=0.8 and an EC_{50}-value of 0.45 mM.

It has been proposed that irradiation of cells can generate so called *bystander effects*. In such a scenario it could be possible that an irradiated cell is producing oxygen radicals, which are then secreted from the irradiated cells into the medium. In the context of the present data it might be possible that channels could be activated by such a bystander-effect, in which H_2O_2 is released by cells into the culture-media (Narayanan, 1997). To test this hypothesis, we irradiated A549 cells with alpha-particles as in Fig. 4. Subsequently we collected the serum of these cells and perfused it over non-irradiated control cells. The data in Fig. 40 report the mean I/V relations of six control cells, which were first incubated in control buffer and subsequently transferred to the serum from cells irradiated with 12.5 cGy alpha-particles. Currents were measured as in Fig. 18. The result of this experiment shows that the serum of irradiated cells contains no factor, which increases the conductance of I_{inst} in A549 cells. The fact that the current density of the control cells is slightly higher than that of the treated cells is presumably the result of the aforementioned run down (Fig. 17).

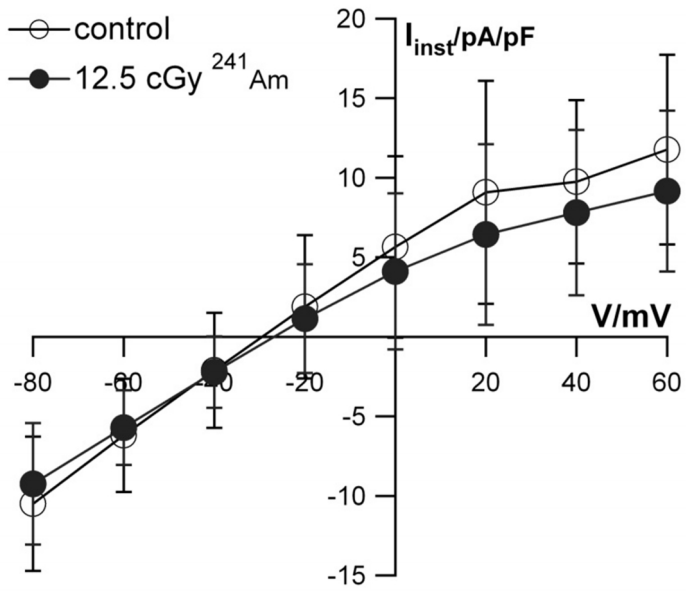

Fig. 40 Medium from A549 cells, which were irradiated with Alpha-particles, does not activate conductance in unirradiated cells.

Mean instantaneous activating I/V relations of A549 cells, which were (filled symbols) or were not (open symbols) exposed to irradiated media with 12 cGy alpha-particles. Data were recorded as in Fig. 5. Currents were measured in the same cell directly before and after perfusion. Data are mean ± standard deviation of n=6 measurements. To account for different cell sizes the currents were normalized to the membrane capacitance of the individual cell; the latter is an indirect measure of the cell surface.

4.1.2. Calcium signaling

Ionizing irradiation frequently causes in cells an elevation of the cytoplasmic concentration of free $[Ca^{2+}]_{cyt}$ (Kuo et al., 1993; Ouadid-Ahidouch & Ahidouch, 2008; Panyi et al., 2004; Todd & Mikkelsen, 1994). This is crucial since Ca^{2+} ions serve as second messenger in cells; they are involved in a large number of cellular reactions including proliferation, migration and apoptosis (Clapham, 2007).

The present data show that the instantaneous activating K^+ current in A549 cells, which is activated by radiation, is mainly conducted by the human intermediate conductance potassium channel hIK. It is well established that this channel is sensitive to $[Ca^{2+}]_{cyt}$; the channel activates at concentrations >200 nM and approaches maximal activity at 1 μM (Grissmer et al., 1993).

To test the dependency of the rise in currents in A549 cells, which are activated after ionizing irradiation, on $[Ca^{2+}]_{cyt}$, A549 cells were perfused with two different internal solutions; one was containing 20 mM EGTA and the other 1 mM EGTA respectively. The increase in currents at +40 mV in response to irradiation with 1 Gy x-ray was then measured as before. The percentage in current increase after ionizing irradiation is shown in Fig. 41. With a high Ca^{2+} buffer concentration the current increases on average by 66.8 ±42%, n=7). A low buffer concentration allows a much stronger rise in current; the average increase in these cells is 497.8 ±178%, (n=4). The difference is statistically significant (p=0.002) in a paired t-test.

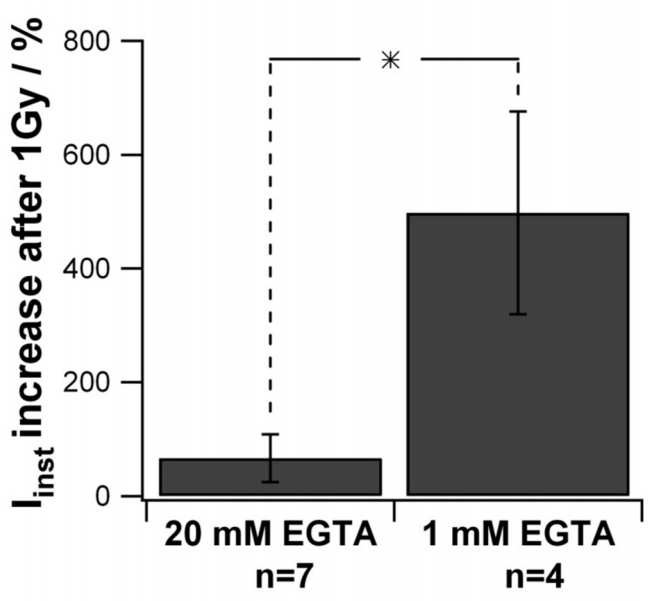

Fig. 41 The activation of K^+ channel activity in A549 cells by ionizing irradiation is suppressed by high cytosolic Ca^{2+} buffer

Mean increase of instantaneous activating current at +40 mV in A549 cells over control value of the same cell after irradiation with 1 Gy x-ray. The free concentration of $[Ca^{2+}]_{cyt}$ was buffered either with 1 mM or 20 mM EGTA in the pipette solution.

4.1.3. Characterization of irradiation and staurosporine induced apoptosis in A549 cells.

Programmed cell death, also known as cell suicide, is the major mechanism for eliminating cells, which are no longer required, or which reveal un-repairable damage. Apoptosis follows a progression of defined biochemical steps leading at the end to the activation of caspases, which finally cause cell death (Chen et al., 2013; Platoshyn et al., 2002; Riedl & Salvesen, 2007).

Apoptosis is often accompanied by changes in ion homeostasis. An essential role in the regulation of apoptosis is played by calcium. It has been reported that even minor increases in $[Ca^{2+}]_{cyt}$ can cause apoptosis in lymphocytes, prostate cells and adenocarcinoma cell (Elliott & Higgins, 2003; Yu et al., 2001). It has further been shown in several studies, that calcium release from the endoplasmic reticulum and influx via calcium activated calcium channels (ICRAC) mediate signal cascades, which are critical for triggering apoptosis (Dangel et al., 2005).

In addition to Ca^{2+} also K^+ ions are associated with apoptosis; it was observed that in several cell lines, which are undergoing apoptosis, K^+ leaks from the cells and this is caused by an

activation of K^+-channels (Singleton et al., 2009; Valencia-Cruz et al., 2009; L. Wang, 2003). Recent findings have shown that apoptosis can be inhibited by raising the extracellular K^+ concentration in lymphocytes (Yu et al., 2001). Also universal K^+ channel blockers like tetraethyl-ammonium-chloride (TEA) and 4-Amminopyridine (4-AP) prevent staurosporine-induced apoptosis and cytochrome-c release in HELA and U937 cells (Benítez-Rangel et al., 2011). Interesting in the context of the present study is the information that an increase in K^+ efflux during apoptosis is mainly mediated by high conductance, non-inactivating and Ca^{2+} dependent channels like hIK channels (Begenisich et al., 2004; Elliott & Higgins, 2003)

To examine the relationship between channel activity in A549 cells as an early response to radiation and apoptosis we used flow cytometry of propidium-iodid stained cells. The DNA intercalator, propidium iodide (PI) binds to DNA after fixation of cells with ethanol. The amount of dye bound correlates with the content of DNA within a given cell. The relative content of DNA indicates the distribution of a population of cells within the cell cycle (Krishan, 1975). For example, cells in the G0/G1 phases are diploid, while S-phase cells have DNA content greater than 2n. Cells undergoing apoptosis show an increase in fragmented DNA (Yan et al., 2006) and are sub-diploid (<2n). In the context of the present work we wanted to examine whether irradiation or staurosporine induces apoptosis in A549 cells and if this is related to the activity of the hIK channel; the latter can for this purpose be blocked specifically by TRAM-34.

The data from FACS measurements show that A549 cells proliferate rapidly and reached 80% confluence after 2 days. Fig. 42 shows histograms of the cell-cycle distributions from flow cytometry measurements of A549 cells under various conditions. A single-parameter histogram with relative DNA fluorescence or light scatter intensity on the x-axis and the number of events on the y-axis allows the discrimination of cell populations in different phases of the cell-cycle. Cell cycle analysis of untreated proliferating cells shows that 49.6 ±3% are in G0-/G1-, 35.2 ±2% in S- and 15.2 ±1.5% in G2-/M-phases, respectively. Treatment of the cells with the hIK blocker TRAM-34 [1 μM] increased the percentage of cells in the G0/G1 phase to 61%. The results of these experiments already imply that the activity of hIK channels is relevant for the regulation of the cell cycle.

Apoptotic cells can be estimated from the percentage of cells in the subG1-phase (Facompré et al., 2000). Under control conditions only 0.76 ±0.2% of the population is present in this phase. Cells, which were fixed and measured 5 hours after irradiation with 1 Gy x-ray showed with 1 ±0.5% only a slightly higher number of apoptotic cells in the subG1 phase. The small increase in apoptotic cells following irradiation could not be suppressed by pretreating cells

with Tram-34 [1 μM] 2 hours prior to irradiation; 1.4 ±0.5% cells were under these conditions detected in the subG1 phase. Interestingly A549 cells irradiated with 1 Gy x-ray showed a strong and significant decrease in cells in G2/M-phase. Compared to the control were 15.8 ±1% cells are in the G2/M-phase, only of 5.3 ±2.2% are found in this phase after irradiation (Fig. 42d). This could indicate that A549 cells are arrested in G0/G1-phase after irradiation with 1 Gy x-ray. Worth noting is that this effect could be reversed by treating the cells with Tram-34 [1 μM] prior to ionizing irradiation to values around 15.1 ±4.3%.

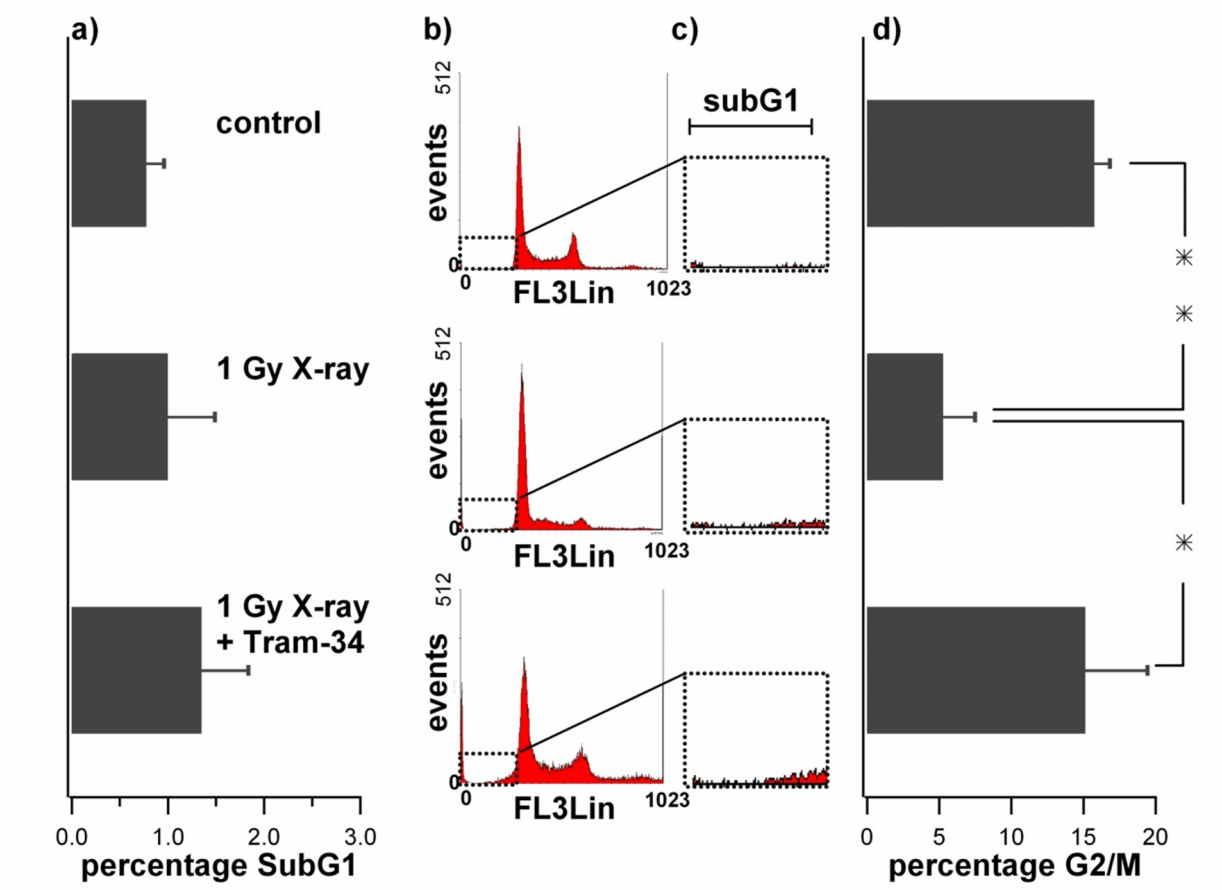

Fig. 42 Irradiation only causes minor apoptosis in A549 cells and effect on cell-cycle distribution by TRAM-34.

A549 cells were treated or were not pre-treated with TRAM-34 [1μM] before irradiation with 1 Gy x-ray. The DNA of cells was then analyzed by flow-cytometry. Plots with the relative distribution (in %) of cells in SubG1- and G2/M-phase under various conditions are shown in (a) and (d) respectively. Representative histograms of DNA content are shown in (b); the fluorescence intensity (FL3Lin) is plotted as a function of the cell counts. The subG1 phase in Fig. 42c is shown as a blow up. The level of significance for a difference in data is indicated by stars were '**' $p<0.005$ '*' $p<0.05$ ($n=5$).

In the next experiment we wanted to figure out whether an inhibition of hIK channels by TRAM-34 could prevent A549 cells from undergoing apoptosis in general. Therefore cells

were fixed and measured 5 hours after treatment cells with staurosporine (STS) [5μM]; this kinase blocker is an established trigger of apoptosis (Bertrand R, Solary E, O'Connor P, Kohn KW, 1994). Staurosporine treated cells were either incubated in the absence or presence of TRAM-34 [1μM]. The data in Fig. 43 show that STS treatment indeed increased the population of apoptotic cells from 1.2 ±0.7% in the control to about 3.2 ±0.6%. Concomitantly the population of G2/M-phase cells decreased as a consequence of STS treatment from 16 ±1.1% to 10.9 ±4.1%. The rise in apoptotic cells after STS treatment could be efficiently suppressed by the hIK channel blocker Tram-34 [1μM]; in the presence of the blocker the amount of apoptotic cells was decreased by 36.9 ±15% to values around. 2 ±0.3%.

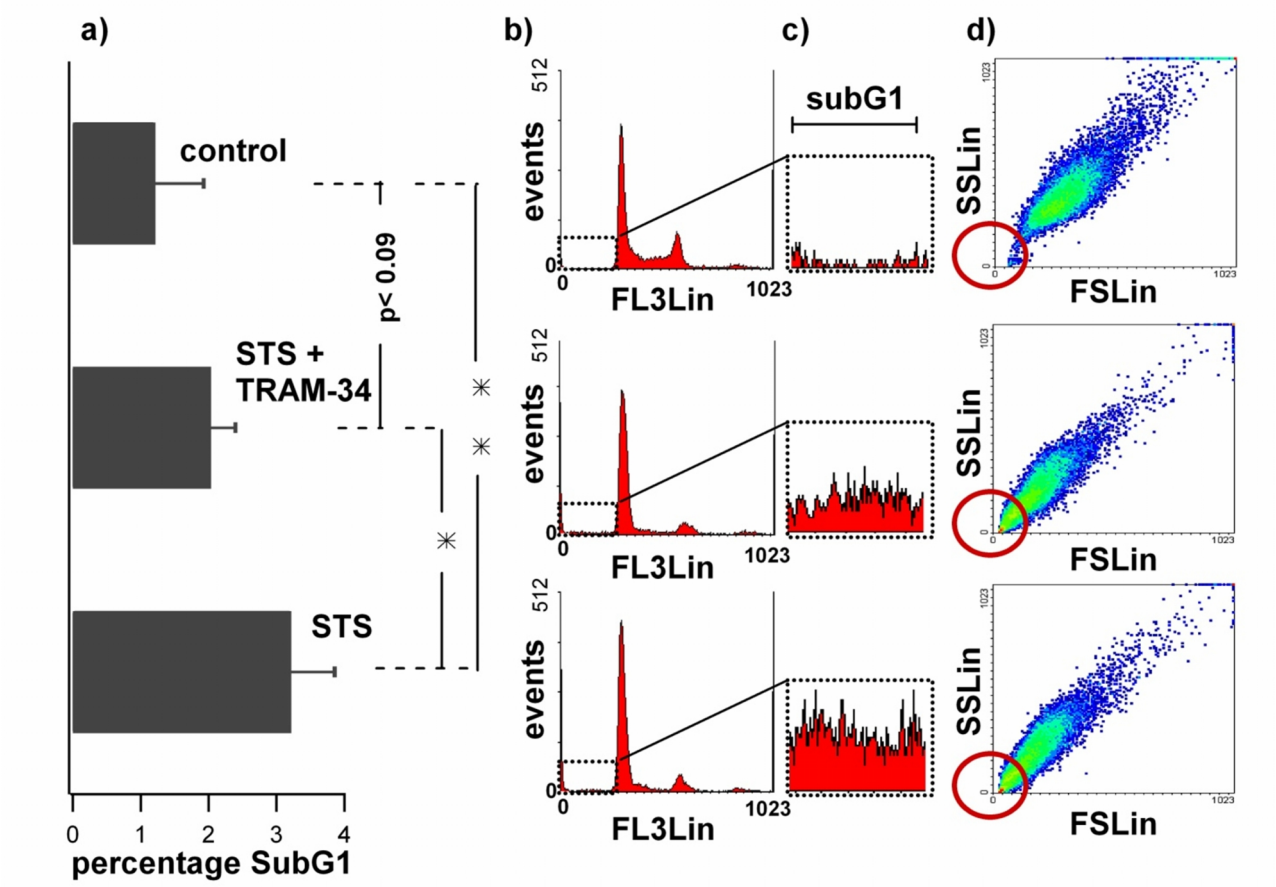

Fig. 43 Staurosporine induces apoptosis in A549 cells can be suppressed by TRAM-34.

A549 cells were treated or not with TRAM-34 [1 μM] and the apoptosis inducer staurosporine [5μM]. Cells were analyzed by flow cytometry for DNA content. Relative distribution (in %) of cells in SubG1-phase under various conditions are shown in (a). Representative histograms of DNA content are shown in (b); the fluorescence intensity (FL3Lin) is plotted against the cell counts. The enlarged excerpt in (c) shows the subG1 phase cells. (d) shows a dot plot of forward light scatter versus side scatter as a measure of cell size and cell granularity respectively, a red circle displays the apoptotic fraction. The statistical significance for the data is given by stars, where '**' represents $p<0.005$ and '*' $p<0.05$. (n=5).

In order to find out, whether proliferation or migration is affected in A549 cells by ionizing irradiation, I analyzed the migration of A549 cells by using two different assays. In a classical scratch assay (Hulkower & Herber, 2011) (Fig. 44a) it was found that, the migration of A549 cells was significantly inhibited by 8.2 ±1.3% with the hIK-channel blocker Tram-34 in comparison to control cells (n=284). In similar experiments we found that cells migrated faster by 6 ±1.5% (n=527 cells) than control cells after irradiation with 1 Gy x-ray (Fig. 44b); this difference is small but statistically significant (p=0.0004).

The difference in the scratch assay between irradiated and non-irradiated cells could result from a difference in cell migration or proliferation. To further examine the mechanism, which is underlying the difference in the scratch assay, we counted the number of A549 cells in the presence and absence of the hIK blocker clotrimazole. The results show the expected exponential increase in cell number under control conditions. In the presence of the channel blocker the rise in cell number is strongly reduced indicating an inhibition of cell proliferation. Differences between the two treatments are already apparent after 24 h of growth.

As a resume the combined electrophysiological recordings and the proliferation and migration assays support the hypothesis that the hIK-channel is activated by ionizing irradiation and that this lead to an enhanced migrating potential.

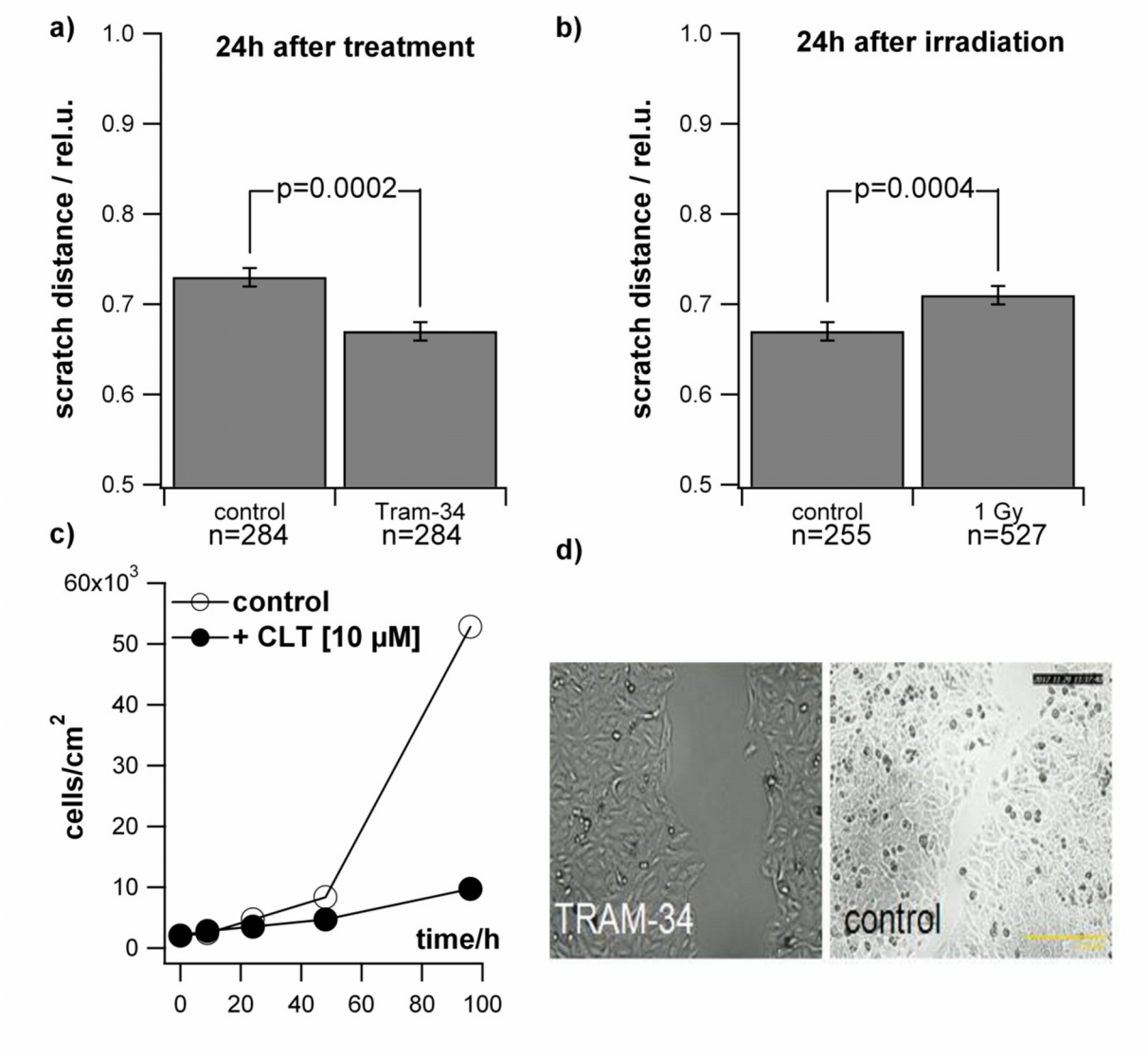

Fig. 44 Blocking the hIK-channel and ionizing irradiation elicit opposite effects in of A549 cells with respect to proliferation and migration.

A549 cells were seeded into culture dishes until full confluence was reached. The cell layer was subsequently scratched as described in materials and methods. Afterwards the cells were treated with Tram-34 [1μM] (n=284) or irradiated with 1 Gy x-ray (n=527) and the closure of the gap was observed by video microscopy. The pictures from one representative experiment are shown in (d). The distance, over which the cells migrated into the scratch in absence and presence of Tram-34 or for un-irradiated and irradiated cells is shown in (a) and (b) respectively. This wound closure was quantified as described in the method section. Values are mean ±SE of n cells from 12 independent experiments. The ability of proliferation was observed by counting the cells in the presence and absence of CLT with an automated cell counter (c).

4.2. Discussion

The dependency of hIK activation by ionizing irradiation on the Ca^{2+} buffer concentration in the cytoplasmic solution is good support for the hypothesis that radiation stress causes in A549 cells a rise in $[Ca^{2+}]_{cyt}$ and that the latter activates the Ca^{2+} sensitive hIK channels. This interpretation is consistent with reports, which show that some cells respond to ionizing irradiation with a rapid increase in $[Ca^{2+}]_{cyt}$ (Todd & Mikkelsen, 1994). Further experiments are required to show if also A549 cells respond to radiation stress by a rise in $[Ca^{2+}]_{cyt}$.

The present experiments show that the hIK conductance can also be activated by H_2O_2. Together with the common believe that ionizing irradiation generates in cells radicals (Muroya et al., 2006; Spitz et al., 2004; Stark, 1991) it is also feasible that hIK channels can be stimulated by radicals. At this point it is however not yet clear whether the two signals operate in parallel or if the ROS signal is upstream of the Ca^{2+}-signal. The second explanation seems to be more reasonable. To date, there are no reports, that the hIK channel does exhibit any obvious redox sites, which would prompt a direct regulation by H_2O_2. Furthermore it was found that the release of Ca^{2+} from internal stores in RBL-2H3 and Jurkat cells is stimulated by oxygen radicals (Grupe et al., 2010). Due to its very short half-life of 10^{-9}s ROS is unlikely responsible for these „Bystander-effects“. However it is conceivable that ROS are generated even after the termination of irradiation stress over a long period up to hours. This ROS production is presumably triggered by chain-reactions, which arises from an initial response to irradiation (Narayanan, 1997). Altogether these data favor a linear signal cascade for the regulation of hIK channels in A549 cells.

We find that staurosporine induces in A549 cells apoptosis and that this process can be effectively abolished by the hIK channel blockers TRAM-34 or CLT. These data on the sensitivity of apoptosis on the function of K^+ channels is in good agreement with the findings of others, which have shown that a programed cell death requires at some stage the activity of K^+ channels (Platoshyn et al., 2002; Z. Wang, 2004). In A549 cells apoptosis seems not to be a relevant response to radiation. But many types of cells respond to radiation stress with an increase in apoptosis. Hence the crucial role of the hIK channel in the complex scenario of apoptosis may suggest that a stimulation of hIK activity by ionizing irradiation could be instrumental for augmenting apoptosis in various cells as part of a radiation response.

The largest impact on the physiological behavior of the A549 cells was discovered in cell migration assays. These experiments show that irradiated A549 cells exhibit an increase in proliferation and migration over the non-irradiated control cells. Such an elevation of proliferation and migration might contribute to the invasiveness of cells after radiation

therapy like it is known for glioblastoma and lung epithelial cells (Jung et al., 2007; Li et al., 2013; Wild-bode et al., 2001). The interpretation that an increase in hIK activity in response to ionizing irradiation is responsible for the increase in cell proliferation and migration is further supported by the effect of hIK blockers. In line with the aforementioned hypothesis these blockers slowed down cell migration and proliferation. Altogether these data imply that ionizing irradiation can stimulate the activity of ion channel, which may enhance tumor invasion after IR. It is a well-known fact that radiotherapy is a useful tool to destroy cancer cells but at the same time it may promote migration and invasion of surviving cells by mechanisms that are not well understood yet (Li et al., 2013; Wild-bode et al., 2001). The discovery of the hIK channel and its responsiveness to ionizing radiation might be an additional factor, which contributes to negative side-effects of tumor treatment by ionizing irradiation.

5. Chapter 3 - Effects of ionizing irradiation on the electrophysiological behavior of radiosensitive primary cells

Blood is composed of different cell types, which can be divided in erythrocytes (red blood cells), leukocytes (white blood cells) and thrombocytes (blood platelets). Fig. 45 shows the progression of all types of human blood cells, which derive from the hematopoietic stem cells (HSC). This is a continuous process since blood cells are continuously regenerated; the life time in the bloodstream is relatively short (Moore, 2002).

Erythrocytes are commonly known to transport oxygen and carbon dioxide whereas thrombocytes play a major role in blood clotting by aggregating with thrombin. The leukocytes are a family of cells generated from lymphoid progenitor cells. These cells, which differentiate from the latter progenitors (Fig. 45) are summarized as peripheral blood lymphocytes (PBLs) and can be sub-divided into macrophages, granulocytes, natural killer cells as well as B- and T-lymphocytes. They all take part in the acquired immune system (Gordon MacPherson, Jon Austyn, 2012).

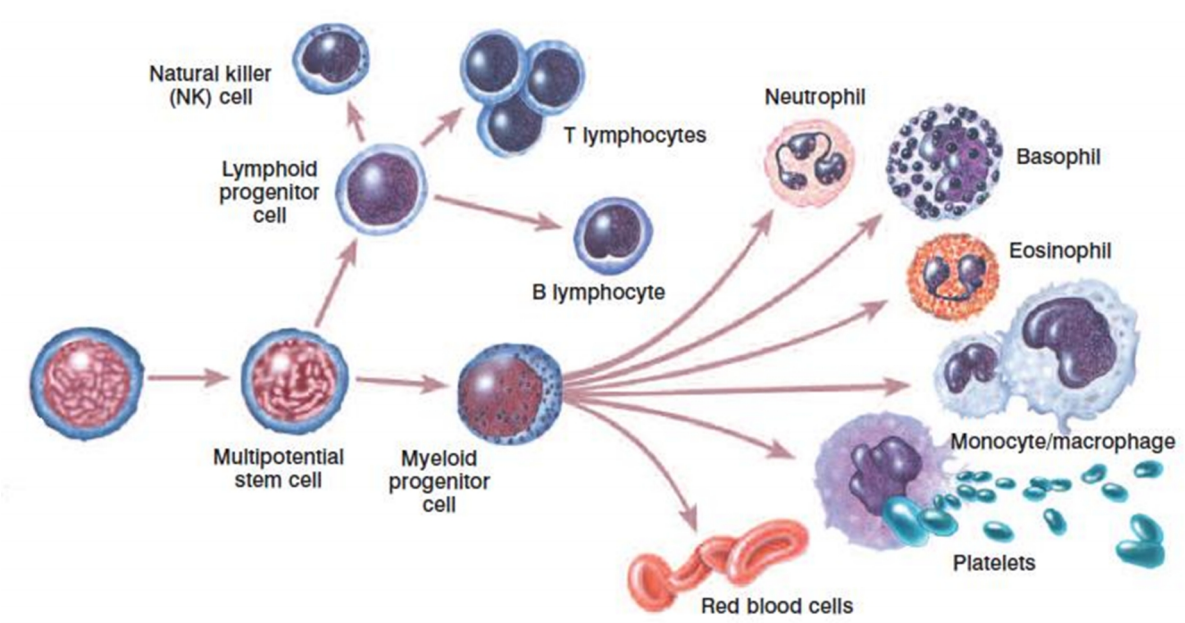

Fig. 45 Hematopoietic cell differentiation

Hematopoietic stem cells are able to form all cells in the hematopoietic system, which includes red blood cells, platelets and the lymphatic system (i.e. T- and B-lymphocytes). From (Winslow, 2006)

The most important cells for the acquired immune response are lymphocytes. Upon activation, lymphocytes differentiate into proliferative cells with effector functions that fight immediate

infection in the so called “primary response”. The lymphocytes with specific receptors for the antigen build up a population of antigen-specific cells, until the infection is successfully eliminated (Moulin AM, 1989).

It is known that blood cells can be the target of ionizing radiation. Within a few years after the invention of the X-ray machine it has been reported that the lymphatic system and individual lymphocytes are extremely radiosensitive (Boreham DR et al., 1996; O. A. Trowell, 1954). The law of Bergonie and Tribondeau (1906) reveals that the radio sensitivity of cell is directly proportional to their reproductive activity and inversely proportional to their degree of differentiation (Alan H. Haber and Barbara E. Rothstein, 1963). Beside germinal and epithelial cells of the gastrointestinal tract, lymphocytes are the most active reproducing cells. Survivors of the atomic bomb explosion or of radiation accidents showed therefore dysfunctions in the immune-system, which are triggered by an altered number of lymphoid cells (Little, 2009). Also in therapeutic medicine radiation is known to cause inflammatory reactions like in fibrosis. In this case various immune cells like lymphocytes are recruited into the lung after thorax irradiation (Cappuccini et al., 2011; Zhao W, 2009). In contrast to these negative effects of ionizing irradiation, low dose radiotherapy is known to cure inflammatory disease like arthritis (Rödel et al., 2007).

Ion-channels are involved in the immune-response by regulating ion fluxes in response to extracellular signals (Michael D Cahalan & Chandy, 2009; Feske, 2007). It is well established that cells of the hematopoietic system alter their electrophysiological properties depending on their functional state and that these alteration in transport properties trigger signal transduction cascades (Pillozzi & Becchetti, 2012). A large body of data has shown that the human intermediate conductance potassium channel hIK is the predominant channel in human lymphocytes (Cahalan & Chandy, 2009; Ghanshani et al., 2000; Khanna, 1999). Following mitogenic stimulation the hIK currents are dramatically up-regulated by a factor of 10 to 25 (R. Lewis & Cahalan, 1995). We have shown in the previous chapters, that low-dose ionizing irradiation evoked in A549 cells an increase in the conductance of this type of K^+ channel. In the context of their crucial role in the immune response and with their potential sensitivity to radiation it is important to understand the role of this channel in lymphocyte immune response after ionizing irradiation.

5.1. Results

5.1.1. Electrophysiological characterization of human peripheral-blood lymphocytes.

Currently five major types of endogenous ion-channels have been found in lymphocytes (Michael D Cahalan & Chandy, 2009). The most abundant ion-channel in resting lymphocytes has been identified as the Kv1.3 channel. From single-channel recordings it has been estimated that approximately 400 active Kv1.3 channels are present in the plasma-membrane of a single lymphocyte cell at rest. During depolarization the Kv1.3 will activate with the consequence that the cell hyperpolarizes until the activation threshold of ca. -60 mV is reached. This feedback-loop together with the slow-recovery from inactivation, which is typical for the Kv1.3 leads to fluctuations of the membrane voltage. By maintaining a negative membrane voltage Kv1.3 channels are responsible for a fine tuning of Ca^{2+}-influx into human lymphocytes (Panyi et al., 2004). The second major common channel in these cells is the intermediate-conductance potassium channel hIK. This voltage independent channel also known as KCa3.1, KCNN4 or IKCa1 ion-channel is activated by a rise in $[Ca^{2+}]_{cyt}$. Mitogenic stimulation causes within the first 2 min a rapid rise in $[Ca^{2+}]_{cyt}$ from the low resting level to 500-2000 nM. The CaM-binding domain in the C-terminus of the hIK channel functions as a Ca^{2+}-sensor and activates the channel in this early phase of stimulation. Because Ca^{2+} entry is greatest when the cell is hyperpolarized, hIK activity is also most elevated and drives the membrane voltage towards E_k. In resting lymphocytes the hIK channel is inactive because of the low resting $[Ca^{2+}]_{cyt}$ at about 50 nM (Michael D Cahalan & Chandy, 2009). This Ca^{2+}-signaling regulates in lymphocytes the expression of cytokines, which then mediate proliferation and differentiation of effector T cells and which regulate the inflammatory response (R. Lewis & Cahalan, 1995).

In addition to these two dominant channels there are reports of a few other K^+ ion–channels in lymphocytes, which only contribute little to the total membrane currents in these cells (Michael D Cahalan & Chandy, 2009). Beside these K^+ selective channels there are also channels with different types of selectivity. These include a Ca^{2+} selective inward current (CRAC) and an ATP-dependent outwardly-rectifying Cl^--current. By omitting ATP in the internal solution this current can be suppressed in experiments.

To examine the effect of ionizing radiation on transport properties of lymphocytes we first measured the currents in cells in the resting state. Fig. 46 shows a typical result from a cell clamped to voltages between -100 mV to 60 mV in 20 mV increments. All measurements have

been carried out like the previously shown recordings in the whole-cell configurations in A549 cells (Fig. 5).

As expected the current responses are composed of the two main components (Fig. 46a). The conductance at voltages more positive than ca. -20 mV is carried by a slow activating outward rectifier. At voltages negative of ca. -20 mV the cell reveals a low conductance with only instantaneously activating currents. This conductance presumably includes a low number of the hIK channels. A voltage-ramp protocol (Fig. 46b) enabling rapid measurement of the hIK conductance (Grissmer et al., 1993) was used to reveal the presence of hIK channels during whole-cell measurements. The protocol is designed in order to differentiate the hIK current from the K^+ outward rectifier. The ramp-current measured in n=21 cells reverses at -3 ±7.5 mV. In a voltage window between -100 to -20 mV the conductance is quasi linear. The measured free running membrane voltage is not identical to the calculated E_K, which is -68 mV under the prevailing recording conditions. This indicates that also the conductance to other ions contributes significantly to the free running membrane voltage. At more positive voltages the currents, which are activated by the ramp protocol, are deflecting upward. This indicates that a voltage-dependent conductance has been activated by the ramp. It is most likely that these currents are carried by Kv1.3 as shown in recent studies (R. Lewis & Cahalan, 1995).

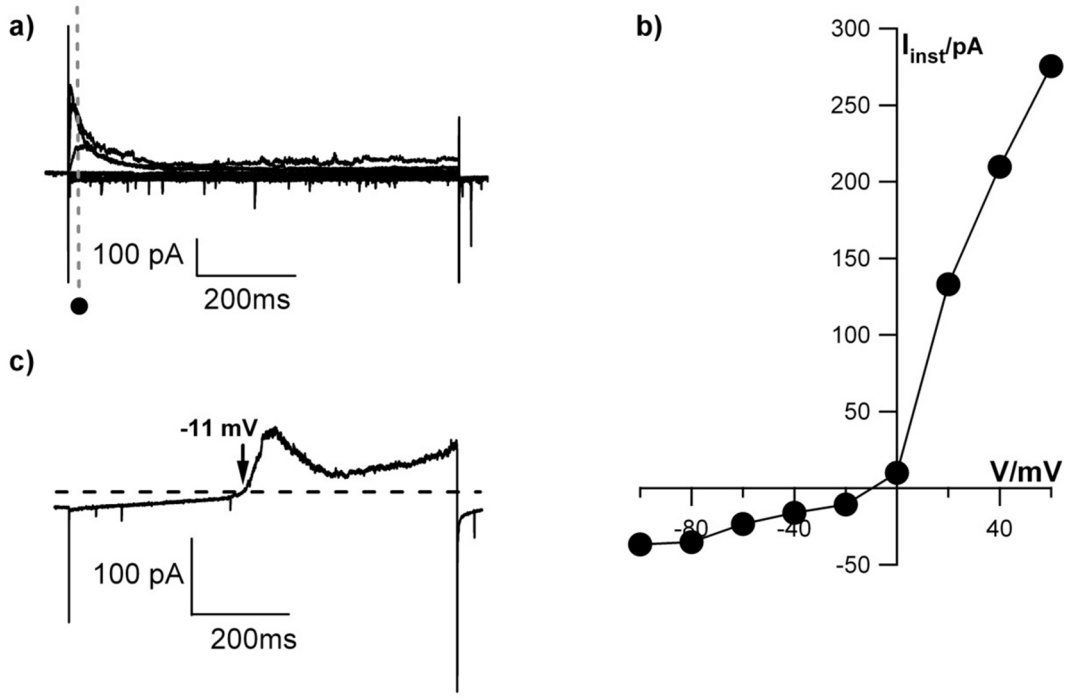

Fig. 46 Current voltage relation of a resting human peripheral-blood lymphocyte.

(a) Typical current response of a resting lymphocyte cell in whole-cell mode to a standard pulse-protocol. The cell was clamped from a holding voltage of -60 mV to test voltages between −100 mV and +60 mV. (b) Corresponding current/voltage (I/V) relation of the rapid activating current; data were collected immediately after clamping to test voltage at time indicated by dashed line. (c) Membrane currents in the same cell elicited by a 800 ms long voltage ramp from -100 to +100 mV. At voltages more negative than ca. -20 mV the conductance is low and quasi-linear; this reflects the activity of voltage-independent channels. At more positive voltages, the current increases exponentially indicating the activation of a K^+ outward rectifier. The measured membrane voltage of the lymphocyte cell is -11 mV. Currents were measured in an external buffer with 4 mM K^+.

Peripheral-blood lymphocytes are normally arrested in the G1-phase of the cell-cycle. They have to be activated by a specific antigen or nonspecific mitogens for progressing into the S-phase and for proliferation. Such responses can be achieved by an activation of specific surface-receptors on the lymphocyte membrane via diverse stimulating agents. An activation of these receptors induces a set of processes, including Ca^{2+} signaling cascades, which finally cause the cells to progress in the cell-cycle (Khanna, 1999). Several publications have underscored the importance of Kv1.3 channels in this activation process (Grissmer et al., 1993; Verheugen & Vijverberg, 1995).

To monitor the change in transport properties of lymphocytes in response to stimulation, cells were treated with the activating mitogen phytohemagglutinin [7.2 μg/ml] (PHA), which induces repetitive oscillations of $[Ca^{2+}]_{cyt}$ (Hayman & Van Der Weyden, 1980; R. S. Lewis & Cahalan, 1989). 48h after stimulation the current voltage properties of these cells were measured as described in Fig. 46. Typical current responses for a stimulated lymphocyte are shown in Fig. 47. The corresponding I/V-relationship for the instantaneously activating currents is significantly different from that of the resting cell. The linear, voltage–independent part of the current/voltage relation becomes at voltages negative of -40 mV much steeper than in resting lymphocytes. This increase in I_{inst} results in a negative shift of the reversal voltage. This means that the free running membrane voltage of the activated cells is much more negative than that of the corresponding resting cells. The mean reversal voltage obtained from 8 mitogen-activated cells is -18.4 ±18.7 mV. This value is closer to the estimated K^+-Nernst voltage of -68 mV than the mean reversal of -3.1 ±7.5 mV recorded in 21 resting cells tested. The results of these experiments indicate that I_{inst} increases substantially. The voltage-dependent outward rectifier at more positive voltages plays after immune-stimulation with PHA a smaller role in the overall conductance. The contribution of the Kv1.3 current appears to be masked by the large instantaneous conductance. The peak current response after PHA activation is also increased by 93 ±60% (n=10) over the corresponding value in resting cells.

Stimulation of lymphocytes with PHA does not only affect the conductance of these cells but also the capacitance. This parameter, which is an indirect measure of the cell surface (Neher & Marty, 1982), increased from an average of 4.8 ±2.3 pF in unstimulated cells (n=17) to 7.2 ±2.9 pF after 48 h of stimulation with PHA (n=10). This apparent difference in cell surface area, which is statistically significant (p=0.002), is consistent with the published increase in lymphocyte diameter. It has been reported that lymphocytes increases from 5-8 μm in non-stimulated cells to a value of 10-30 μm after mitogen stimulation (Cuschieri & Mughal, 1985; Decoursey et al., 1987). The increase in surface area can also be correlated with the observed increase in membrane conductance, which increases in response to PHA stimulation.

To test whether the instantaneous activating conductance includes activity of the hIK channel the same PHA stimulated lymphocyte was treated with the hIK channel blocker clotrimazole. A comparison of a current response of a lymphocyte to a test voltage from -60 to 40 mV before and after addition of 10 μM clotrimazole shows that the blocker reduces the respective current by 75% (Fig. 47d). The remaining current is most likely the voltage-dependent Kv1.3.

The results of these experiments are in agreement with published data, which have shown that the surface expression of the hIK channel is increased in lymphocytes 65-fold after stimulation by PHA; Kv1.3 channels increase only modestly 1.5-fold (Cahalan et al., 2001). As a consequence of the increase in K^+ conductance, the free running membrane voltage of the cells hyperpolarizes (Grissmer et al., 1993).

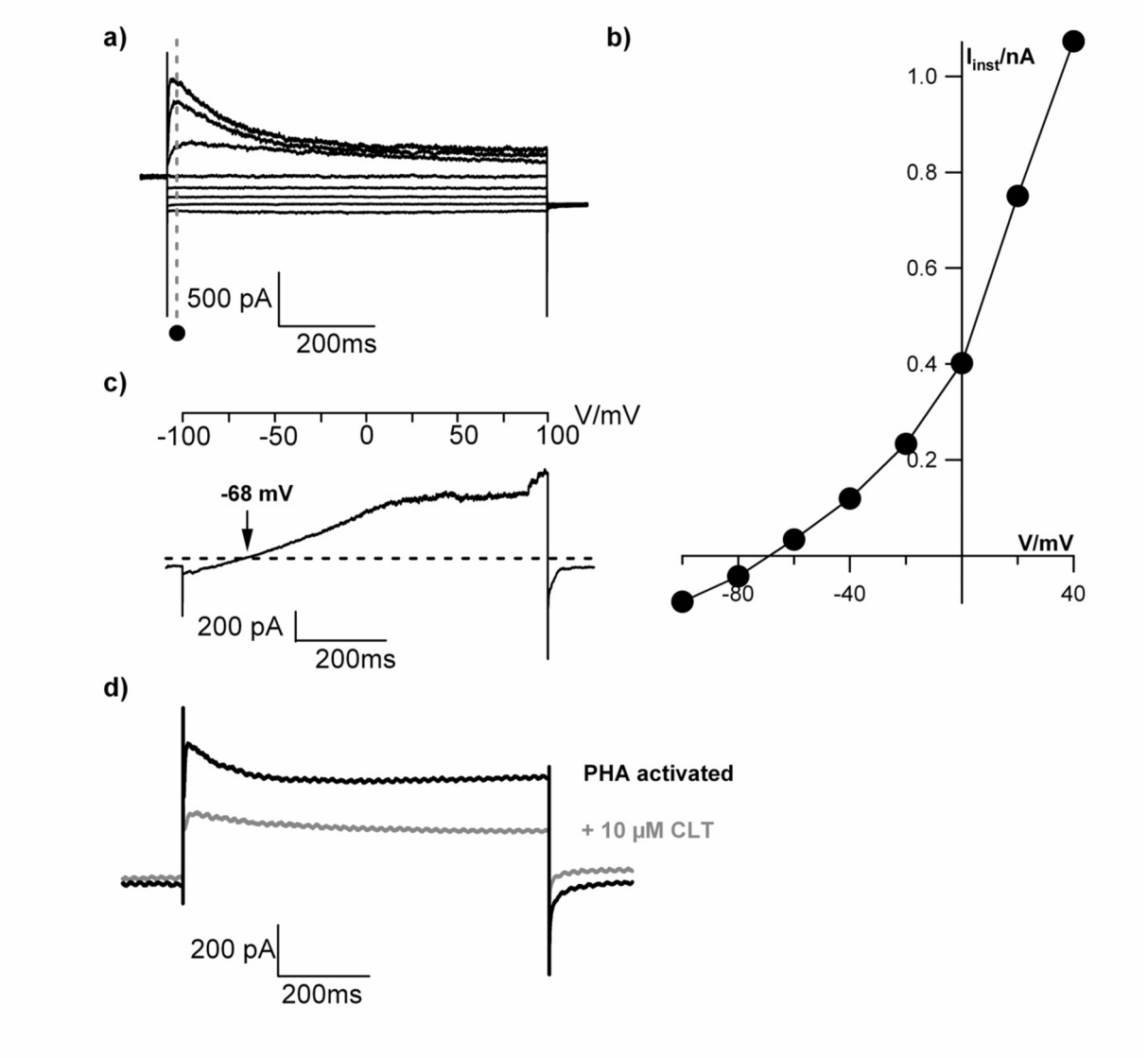

Fig. 47 Current voltage relation of a human peripheral-blood lymphocyte after stimulation with phytohemagglutinin.

(a) Typical current response of a lymphocyte cell 48h after PHA-stimulation. Currents were elicited with standard pulse-protocol from holding voltages (-60 mV) to test voltages between −100 mV and +40 mV. The corresponding current/voltage (I/V) relation of the early current response is shown in (b). The currents were sampled at the time indicated in a). Currents of the same cell were also elicited by a 800 ms long voltage ramp from -100 to +100 mV (c). The linear part of the current/voltage relation at negative voltages below -40 mV is dominated by voltage-independent currents. The nonlinear part at more positive voltages reflects the activity of the activating and inactivating outward rectifier. The membrane voltage obtained from the reversal voltage is negative at -68 mV. (d) Current response of a PHA-stimulated lymphocyte to a voltage step from -60 mV to 40 mV before and 3 min after adding clotrimazole $[10\ \mu M]_{ex}$ to the external buffer solution. Currents were measured in an external buffer with 4 mM K^+.

5.1.2. Effects of IR on the ion-channel activity in human peripheral-blood lymphocytes

To examine the effect of ionizing radiation on the K^+ conductance in lymphocytes, we compared the current voltage relations of a population of control cells with those irradiated with 1 Gy x-ray. For this purpose we measured I/V relations of lymphocytes >30 min after radiation with x-ray and of control cells from the same batch. Fig. 48 shows a typical example of lymphocyte cell after exposure to x-ray. The exemplary current responses taken 30 min after irradiation with 1 Gy x-ray are shown. Similar to the PHA-stimulated lymphocytes, the cells from the irradiated population, exhibit a pronounced activation/inactivation kinetic at positive clamp voltages; this behavior is typical for the Kv1.3 channel. Upon close scrutiny, it is apparent that the inactivation of the outward rectifier in the irradiated cells is much slower than in resting cells. This can be an indication for the removal of c-type inactivation in response to irradiation induced ROS (Ruppersberg et al., 1991; Xu et al., 2001). In addition we could observe an increase in conductance after irradiating the lymphocytes with 1 Gy x-ray over that of resting non-irradiated lymphocytes. The mean reversal voltage obtained from 10 irradiated cells is -12.2 ±5 mV. This value is again higher than the membrane voltage of resting lymphocytes -3 ±7.5 mV (n=21). The hyperpolarization towards the K^+ Nernst voltage in response to irradiation is presumably the result of an activation of a K^+ conductance.

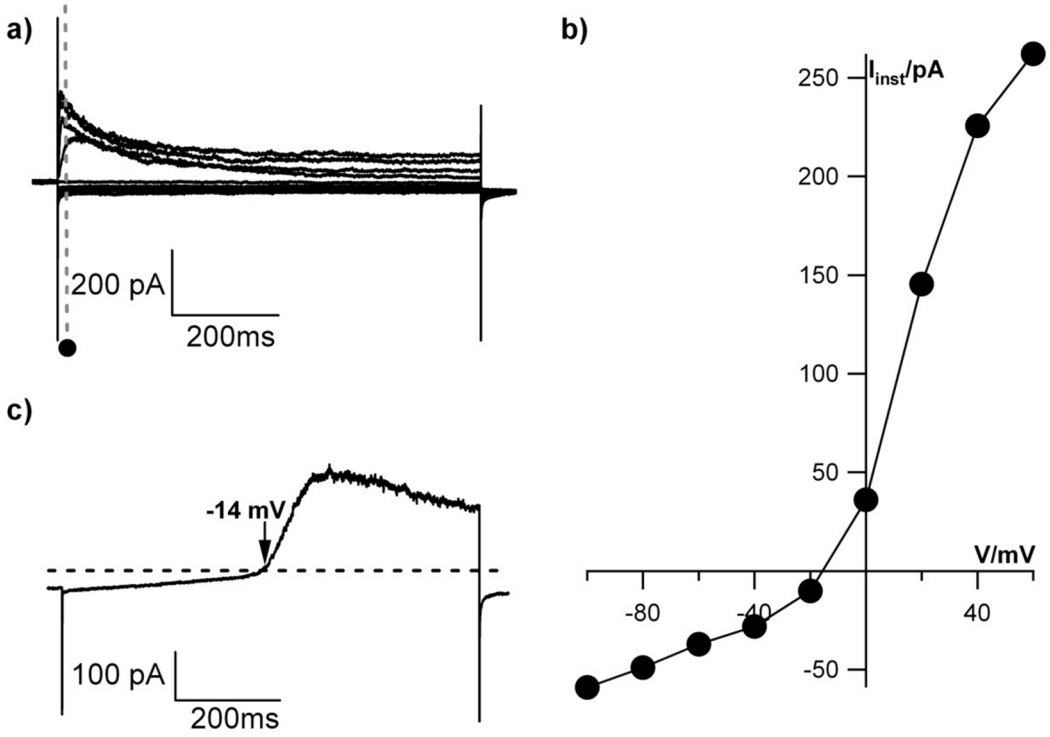

Fig. 48 Membrane conductance of non-activated human peripheral-blood lymphocytes after ionizing irradiation.

Whole cell currents in non-stimulated lymphocyte 20 min after irradiation with 1 Gy X-ray. Currents were elicited by stepwise increasing test voltages from -100 to +60 mV (a). Both currents, the instantaneous activating and the time-dependent activating current, are larger than in resting lymphocytes. (b) Shows the resulting I/V-relationship of the early peak current sampled at the time indicated in (a). Currents were also elicited by 800 ms long voltage ramps from -100 to +100 mV (c). The linear part at negative voltages below -20 mV represents voltage-independent currents; the steep increase at depolarizing voltages reflects the activation and inactivation of the Kv1.3 channel. The measured membrane voltage is -14 mV. Currents were measured in an external buffer with 4 mM K^+.

In order to quantify the total conductance of lymphocytes after ionizing irradiation the peak current at 20 mV was determined for resting and irradiated cells as well as for cells stimulated for 48h with PHA. The plot of peak currents from different cell populations in Fig. 49 show the highest conductance in the population of PHA stimulated cells; the mean value is 303 ±136 pA (n=10). This value is significantly higher ($p<0.001$) than that of the resting cells where the corresponding value is 60 ±46 pA (n=21). The analysis also discloses a significant ($p<0.01$) increase in the peak conductance of irradiated cells over that of the control; the mean peak current value in this population is 128 ±89 pA (n=12) compared with controls. At

the test voltage of 20 mV both K^+ conductance in lymphocytes namely Kv1.3 and hIK are active. Hence both conductances can contribute to the elevation of the peak current in response to irradiation.

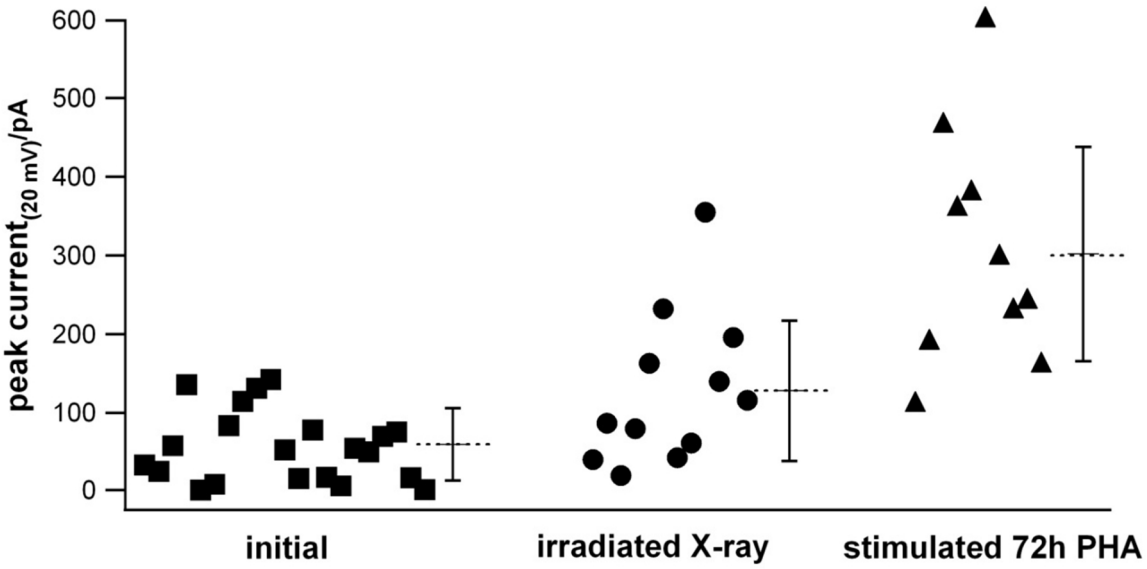

Fig. 49 Increase of peak current amplitude at 20 mV in irradiated lymphocytes.

Instantaneous conductance was quantified from buffy coat isolated lymphocytes ("initial", n=21), 2-6h post irradiation with 1 Gy X-ray ("irradiated X-ray", n=12), and after 72h culture stimulated with phytohemagglutinin (PHA) ("stimulated 72h PHA", n=10). Each point represents the peak current at 20 mV from an individual cell. The lymphocytes used in this analysis originate from 5 independent blood samples. Dashed lines represent averages of the n experiments and the error bars show standard deviation.

To estimate whether the elevated peak current after irradiation is more due to an increase in hIK or Kv1.3 activity, I tried to deconvolute the I/V data. It is known, that the hIK-channel has a linear current voltage relation over the wide range between -100 mV and +40 mV (Bondarenko et al., 2011). By contrast the Kv1.3 channel is not active at very hyperpolarized voltages (Wulff et al., 2004). Hence the activity of Kv1.3 does not contribute to the current at voltages between -100 mV and -60 mV. The contribution of Kv1.3 currents to the overall membrane currents was therefore estimated by fitting and extrapolating the linear current between -100 mV and -60 mV. The extrapolated straight line, which is a good approximation of the current/voltage dependency of the hIK channel, (Fig. 47c) was subtracted from the whole-cell current at depolarizing voltages. This gives rise to an I/V-relationship, which only

includes Kv1.3 currents (Fig. 50a). From the data it can be seen, that a stimulation of lymphocytes with PHA for 48 h causes a strong increase in Kv1.3 conductance; the mean current, which can be attributed to Kv1.3 is 167 ± 119 pA (n=11) at 20 mV. The corresponding Kv1.3 current in cells after irradiation with 1 Gy x-ray is 96 ± 53 pA (n=9) and that of the control in resting cells is 99 ± 69 pA (n=8). The result of this analysis implies that the rise in membrane conductance following ionizing irradiation is presumably not caused by Kv1.3 conductance but by an increase in hIK conductance.

It has been mentioned before that the membrane capacity of lymphocytes almost doubled after 48h of stimulation with PHA. To account for this increase in membrane surface we express the data as current densities. This procedure normalizes the measured Kv1.3 current to the cell surface area. The data show that the currents are after normalization basically the same in lymphocytes, which were stimulated by PHA, irradiated with 1 Gy x-ray or untreated control cells (Fig. 50b). This analysis suggests that PHA-stimulation increases the absolute number of Kv1.3 channels in the membrane but not the current density. Furthermore this implies that PHA has no appreciable effect on the activity of these channels. Furthermore the increase in peak current amplitude at +20 mV in irradiated lymphocytes (Fig. 49) is not caused by an increase in the Kv1.3-channel activity.

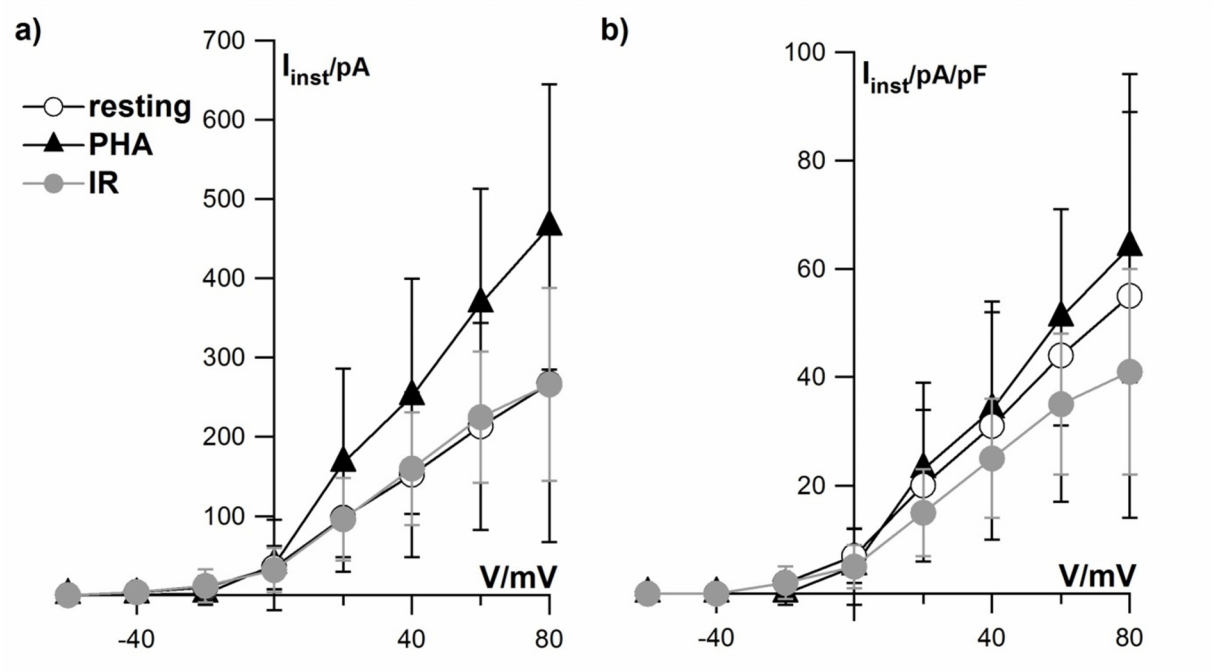

Fig. 50 Separation of Kv1.3 currents from total whole-cell currents in control lymphocytes and lymphocytes activated with PHA or irradiated with 1 Gy x-ray

Resting lymphocytes were not treated (control) or treated for 48 h with PHA [7.2 μg/ml] or irradiated before current recordings with 1 Gy x-ray. For details of the procedures see materials and methods. The I/V-relationships of Kv1.3 in a) were obtained by subtracting from the total membrane current a linear hIK current. The latter was obtained by a linear extrapolation of the current between -140 and -100 mV. b) To account for different cell sizes the currents from a) were normalized to the membrane capacitance of the individual cell; the latter is an indirect measure of the cell surface. Data are mean ± standard deviation.

In the next step the instantaneous currents collected at 20 mV from lymphocytes with different treatments were normalized to their membrane capacitance. This procedure results in a significant difference in the conductance between control cells and cells treated with 1 Gy x-rays. The value is 17.8 ±12.9 pA/pF (n=9) in control cells and 5.8 ±4.5 pA/pF (n=8) in irradiated cells (Fig. 51). The results of this analysis imply that irradiation with x-ray augments the conductance of hIK channels. The significant increase in hIK conductance in lymphocytes after PHA activation (Fig. 54), which has already been described elsewhere, (Wulff et al., 2004), underlines this conclusion .

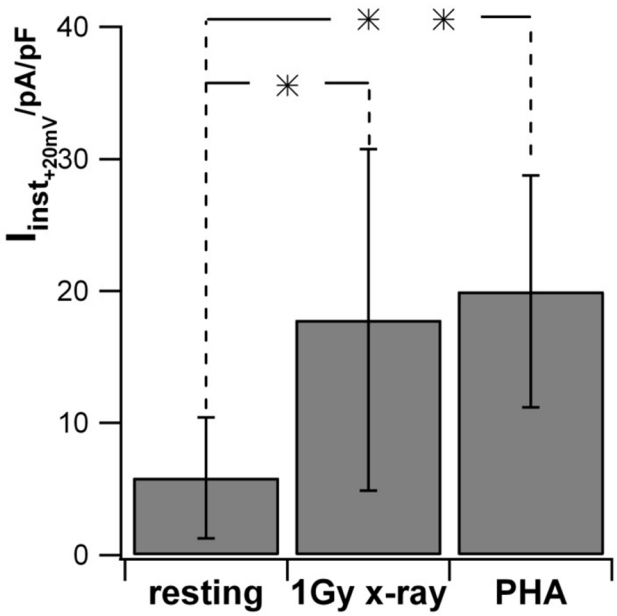

Fig. 51 The IR evoked increase in conductance in lymphocytes is carried by an increase in hIK activity

Average instantaneous current density at +20 mV after correction for Kv1.3 activity; currents were normalized to the membrane capacitance of the individual cells. The instantaneous activating current, which is a measure for the hIK activity, increases significantly over that in control cells after irradiation with 1 Gy x-ray or after treating the cells with PHA [7.2 μg/ml] for 48 h. The level of significance for a difference in data is indicated by stars were '**' indicates $p<0.005$ and '*' $p<0.05$ ($n=5$).

5.2. Discussion

Our experiments and the work of others (Cahalan & Chandy, 2009; Grissmer et al., 1993; R. Lewis & Cahalan, 1995; Panyi et al., 2004) have shown that the plasma membrane conductance of lymphocytes is dominated by two endogenous potassium channels, the voltage independent intermediate-conductance Ca^{2+}-activated potassium channel (hIK) and the voltage activated potassium channel Kv1.3. Both channels can be activated by incubating the cells for 48h with PHA. This is fully consistent with a previous study, which showed an increased expression of hIK and Kv1.3 channels after mitogen stimulation in lymphocytes (Khanna, 1999). Furthermore, the present data also show that ionizing irradiation with x-rays evoked in these cells an increase in membrane conductance. This rise in conductance occurred within minutes after irradiation e.g. the response of lymphocytes occurred in the same time window as that in A549 cells (Fig. 18). Separation of the global current response of lymphocytes into the individual conductance components indicates that the irradiation evoked increase in current is caused, at least in part, by a rise in the activity of the hIK-channel. The

activation of hIK activity in lymphocytes after x-ray irradiation is a further parallel with the reaction of A549 cells to this stress; also the latter cells showed a rapid and strong increase in hIK channel activity after this treatment. Collectively the results of these experiments are in good agreement with the hypothesis that cells, which express the hIK channel, respond rapidly to ionizing irradiation.

The present results suggest that ionizing irradiation may trigger a signaling cascade, which activates hIK channels. Because of the rapid response of lymphocytes to the irradiation stress it is unlikely that the increase in hIK conductance is the result of an elevated expression and an increased number of channel proteins in the membrane. The latter scenario accounts for the elevation of hIK activity in lymphocytes following PHA stimulation (Ghanshani et al., 2000). In the case of the rapid response to ionizing irradiation a more immediate mode of regulation must be considered. It is well established that the regulation of hIK channel activity in lymphocytes is strongly connected to Ca^{2+} signaling cascades (Feske, 2007). In the context of experimental data, which report that ionizing irradiation causes in some types of cells a rise in $[Ca^{2+}]_{cyt}$ (Palme et al., 2013; Todd & Mikkelsen, 1994) it is reasonable to speculate that such a signaling cascade stimulates hIK activation also in lymphocytes. The consequent activation of hIK channels will cause a hyperpolarization of the cells with the final result that the lymphocytes enter and progress through the cell-cycle. The causal relation of hIK activation hyperpolarization and lymphocyte activation has already been reported for other stimuli (Wonderlin & Strobl, 1996). Altogether the data foster the hypothesis that ionizing irradiation is stimulating an immune response in lymphocytes via activation of hIK channels.

6. Conclusion

Here the response of membrane transport properties to ionizing irradiation was studied in different human cell lines with electrophysiological methods. By using K^+ channel activators and blockers it was possible to identify the hIK channel as a putative molecular switch in A549 and lymphocyte cells. This finding is an extension of a previous study by Kuo et al., 1993 who found an increase in steady-state current after irradiation with gamma-rays in A549 cells. Here we further specify this cellular reaction and identify the hIK channel as the main targets of irradiation. This channel is activated within minutes after the irradiation stress and affects the differentiation of these cells. The data show that irradiation can stimulate cell proliferation and migration in A549 cells by activating the hIK channel; a membrane hyperpolarization, which is a consequence of the hIK activation, is presumably instrumental for this impact on cell differentiation. The causal relation between hIK channel activity and cell proliferation/migration is supported by the findings that specific blockers of the hIK channel are able to reverse the effects, which were stimulated by irradiation.

The response of hIK channels to radiation stress is rapid and occurs within minutes after the stress. This implies that a signal transduction cascade must link the radiation stress with a modulation of channel activity. The finding that the same kind of hIK channel activity can also be increased by ROS suggests a causal relationship between radiation-induced free radical production and ion-channel response. A direct regulation of the hIK channel however is unlikely because the irradiation effect can be suppressed by elevating the Ca^{2+} buffer concentration. Taken together the data suggest that ionizing irradiation generates ROS in cells, which in turn causes a rise in $[Ca^{2+}]_{cyt}$. The latter then activates the Ca^{2+} sensitive hIK channels. The elevated hIK channel activity drives the free running membrane voltage towards the Nernst voltage for K^+, which in general causes a hyperpolarization of the cells. This parameter is required for migration and proliferation of A549 cells. Presumably the same scenario occurs in lymphocytes, which also express the hIK channel. The resulting hyperpolarization of the lymphocytes may be a key step for an immune activation of these cells.

The key function of the hIK channel in regulating cell proliferation and migration and the discovery of its sensitivity to ionizing irradiation implies that this channel could be very important in radiotherapy for cancer. It may be speculated here that a treatment with ionizing radiation may stimulate negative side effects by increasing cell motility; the latter may be inhibited by specific blockers of the hIK channel. Examination of this possibility in in-vivo experiments will be an important future direction.

7. References

Alan H. Haber and Barbara E. Rothstein. (1963). Radiosensitivity and Rate of Cell Division: “Law of Bergonie and Tribondeau.” *Science*, *163*, 1338–1339.

AMENTA PS. (1962). The effects of ultraviolet microbeam irradiation on the eosinophil granular leukocytes of Triturus viridescens. *Anatomical record*, *142*, 81–87.

Arcangeli, A., & Becchetti, A. (2006). Complex functional interaction between integrin receptors and ion channels. *Trends in cell biology*, *16*(12), 631–9.

Becher, W., Konradt, M., Lenz, G., & Lotz, R. (2002). A new irradiation facility for biological samples at the UNILAC. *GSI scientific report*, *168*, 1980.

Begenisich, T., Nakamoto, T., Ovitt, C. E., Nehrke, K., Brugnara, C., Alper, S. L., & Melvin, J. E. (2004). Physiological roles of the intermediate conductance, Ca2+-activated potassium channel Kcnn4. *The Journal of biological chemistry*, *279*(46), 47681–7.

Benítez-Rangel, E., García, L., Namorado, M. C., Reyes, J. L., & Guerrero-Hernández, a. (2011). Ion channel inhibitors block caspase activation by mechanisms other than restoring intracellular potassium concentration. *Cell death & disease*, *2*, e113.

Bertrand R, Solary E, O’Connor P, Kohn KW, P. Y. (1994). Induction of a common pathway of apoptosis by staurosporine. *Exp Cell Res*, *211*(2), 314–321.

Bielanska, J., Hernández-Losa, J., Moline, T., Somoza, R., Cajal, S. R. Y., Condom, E., … Felipe, A. (2012). Increased voltage-dependent K(+) channel Kv1.3 and Kv1.5 expression correlates with leiomyosarcoma aggressiveness. *Oncology letters*, *4*(2), 227–230.

Bienert, G. P., Møller, A. L. B., Kristiansen, K. a, Schulz, A., Møller, I. M., Schjoerring, J. K., & Jahn, T. P. (2007). Specific aquaporins facilitate the diffusion of hydrogen peroxide across membranes. *The Journal of biological chemistry*, *282*(2), 1183–92.

Bionda, C., Hadchity, E., Alphonse, G., Chapet, O., Rousson, R., Rodriguez-Lafrasse, C., & Ardail, D. (2007). Radioresistance of human carcinoma cells is correlated to a defect in raft membrane clustering. *Free radical biology & medicine*, *43*(5), 681–94.

Bondarenko, A. I., Malli, R., & Graier, W. F. (2011). The GPR55 agonist lysophosphatidylinositol directly activates intermediate-conductance Ca2+ -activated K+ channels. *Pflügers Archiv : European journal of physiology*, *462*(2), 245–55.

Boreham DR, Gale KL, Maves SR, Walker JA, M. D. (1996). Radiation-induced apoptosis in human lymphocytes: potential as a biological dosimeter. *Health Phys.*, *71*(5), 685–91.

Bøyum A. (1976). Isolation of lymphocytes, granulocytes and macrophages. *Scand J Immunol*, 9–15.

Brugnara, C., Gee, B., Armsby, C. C., Kurth, S., Sakamoto, M., Rifai, N., … Platt, O. S. (1996). Therapy with oral clotrimazole induces inhibition of the Gardos channel and reduction of

erythrocyte dehydration in patients with sickle cell disease. *The Journal of clinical investigation*, *97*(5), 1227–34.

Cahalan, M D. (1985). A voltage-gated potassium channel in human t lymphocytes. *J. Physiol.*, *358*, 197–237.

Cahalan, M D, Wulff, H., & Chandy, K. G. (2001). Molecular properties and physiological roles of ion channels in the immune system. *Journal of clinical immunology*, *21*(4), 235–52.

Cahalan, Michael D, & Chandy, K. G. (2009). The functional network of ion channels in T lymphocytes. *Immunological reviews*, *231*(1), 59–87.

Caouette, D., Dongmo, C., Bérubé, J., Fournier, D., & Daleau, P. (2003). Hydrogen peroxide modulates the Kv1.5 channel expressed in a mammalian cell line. *Naunyn-Schmiedeberg's archives of pharmacology*, *368*(6), 479–86.

Cappuccini, F., Eldh, T., Bruder, D., Gereke, M., Jastrow, H., Schulze-Osthoff, K., … Jendrossek, V. (2011). New insights into the molecular pathology of radiation-induced pneumopathy. *Radiotherapy and oncology : journal of the European Society for Therapeutic Radiology and Oncology*, *101*(1), 86–92.

Catacuzzeno, L., Fioretti, B., & Franciolini, F. (2012). Expression and Role of the Intermediate-Conductance Calcium-Activated Potassium Channel KCa3.1 in Glioblastoma. *Journal of signal transduction*, *2012*, 421564.

Cecilia Vergara. (1998). Calcium-activated potassium channels. *Current Opinion in neurobiologypinion in neurobiology*, *8*, 321–329.

Chen, T., Chen, M., & Chen, J. (2013). Ionizing radiation potentiates dihydroartemisinin-induced apoptosis of A549 cells via a caspase-8-dependent pathway. *PloS one*, *8*(3), e59827.

Clapham, D. E. (2003). TRP channels as cellular sensors. *Nature*, *426*(6966), 517–24.

Clapham, D. E. (2007). Calcium signaling. *Cell*, *131*(6), 1047–58.

Corre, I., Niaudet, C., & Paris, F. (2010). Plasma membrane signaling induced by ionizing radiation. *Mutation research*, *704*(1-3), 61–7.

Croce, M. V, Colussi, a G., Price, M. R., & Segal-Eiras, a. (1999). Identification and characterization of different subpopulations in a human lung adenocarcinoma cell line (A549). *Pathology oncology research : POR*, *5*(3), 197–204.

Cuschieri, A., & Mughal, S. (1985). Surface morphology of mitogen-activated human lymphocytes and their derivatives in vitro. *Journal of anatomy*, 93–104.

Dangel, G., Lang, F., & Lepple-Wienhues, A. (2005). Effect of sphingosine on Ca2+ entry and mitochondrial potential of Jurkat T cells-interaction with Bcl2. *Cellular Physiology and …*.

Decoursey, T. E., Chandy, K. G., Gupta, S., & Cahalan, M. D. (1987). Mitogen induction of ion channels in murine T lymphocytes. *The Journal of general physiology*, *89*(3), 405–20.

Deshpande A. (1996). Alpha-particle-induced sister chromatid exchange in normal human lung fibroblasts: evidence for an extranuclear target. *Radiat Res.*, *145*(3), 260–267.

Devor, D. C., Singh, a K., Frizzell, R. a, & Bridges, R. J. (1996). Modulation of Cl- secretion by benzimidazolones. I. Direct activation of a Ca(2+)-dependent K+ channel. *The American journal of physiology*, *271*(5 Pt 1), L775–84.

Dimitrijevic-Bussod, M. (1999). Extracellular matrix and radiation G1 cell cycle arrest in human fibroblasts. *Cancer research*, 4843–4847.

Durante, M., & Cucinotta, F. a. (2008). Heavy ion carcinogenesis and human space exploration. *Nature reviews. Cancer*, *8*(6), 465–72.

Elliott, J. I., & Higgins, C. F. (2003). IKCa1 activity is required for cell shrinkage, phosphatidylserine translocation and death in T lymphocyte apoptosis. *EMBO reports*, *4*(2), 189–94.

Facompré, M., Wattez, N., Kluza, J., Lansiaux, a, & Bailly, C. (2000). Relationship between cell cycle changes and variations of the mitochondrial membrane potential induced by etoposide. *Molecular cell biology research communications : MCBRC*, *4*(1), 37–42.

Failla, G. (1931). The Relative Biological Effectiveness of X-rays and Gamma Rays. *Radiology*, *17*, 1–43.

Fanger, C. M., Ghanshani, S., Logsdon, N. J., Rauer, H., Kalman, K., Zhou, J., … Aiyar, J. (1999). Calmodulin mediates calcium-dependent activation of the intermediate conductance KCa channel, IKCa1. *The Journal of biological chemistry*, *274*(9), 5746–54.

Fertig, N., Blick, R. H., & Behrends, J. C. (2002). Whole cell patch clamp recording performed on a planar glass chip. *Biophysical journal*, *82*(6), 3056–62.

Feske, S. (2007). Calcium signalling in lymphocyte activation and disease. *Nature reviews. Immunology*, *7*(9), 690–702.

Garcia-Calvo, M., Leonard, R. J., Novick, J., Stevens, S. P., Schmalhofer, W., Kaczorowski, G. J., & Garcia, M. L. (1993). Purification, characterization, and biosynthesis of margatoxin, a component of Centruroides margaritatus venom that selectively inhibits voltage-dependent potassium channels. *The Journal of biological chemistry*, *268*(25), 18866–74.

Gazzarrini, S. (2003). The viral potassium channel Kcv: structural and functional features. *FEBS Letters*, *552*(1), 12–16.

Gerlach, a. C. (2000). Kinase-dependent Regulation of the Intermediate Conductance, Calcium-dependent Potassium Channel, hIK1. *Journal of Biological Chemistry*, *275*(1), 585–598.

Ghanshani, S., Wulff, H., Miller, M. J., Rohm, H., Neben, A., Gutman, G. a, … Chandy, K. G. (2000). Up-regulation of the IKCa1 potassium channel during T-cell activation. Molecular mechanism and functional consequences. *The Journal of biological chemistry*, *275*(47), 37137–49.

Gordon MacPherson Jon Austyn. (2012). *Exploring Immunology: Concepts and Evidence* (First Edit.). Wiley-VCH Verlag GmbH & Co. KGaA.

Graham, F. L., Smiley, J., Russell, W. C., & Nairn, R. (1977). Characteristics of a human cell line transformed by DNA from human adenovirus type 5. *The Journal of general virology*, *36*(1), 59–74.

Grgic, I., Eichler, I., Heinau, P., Si, H., Brakemeier, S., Hoyer, J., & Köhler, R. (2005). Selective blockade of the intermediate-conductance Ca2+-activated K+ channel suppresses proliferation of microvascular and macrovascular endothelial cells and angiogenesis in vivo. *Arteriosclerosis, thrombosis, and vascular biology*, *25*(4), 704–9.

Grissmer, S., Nguyen, a N., & Cahalan, M. D. (1993). Calcium-activated potassium channels in resting and activated human T lymphocytes. Expression levels, calcium dependence, ion selectivity, and pharmacology. *The Journal of general physiology*, *102*(4), 601–30.

Grupe, M., Myers, G., Penner, R., & Fleig, A. (2010). Activation of store-operated I(CRAC) by hydrogen peroxide. *Cell calcium*, *48*(1), 1–9.

Gupta, S. C., Hevia, D., Patchva, S., Park, B., Koh, W., & Aggarwal, B. B. (2012). Upsides and downsides of reactive oxygen species for cancer: the roles of reactive oxygen species in tumorigenesis, prevention, and therapy. *Antioxidants & redox signaling*, *16*(11), 1295–322.

Hall. (2005). *Radiobiology for the Radiologist*. Lippincott Williams & Wilkins Hardcover.

Hamill, O. P., Marty, A., Neher, E., Sakmann, B., & Sigworth, F. J. (1981). Improved patch-clamp techniques for high-resolution current recording from cells and cell-free membrane patches. *Pfluegers Archiv European Journal of Physiology*, *391*(2), 85–100.

Hayman, R. J., & Van Der Weyden, M. B. (1980). Phytohemagglutinin-stimulated normal human peripheral blood lymphocytes in folate-depleted medium: an in vitro model for megaloblastic hemopoiesis. *Blood*, *55*(5), 863–5.

Heitzmann, D., & Warth, R. (2008). Physiology and pathophysiology of potassium channels in gastrointestinal epithelia. *Physiological reviews*, 1119–1182.

Hille, B. (1992). *Ionic Channels of Excitable Membranes*. Sunderland, MA: Sinauer Verlag.

Hille, B. (2001). *Ion Channels of Excitable Membranes, 3nd edn.* Sunderland, MA.: Sinauer Associates Inc.

Hollaender, A. (1954). High Energy Radiation. *Radiation Biology*, *1*, 1265.

Horváth, F., Wodala, B., Erdei, L., Moroni, A., Etten, J. Van, & Thiel, G. (2002). pH-dependent regulation of a potassium channel protein encoded by a Chlorella virus PBCV-1. *Acta Biologica Szegediensis*, *46*(mM), 21–22.

Hulkower, K. I., & Herber, R. L. (2011). Cell Migration and Invasion Assays as Tools for Drug Discovery. *Pharmaceutics*, *3*(1), 107–124.

Iftinca, M., Waldron, G. J., Triggle, C. R., & Cole, W. C. (2001). State-dependent block of rabbit vascular smooth muscle delayed rectifier and Kv1.5 channels by inhibitors of cytochrome P450-dependent enzymes. *The Journal of pharmacology and experimental therapeutics*, *298*(2), 718–28.

Jehle, J., Schweizer, P. a, Katus, H. a, & Thomas, D. (2011). Novel roles for hERG K(+) channels in cell proliferation and apoptosis. *Cell death & disease*, *2*(8), e193.

Jensen, B S, Strøbaek, D., Olesen, S. P., & Christophersen, P. (2001). The Ca2+-activated K+ channel of intermediate conductance: a molecular target for novel treatments? *Current drug targets*, *2*(4), 401–22.

Jensen, Bo Skaaning, Strøbæk, D., Christophersen, P., Jørgensen, T. D., Hansen, C., Silahtaroglu, A., … Kiær, P. (1998). Characterization of the cloned human intermediate-conductance Ca 2+-activated K+ channel. *American journal of physiology. Cell physiology*, *275*, 848–856.

Jiang, R., Shen, H., & Piao, Y.-J. (2010). The morphometrical analysis on the ultrastructure of A549 cells. *Romanian journal of morphology and embryology = Revue roumaine de morphologie et embryologie*, *51*(4), 663–7.

Jiang, Y., Ruta, V., Chen, J., Lee, A., & MacKinnon, R. (2003). The principle of gating charge movement in a voltage-dependent K+ channel. *Nature*, *423*(May), 42–48.

Jung, J.-W., Hwang, S.-Y., Hwang, J.-S., Oh, E.-S., Park, S., & Han, I.-O. (2007). Ionising radiation induces changes associated with epithelial-mesenchymal transdifferentiation and increased cell motility of A549 lung epithelial cells. *European journal of cancer (Oxford, England : 1990)*, *43*(7), 1214–24.

Kauffmann G.W. (2006). *Radiologie* (3rd ed.). Elsevier.

Khanna, R. (1999). hSK4/hIK1, a Calmodulin-binding KCa Channel in Human T Lymphocytes. ROLES IN PROLIFERATION AND VOLUME REGULATION. *Journal of Biological Chemistry*, *274*(21), 14838–14849.

Kraft G, Krämer M, S. M. (1992). LET, track structure and models. A review. *Radiat Environ Biophys.*, *31*(3), 161–180.

Krämer, M., & Kraft, G. (1994). Calculations of heavy-ion track structure. *Radiation and environmental biophysics*, *33*(2), 91–109.

Krishan, A. (1975). Rapid flow cytofluorometric analysis of mammalian cell cycle by propidium iodide staining. *The Journal of cell biology*, *66*.

Kunzelmann, K. (2005). Ion channels and cancer. *The Journal of membrane biology*, *205*(3), 159–73.

Kuo, S. S., Saad, a H., Koong, a C., Hahn, G. M., & Giaccia, a J. (1993). Potassium-channel activation in response to low doses of gamma-irradiation involves reactive oxygen intermediates in nonexcitatory cells. *Proceedings of the National Academy of Sciences of the United States of America*, *90*(3), 908–12.

Lang, F., Ritter, M., Gamper, N., Huber, S., Tanneur, V., Lepple-wienhues, A., … Gulbins, E. (2000). Cellular Physiology and Biochemistry Cell Volume in the Regulation of Cell Proliferation and Apoptotic Cell Death. *Cellular Physiology and Biochemistry*, 417–428.

Laverne, J., & Laveme, J. A. (1996). Development of radiation chemistry studies of aqueous solutions with heavy ions. *Nuclear Instruments and Methods in Physics Research Section B: Beam Interactions with Materials and Atoms*, *107*(1-4), 302–307.

Lehen'kyi, V., Shapovalov, G., Skryma, R., & Prevarskaya, N. (2011). Ion Channels in Control of Cancer and Cell Apoptosis. *American journal of physiology. Cell physiology*, *301*(6), C1281–9.

Lewis, R., & Cahalan, M. (1995). Potassium and calcium channels in lymphocytes. *Annual review of immunology*.

Lewis, R. S., & Cahalan, M. D. (1989). Mitogen-induced oscillations of cytosolic Ca2+ and transmembrane Ca2+ current in human leukemic T cells. *Cell regulation*, *1*(1), 99–112.

Li, X., Ishihara, S., Yasuda, M., Nishioka, T., Mizutani, T., Ishikawa, M., … Haga, H. (2013). Lung cancer cells that survive ionizing radiation show increased integrin α2β1- and EGFR-dependent invasiveness. *PloS one*, *8*(8), e70905.

Lin, B. C. S., Boltz, R. C., Blake, J. T., Nguyen, M., Talento, A., Fischer, P. A., … Koo, G. C. (1993). Voltage-gated Potassium Channels Regulate Calcium-dependent Pathways Involved in Human T Lymphocyte Activation. *J. Exp. Med.*, *177*(March).

Little, M. P. (2009). Cancer and non-cancer effects in Japanese atomic bomb survivors. *Journal of radiological protection : official journal of the Society for Radiological Protection*, *29*(2A), A43–59.

MacKinnon, R. (2004). Potassium channels and the atomic basis of selective ion conduction (Nobel Lecture). *Angewandte Chemie (International ed. in English)*, *43*(33), 4265–77.

Maher, A. D., & Kuchel, P. W. (2003). The Gárdos channel: a review of the Ca2+-activated K+ channel in human erythrocytes. *The international journal of biochemistry & cell biology*, *35*(8), 1182–97.

Mikkelsen, R. B., & Wardman, P. (2003). Biological chemistry of reactive oxygen and nitrogen and radiation-induced signal transduction mechanisms. *Oncogene*, *22*(37), 5734–54.

Moore, M. a. S. (2002). Cytokine and chemokine networks influencing stem cell proliferation, differentiation, and marrow homing. *Journal of Cellular Biochemistry*, *85*(S38), 29–38.

Mothersill, C., & Seymour, C. (2012). Changing paradigms in radiobiology. *Mutation research*, *750*(2), 85–95.

Moulin AM. (1989). The immune system: a key concept for the history of immunology. *Hist Philos Life Sci.*, *11*(2), 221–236.

Munro TR. (1970). The relative radiosensitivity of the nucleus and cytoplasm of Chinese hamster fibroblastsNo Title. *Radiat Res.*, *42*(3), 451–470.

Muroya, Y., Plante, I., Azzam, E. I., Meesungnoen, J., Katsumura, Y., Jay-gerin, J.-P., & Radiolysis, J. H. I. (2006). High-LET Ion Radiolysis of Water: Visualization of the Formation and Evolution of Ion Tracks and Relevance to the Radiation-Induced Bystander Effect. *Radiation Research*, *165*(4), 485–491.

Mustafa, A., Gadalla, M., & Snyder, S. (2009). Signaling by gasotransmitters. *Science signaling*, *2*(68).

Nagasawa H. (1991). Response of X-ray-sensitive CHO mutant cells (xrs-6c) to radiation. II. Relationship between cell survival and the induction of chromosomal damage with low doses of alpha particles. *Radiat Res.*, *126*(3), 280–288.

Narayanan, P. K. et al. (1997). Alpha particles initiate biological production of superoxide anions and hydrogen peroxide in human cells. *Cancer research*, *57*(18), 3963–71.

Neher, E., & Marty, A. (1982). Discrete changes of cell membrane capacitance observed under conditions of enhanced secretion in bovine adrenal chromaffin cells. *Proceedings of the National Academy of …*, *79*(November), 6712–6716.

Nicholson, G. M. (2007). Insect-selective spider toxins targeting voltage-gated sodium channels. *Toxicon : official journal of the International Society on Toxinology*, *49*(4), 490–512.

Nicoletti, I., Migliorati, G., Pagliacci, M. C., Grignani, F., & Riccardi, C. (1991). A rapid and simple method for measuring thymocyte apoptosis by propidium iodide staining and flow cytometry. *Journal of immunological methods*, *139*(2), 271–9.

Noskov, S. Y., & Roux, B. (2006). Ion selectivity in potassium channels. *Biophysical chemistry*, *124*(3), 279–91.

O. A. Trowell. (1954). THE SENSITIVITY OF LYMPHOCYTES TO IONISING RADIATION. *The Journal of Pathology and Bacteriology*, *64*(4), 687–704.

Ouadid-Ahidouch, H., & Ahidouch, A. (2008). K+ channel expression in human breast cancer cells: involvement in cell cycle regulation and carcinogenesis. *The Journal of membrane biology*, *221*(1), 1–6.

Ouadid-Ahidouch, H., Roudbaraki, M., Delcourt, P., Ahidouch, A., Joury, N., & Prevarskaya, N. (2004). Functional and molecular identification of intermediate-conductance Ca(2+)-activated K(+) channels in breast cancer cells: association with cell cycle progression. *American journal of physiology. Cell physiology*, *287*(1), C125–34.

Palme, D., Misovic, M., Schmid, E., Klumpp, D., Salih, H. R., Rudner, J., & Huber, S. M. (2013). Kv3.4 potassium channel-mediated electrosignaling controls cell cycle and survival of irradiated leukemia cells. *Pflügers Archiv : European journal of physiology*, *465*(8), 1209–21.

Panyi et al. (2004). Ion channels and lymphocyte activation. *Immunology letters*, *92*(1-2), 55–66.

Panyi, G., Sheng, Z., & Deutsch, C. (1995). C-type inactivation of a voltage-gated K+ channel occurs by a cooperative mechanism. *Biophysical journal*, *69*(3), 896–903.

Pedersen, K. a, Schrøder, R. L., Skaaning-Jensen, B., Strøbaek, D., Olesen, S. P., & Christophersen, P. (1999). Activation of the human intermediate-conductance Ca(2+)-activated K(+) channel by 1-ethyl-2-benzimidazolinone is strongly Ca(2+)-dependent. *Biochimica et biophysica acta*, *1420*(1-2), 231–40.

Pietenpol, J. a, & Stewart, Z. a. (2002). Cell cycle checkpoint signaling: cell cycle arrest versus apoptosis. *Toxicology*, *181-182*, 475–81.

Pillozzi, S., & Becchetti, A. (2012). Ion channels in hematopoietic and mesenchymal stem cells. *Stem cells international*, *2012*, 217910.

Platoshyn, O., Zhang, S., McDaniel, S. S., & Yuan, J. X.-J. (2002). Cytochrome c activates K+ channels before inducing apoptosis. *American journal of physiology. Cell physiology*, *283*(4), C1298–305.

Quintero-Hernández, V., Jiménez-Vargas, J. M., Gurrola, G. B., Valdivia, H. H., & Possani, L. D. (2013). Scorpion venom components that affect ion-channels function. *Toxicon : official journal of the International Society on Toxinology*, *72*, 1–15.

Remillard, C. V, & Yuan, J. X.-J. (2004). Activation of K+ channels: an essential pathway in programmed cell death. *American journal of physiology. Lung cellular and molecular physiology*, *286*(1), L49–67.

Restrepo-Angulo, I., De Vizcaya-Ruiz, A., & Camacho, J. (2010). Ion channels in toxicology. *Journal of applied toxicology : JAT*, *30*(6), 497–512.

Rhyu, D. Y. et al. (2012). Role of reactive oxygen species in transforming growth factor-beta1-induced extracellular matrix accumulation in renal tubular epithelial cells. *Transplantation proceedings*, *44*(3), 625–8.

Riedl, S. J., & Salvesen, G. S. (2007). The apoptosome: signalling platform of cell death. *Nature reviews. Molecular cell biology*, *8*(5), 405–13.

Robinson, R.A. and Stokes, R. H. (1965). *Electrolyte Solutions. (2nd ed.revised)*. London: Butterworth's.

Rödel, F., Keilholz, L., Herrmann, M., Sauer, R., & Hildebrandt, G. (2007). Radiobiological mechanisms in inflammatory diseases of low-dose radiation therapy. *International journal of radiation biology*, *83*(6), 357–66.

Roux, B. (2002). What can be deduced about the structure of Shaker from available data? *Novartis Foundation symposium*, *245*(MacKinnon 1991), 84–101; discussion 101–8, 165–8.

Ruppersberg, J., Stacker, M., & Pongs, O. (1991). Regulation of fast inactivation of cloned mammalian IK (A) channels by cysteine oxidation. *Nature*, *352*.

Sahoo, N., Hoshi, T., & Heinemann, S. H. (2013). Oxidative Modulation of Voltage-Gated Potassium Channels. *Antioxidants & redox signaling*, *00*(00).

Samet, J. M. (1989). Radon and Lung Cancer. *JNCI Journal of the National Cancer Institute*, *81*(10), 745–758.

Schmidt-Ullrich, R K, Contessa, J. N., Dent, P., Mikkelsen, R. B., Valerie, K., Reardon, D. B., … Lin, P. S. (1999). Molecular mechanisms of radiation-induced accelerated repopulation. *Radiation oncology investigations*, *7*(6), 321–30.

Schmidt-Ullrich, R K, Mikkelsen, R. B., Dent, P., Todd, D. G., Valerie, K., Kavanagh, B. D., … Chen, P. B. (1997). Radiation-induced proliferation of the human A431 squamous carcinoma cells is dependent on EGFR tyrosine phosphorylation. *Oncogene*, *15*(10), 1191–7.

Schmidt-Ullrich, Rupert K. (2000). Signal Transduction and Cellular Radiation Responses. *Radiation Research*, *153*(3), 245–257.

Scholz M, Kraft-Weyrather W, Ritter S, K. G. (1994). Cell cycle delays induced by heavy ion irradiation of synchronous mammalian cells. *Int J Radiat Biol.*, *66*(1), 59–75.

Schwab, A., Fabian, A., Hanley, P. J., & Stock, C. (2012). Role of ion channels and transporters in cell migration. *Physiological reviews*, *92*(4), 1865–913.

Seddon, M., Looi, Y. H., & Shah, A. M. (2007). Oxidative stress and redox signalling in cardiac hypertrophy and heart failure. *Heart (British Cardiac Society)*, *93*(8), 903–7.

Shao, C., Folkard, M., Michael, B. D., & Prise, K. M. (2004). Targeted cytoplasmic irradiation induces bystander responses. *Proceedings of the National Academy of Sciences of the United States of America*, *101*(37), 13495–500.

Sheppard, D. N., & Welsh, M. J. (1999). Structure and function of the CFTR chloride channel. *Physiological reviews*, *79*(1 Suppl), S23–45.

Shieh, C. C., Coghlan, M., Sullivan, J. P., & Gopalakrishnan, M. (2000). Potassium channels: molecular defects, diseases, and therapeutic opportunities. *Pharmacological reviews*, *52*(4), 557–94.

Singh, H., Saroya, R., Smith, R., Mantha, R., Guindon, L., Mitchel, R. E. J., … Mothersill, C. (2011). Radiation induced bystander effects in mice given low doses of radiation in vivo. *Dose-response : a publication of International Hormesis Society*, *9*(2), 225–42.

Singleton, K. R., Will, D. S., Schotanus, M. P., Haarsma, L. D., Koetje, L. R., Bardolph, S. L., & Ubels, J. L. (2009). Elevated extracellular K+ inhibits apoptosis of corneal epithelial cells exposed to UV-B radiation. *Experimental eye research*, *89*(2), 140–51.

Spitz, D. R., Azzam, E. I., Li, J. J., & Gius, D. (2004). Metabolic oxidation/reduction reactions and cellular responses to ionizing radiation: a unifying concept in stress response biology. *Cancer metastasis reviews*, *23*(3-4), 311–22.

Stark, G. (1991). The effect of ionizing radiation on lipid membranes. *Biochimica et biophysica acta*, *1071*(2), 103–22.

Sundelacruz, S., Levin, M., & Kaplan, D. L. (2009). Role of membrane potential in the regulation of cell proliferation and differentiation. *Stem cell reviews*, *5*(3), 231–46.

Sze, H., & Solomon, a K. (1979). Calcium-induced potassium pathway in sided erythrocyte membrane vesicles. *Biochimica et biophysica acta*, *554*(1), 180–94.

Tharp, D. L., & Bowles, D. K. (2009). The intermediate-conductance Ca2+ -activated K+ channel (KCa3.1) in vascular disease. *Cardiovascular & hematological agents in medicinal chemistry*, *7*(1), 1–11.

Tochhawng et al. (2013). Redox regulation of cancer cell migration and invasion. *Mitochondrion*, *13*(3), 246–53.

Todd, D. G., & Mikkelsen, R. B. (1994). Ionizing radiation induces a transient increase in cytosolic free [Ca2+] in human epithelial tumor cells. *Cancer research*, *54*(19), 5224–30.

Valencia-Cruz, G., Shabala, L., Delgado-Enciso, I., Shabala, S., Bonales-Alatorre, E., Pottosin, I. I., & Dobrovinskaya, O. R. (2009). K(bg) and Kv1.3 channels mediate potassium efflux in the early phase of apoptosis in Jurkat T lymphocytes. *American journal of physiology. Cell physiology*, *297*(6), C1544–53.

Vandorpe, D. H. (1998). cDNA Cloning and Functional Characterization of the Mouse Ca2+-gated K+ Channel, mIK1. ROLES IN REGULATORY VOLUME DECREASE AND ERYTHROID DIFFERENTIATION. *Journal of Biological Chemistry*, *273*(34), 21542–21553.

Verheugen, J. a. H., & Vijverberg, H. P. M. (1995). Intracellular Ca2+ oscillations and membrane potential fluctuations in intact human T lymphocytes: role of K+ channels in Ca2+ signaling. *Cell Calcium*, *17*(4), 287–300.

Wang, H., Zhang, Y., Cao, L., Han, H., & Wang, J. (2002). HERG K+ channel, a regulator of tumor cell apoptosis and proliferation. *Cancer research*, 4843–4848.

Wang, L. (2003). UV-Induced Corneal Epithelial Cell Death by Activation of Potassium Channels. *Investigative Ophthalmology & Visual Science*, *44*(12), 5095–5101.

Wang, S., Melkoumian, Z., Woodfork, K. a, Cather, C., Davidson, a G., Wonderlin, W. F., & Strobl, J. S. (1998). Evidence for an early G1 ionic event necessary for cell cycle progression and survival in the MCF-7 human breast carcinoma cell line. *Journal of cellular physiology*, *176*(3), 456–64.

Wang, Z. (2004). Roles of K+ channels in regulating tumour cell proliferation and apoptosis. *Pflügers Archiv : European journal of physiology*, *448*(3), 274–86.

Ward JF. (1994). DNA damage as the cause of ionizing radiation-induced gene activation. *Radiat. Res.*, *138*, 85–88.

Wardman, P. (1996). Fenton chemistry: an introduction. *Radiat Res.*, *145*(5), 523–531.

Warth, R., Hamm, K., Bleich, M., Kunzelmann, K., von Hahn, T., Schreiber, R., … Greger, R. (1999). Molecular and functional characterization of the small Ca(2+)-regulated K+ channel (rSK4) of colonic crypts. *Pflügers Archiv : European journal of physiology*, *438*(4), 437–44.

Wild-bode, C., Weller, M., Rimner, A., Dichgans, J., & Wick, W. (2001). Sublethal Irradiation Promotes Migration and Invasiveness of Glioma Cells : Implications for Radiotherapy of Human Glioblastoma. *Cancer research*, *61*, 2744–2750.

Winslow, T. (2006). Regenerative Medicine 2006 © 2006.

Wonderlin, W. F., Woodfork, K. a, & Strobl, J. S. (1995). Changes in membrane potential during the progression of MCF-7 human mammary tumor cells through the cell cycle. *Journal of cellular physiology*, *165*(1), 177–85.

Wonderlin, W., & Strobl, J. (1996). Potassium channels, proliferation and G1 progression. *Journal of Membrane Biology*, *107*, 91–107.

Wulff, H, Gutman, G. a, Cahalan, M. D., & Chandy, K. G. (2001). Delineation of the clotrimazole/TRAM-34 binding site on the intermediate conductance calcium-activated potassium channel, IKCa1. *The Journal of biological chemistry*, *276*(34), 32040–5.

Wulff, Heike, Knaus, H.-G., Pennington, M., & Chandy, K. G. (2004). K+ channel expression during B cell differentiation: implications for immunomodulation and autoimmunity. *Journal of immunology (Baltimore, Md. : 1950)*, *173*(2), 776–86.

Xu, L., Enyeart, J. a, & Enyeart, J. J. (2001). Neuroprotective agent riluzole dramatically slows inactivation of Kv1.4 potassium channels by a voltage-dependent oxidative mechanism. *The Journal of pharmacology and experimental therapeutics*, *299*(1), 227–37.

Yan, B., Wang, H., Li, F., & Li, C.-Y. (2006). Regulation of mammalian horizontal gene transfer by apoptotic DNA fragmentation. *British journal of cancer*, *95*(12), 1696–700.

Yang, J. (1999). Human Endothelial Cell Life Extension by Telomerase Expression. *Journal of Biological Chemistry*, *274*(37), 26141–26148.

Yao SX. (1994). Exposure to radon progeny, tobacco use and lung cancer in a case-control study in southern China. *Radiat Res.*, *138*(3), 326–336.

Yu, S. P., Canzoniero, L. M. ., & Choi, D. W. (2001). Ion homeostasis and apoptosis. *Current Opinion in Cell Biology*, *13*(4), 405–411.

Zatalia, S. R., & Sanusi, H. (2013). The role of antioxidants in the pathophysiology, complications, and management of diabetes mellitus. *Acta medica Indonesiana*, *45*(2), 141–7.

Zdrojewicz, Z., & Strzelczyk, J. J. (2006). Radon treatment controversy. *Dose-response : a publication of International Hormesis Society*, *4*(2), 106–18.

Zhang, D., Spielmann, a, Wang, L., Ding, G., Huang, F., Gu, Q., & Schwarz, W. (2012). Mast-cell degranulation induced by physical stimuli involves the activation of transient-receptor-potential channel TRPV2. *Physiological research / Academia Scientiarum Bohemoslovaca*, *61*(1), 113–24.

Zhao W, R. M. (2009). Inflammation and chronic oxidative stress in radiation-induced late normal tissue injury: therapeutic implications. *Curr Med Chem*, *16*(2), 130–143.

Zhou, H., Hong, M., Chai, Y., & Hei, T. K. (2009). Consequences of Cytoplasmic Irradiation: Studies from Microbeam. *Journal of Radiation Research*, *50*(Suppl.A), A59–A65.

8. List of figures

9. List of abbreviations

1

1-EBIO · *1-ethyl-2-benzimidazolinone*

4

4-AP · *4-Amminopyridine*

A

ATP · *Adenosintriphosphat*

B

BIBA · *Biologische Bestrahlungs-Anlage*
BK · *big conductance potassium channel*

C

CaM · *Calmodulin*
cDNA · Complementary DNA
CFTR · *Cystic Fibrosis Transmembrane Conductance Regulator*
CLT · *Clotrimazole*

D

DAPI · *4`, 6-diamidin-2-phenylidol*
DMEM · Dulbecco´s modified minimal essential medium
DMSO · *Dimethylsulfoxid*, *Dimethyl sulfoxide*
DNA · Deoxyribonucleic acid
dNTPs · *deoxyribonucleotides*
DTT · *Dithiothreitol*

E

EDTA · *Ethylenediaminetetraacetic acid*
EGF · *epidermal growth factor*
E_k · *potassium equilibrium potential*

F

FACS · *fluorescence-activated cell sorting*
FCS · *fetal calve serum*

G

G1-phase · *Gap1-phase in cell-cycle*
GAPDH · *Glycerinaldehyd-3-phosphat-Dehydrogenase*
GSI · *Helmholtzzentrum für Schwerionenforschung GmbH*

H

hEAG · *Homo sapiens potassium voltage-gated channel, subfamily H (eag-related), member 1 (KCNH1)*
HEK 293 · human embryonic kidney cells
hERG · *Homo sapiens potassium voltage-gated channel, subfamily H (eag-related), member 2 (KCNH2)*
hIK · *human intermediate conductance Ca2+-activated potassium channel*
hTERT · human telomerase reverse transcriptase

I

ICRAC · *Calcium Release Activated Channel*
I_{inst} · *instantaneous current*
IK · *intermediate conductance potassium channel*
IP_3 · *inositoltriphosphate*
I_{td} · *time dependent current*

K

KCNA3
Kv1.3 · *Potassium voltage-gated channel, shaker-related subfamily, member 3*

L

LET · *linear energy transfer*
L-Glu · *L-Glutamin*

M

MCF-7 · *Michigan Cancer Foundation - 7*
MEM · Minimal essential medium
MGTX · *Margatoxin*

N

NEAA · *non-essential amino acids*

NMDG · *N-methyl-d-glucamine*

P

PBL · *peripheral blood lymphocytes*, Human peripheral blood lymphocytes
PBS · *phosphate-buffered saline*
PCR · *Polymerase chain reaction*
PE · *photoelectric effect*
pH · *potential hydrogen*
PHA · *phytohaemagglutinin*, *phytohemagglutinin*
PI · *propidium iodide*

R

RBE · *relative biological effectiveness*
RNAse · *Ribonuclease*
ROS · *Reactive oxygen species*, *reactive oxygen species*
RPMI · *Roswell Park Memorial Institute medium*
RT · *room-temperature*
RT-PCR · *Reverse transcription polymerase chain reaction*

S

SE · *standard error*
SIS · *Heavy Ion Synchrotron*
SK · *small conductance potassium channel*
S-phase · *Synthese-phase in cell-cycle*
STD · *Standard deviation*
STS · *Staurosporine*

T

TEA · *tetraethyl-ammonium-chloride*
TEM · *Transmission electron microscopy*
TNF · tumor necrosis factor

U

UNILAC · *Universal Linear Accelerator*

10. Acknowledgements

Zum Abschluss dieser Arbeit ist es an der Zeit, mich bei denjenigen zu bedanken, die mich in dieser spannenden Phase meiner akademischen Laufbahn begleitet haben. Dabei gilt mein besonderer Dank vor allem:

Prof. Dr. Gerhard Thiel, für die Betreuung dieser interessanten und spannenden Arbeit. Für die stetige Unterstützung während der Arbeit, aber auch während der etwas schwierigeren Zeit, in der ich auf viel Verständnis gestossen bin. Für die jederzeit angenehme Atmosphäre am Arbeitsplatz, die mich immer motiviert hat und mich weiter motivieren wird. Das von ihm entgegengebrachte Vetrauen und die Möglichkeit mich auf vielen Konferenzen mit anderen Wissenschaftlern auszutauschen.

Prof. PhD. Marco Durante, für die Möglichkeit dieses spannende Projekt durchzuführen und die Übernahme des Koreferats.

Dr. Claudia Fournier, für die immer geduldige Beantwortung all meiner Fragen bezüglich Strahlenbiohysik und ihre unentbehrliche Hilfestellung bei allen Strahlzeiten an der GSI. Sowie ihrem Ideenreichtum um dieses Projekt weiter voranzutreiben.

Dr. Brigitte Hertel, für die schöne Zeit in der Arbeitsgruppe und ihr offenes Ohr bei allen wissenschaftlichen, aber auch unwissenschaftlichen Problemen. Sowie die viele Motivase.

Dr. Indra Schröder und **Dr. Tobias Meckel**, die jederzeit mit Rat und Tat zu Seite standen und mir neue Denkanstöße lieferten.

Meinen „alten“ und „neuen“ Zimmergenossen, mit denen ich eine wunderbare Zeit in der Arbeitsgruppe, aber auch ausserhalb der Labore verleben konnte. **Thomas Guthmann**, mein Studienweggefährte, mit dem ich den Weg in die AG fand. **Christian Braun** und **Timo Wulfmeyer**, ohne die der Arbeitstag manchmal früher geendet hätte. **Vera Bandmann** und **Lucia Carillo**, für die schöne Zeit auf Timo Greiners Spuren, Cappuccino Pausen sowie Gespräche und Aktivitäten ausserhalb der AG. **Charlotte von Chappuis**, für die sportlichen Auszeiten am Kicker sowie Reitstunden auf Emily. **Timo Greiner** und **Manuela Gebhardt**, ohne die es nur halb so lustig geworden wäre. **Christine Gibhardt**, meine Reisebegleitung im Auftrag der Elektrophysiologie und Strahlenbiologie sowie **Anne Berthold**, wegen der ich sicherlich während der Doktorandenzeit zugenommen habe. Der gesamten restlichen **AG Thiel und Meckel** besonders **Barbara Reinhards**, **Silvia Lenz**, **Sylvia Haase**, **Brigitte Hehl**, **Barbara Wolf** und **Mirja Manthey**, die immer ein Lächeln übrig haben und ohne die, die Arbeitsgruppe nicht laufen würde.

Danke auch an alle meine Freunde und Volleyballspielerinnen, die gerade am Ende meiner Arbeit mit einigen Stimmungsschwankungen zu kämpfen hatten und sie ertragen haben.

Besonderer Dank gilt meinen Eltern **Elfi** und **Hans-Joachim Roth** sowie meinem Bruder **Martin**, die mir das alles ermöglicht haben und immer für mich da waren.

Weiterer Dank gilt meiner Freundin **Isabelle Prediger**, für all die Liebe und Unterstützung während der gesamten Zeit.

11. Eidesstattliche Erklärung

"Ich erkläre hiermit ehrenwörtlich, dass ich die vorliegende Arbeit entsprechend den Regeln guter wissenschaftlicher Praxis selbstständig und ohne unzulässige Hilfe Dritter angefertigt habe. Sämtliche aus fremden Quellen direkt oder indirekt übernommenen Gedanken sowie sämtliche von Anderen direkt oder indirekt übernommenen Daten, Techniken und Materialien sind als solche kenntlich gemacht. Die Arbeit wurde bisher bei keiner anderen Hochschule zu Prüfungszwecken eingereicht."

Darmstadt, den _____

_____

Bastian Roth

12. Own work

Experiments, data analysis and writing of the present thesis with exception of the following items, were all done by myself.

- The RT-PCR in Figs. Fig. 9, Fig. 34 and Fig. 36 were done by Dr. Manuela Gebhardt (TU-Darmstadt, Germany).

- The Overview-image of cell-cycle distribution in Fig. 23 was done by Anne Berthold (TU-Darmstadt, Germany)

- The proliferation assay in the presence of CLT in Fig. 44c was done by Jan Knoop (GSI, Germany).

- Parts of the data for Fig. 25 were part of the diploma thesis: “Einfluss ionisierender Strahlung auf Ionenkanalaktivität” by Bastian Roth, 2009 (TU-Darmstadt, Germany).

13. Curriculum Vitae

Education

1985 – 1989	Hirschbachschule Reinheim/Zeilhard
1989 – 1991	Dr. Kurt-Schumacher-Schule Reinheim
1991 – 1998	Albert-Einstein-Schule Groß-Bieberau
1999 – 2000	Zivildienst Johanniter-Unfallhilfe E.V.
2000 – 2001	Technische Universität Darmstadt – Computer Science
2001 – 2009	Technische Universität Darmstadt – Biology
since 2010	Technische Universität Darmstadt – Doctoral program

Degrees:	General qualification for university entrance
	Pre-degree

the Diploma thesis “Einfluss ionisierender Strahlung auf Ionen-Kanal Aktivität”, 2009

Skills acquired during studies

2010 scholarship student and member of the Helmholtz-Graduate School HGS-HIRe

2010 Poster presentation at the Annual Meeting of the German Biophysical Society, Bochum

2010 Soft-Skill Course “Writing Scientific Papers in English”

2010 Lecture Week “The Physics of Strong Coulomb Fields - Precision Studies with Highly Charged Ions”

2010 Conference “Biotec meets Optics”, Hannover

2011 Member of the Graduate-School GRK1657

2011 Poster presentation at the Erice School of Biophysics “Channels and Transporters”, Erice

2011 Poster presentation at the 12th International Wolfsberg Meeting on Molecular Radiation Biology/Oncology

2011 Workshop “Ionizing radiation epidemiology”, Mainz

2011 Chairman at the HGS-HIRe Graduate-Days 2011

2012 Oral presentation at the “International Meeting on Ion Transport and Cancer” (ITC 2012), Würzburg

2012 Poster presentation at the 15th Annual Meeting of the GBS, Munich

2012 Poster presentation at the HGS-HIRe Graduate-Days 2012, Mainz

2013 Poster presentation at the 9th European Biophysics Congress, Lisbon